



This is to certify that the
dissertation entitled

Control of Aerobic Metabolism
in Skeletal Muscle
presented by

Susan Jill Harkema

has been accepted towards fulfillment
of the requirements for

Ph.D. degree in Physiology



Major professor

Date 9/27/93

LIBRARY
Michigan State
University

PLACE IN RETURN BOX to remove this checkout from your record.
TO AVOID FINES return on or before date due.

DATE DUE	DATE DUE	DATE DUE
MAR 25 1999 1-75	_____	_____
_____	_____	_____
_____	_____	_____
_____	_____	_____
_____	_____	_____
_____	_____	_____
_____	_____	_____

MSU Is An Affirmative Action/Equal Opportunity Institution

CONTROL OF AEROBIC METABOLISM IN SKELETAL MUSCLE

By

Susan Jill Harkema

A DISSERTATION

Submitted to
Michigan State University
in partial fulfillment of the requirements
for the degree of

DOCTOR OF PHILOSOPHY

Department of Physiology

1993

ABSTRACT

CONTROL OF AEROBIC METABOLISM IN SKELETAL MUSCLE

By

Susan Jill Harkema

The primary focus of this research was to test the two prominent models of the control of respiration in skeletal muscle. The two models are: 1) simple kinetic control, or control by total cytoplasmic ADP and 2) thermodynamic control, or control by cytoplasmic phosphorylation potential. These two hypotheses are difficult to distinguish by simple correlative experiments because both ADP and cytoplasmic phosphorylation potential change in tandem during muscle stimulation. However, it had been shown that the study of contracting muscles during experimentally induced acidosis could, in principle distinguish between the two models. Therefore, the primary research objective was to examine the effects of acidosis on respiratory control during submaximal ATPase rates in skeletal muscle.

Although there is general agreement that respiration is controlled by "phosphorylation state" (either ADP, or

cytoplasmic phosphorylation potential) in most skeletal muscles, there was some evidence that phosphorylation state is not the sole controller of respiration in slow-twitch muscle at higher respiration rates. Therefore, the initial focus of this research was to re-investigate this phenomenon in intact slow-twitch muscle. We examined the relationship between phosphorylation state and oxygen consumption in cat soleus muscle *in situ*. One series of experiments monitored PCr, ATP, Pi and pH noninvasively during submaximal stimulation in intact soleus muscles using ^{31}P -NMR. Another series measured oxygen consumption during steady-state conditions at identical stimulation rates. The results did not confirm the previous studies and suggested that phosphorylation state is the dominant regulator of respiration in slow-twitch muscle.

The remainder of the research focused on distinguishing between the two models of the control of respiration by experimentally manipulating the intracellular concentration of hydrogen ion. A potential obstacle to the design of this study was the possibility that acidosis alters the utilization of ATP, as well as ATP synthesis. For example, if acidosis profoundly inhibits cross-bridge cycling, it would be difficult to increase respiratory rate by muscle stimulation in acidic muscles. Therefore, the purpose of the second study was to directly measure the effect of hypercapnic acidosis on ATP utilization during isometric contractions of perfused

cat fast- and slow-twitch muscles. ATP utilization was observed during acidosis using gated ^{31}P -NMR in isolated cats soleus and biceps muscles. The results showed that the ATP cost of tetanic contractions is reduced in proportion to the reduction in force. Thus, the intrinsic rate of cross-bridge cycling and the economy of force development appeared not to be sensitive to lowered pH.

The final series of experiments were then designed and implemented to test the control of respiration in slow-twitch muscle. We examined the effect of hypercapnic acidosis on the relationship between PCr, ADP, and phosphorylation potential versus respiratory rate in intact cat soleus muscle at rest and during moderate stimulation. Intracellular pH was decreased by changing the gas content of the perfusate, metabolite concentrations (PCr, Pi, ATP, and pH) were measured by ^{31}P -NMR, and oxidative rates were calculated from oxygen consumption measurements in the slow-twitch muscles. Although interpretation of the study was complicated by the observation that acidosis decreased the maximum aerobic capacity of muscle, the results were clearly not consistent with the simple ADP model of respiratory control, but did remain consistent with thermodynamic models. We conclude that the control of respiration is regulated by cytosolic phosphorylation potential and not by ADP availability in skeletal muscle.

Copyright by
SUSAN JILL HARKEMA
1993

I dedicate this thesis to my family and friends who made
this possible:

Mom and Dad,
Julie, Tommy, and Sallie,
your continued love, support, and encouragement never
ceases and for that I am truly fortunate;

Kate and Todd,
you've seen me through the tough times, and of course, the
good times;

Glenna and Marsha,
you've always accepted who I am and believed in me;

Steve and Linda,
you were there when I most needed you, and of course,
your *funny*;

Van,
your patience, trust, understanding, and love is a miracle.

ACKNOWLEDGMENTS

I would like to thank Dr. Ronald Meyer for providing me with the opportunity to do exciting research and learn innovative technology under his direction. I am extremely fortunate to have you as a mentor and most admire you for your straightforward, intelligent approach to science and your pure quest for fully supported scientific answers.

I greatly appreciate the contributions of my thesis committee members. Dr. Adams your encouragement and guidance was very valuable to me. There are so many students over the years who have benefited from your wisdom and I feel very fortunate to be one of them. Dr. Chaudry, I especially thank you for giving me the encouragement to pursue graduate work. Dr. Jump, I have learned many aspects of becoming a successful scientist by your example and only hope I can reach the consistent level of hard work and perseverance you maintain every day. Dr. Hollingsworth, I appreciate your participation on my committee and your insightful suggestions. Dr. Krier, your motivational talks and sound scientific advice were very valuable in my early development as a scientist.

I would like to sincerely thank the members of the RAM lab for there support. Dr. Greg Adams, thanks so much for

your "million" ideas, but most important is that almost every one was a good one. Your contribution to my work was significant and I look forward to future collaboration during our careers. Dr. Jeanne Foley, I appreciate your contributions to my graduate experience and especially enjoyed the "weekend" experiments. Mary Peterson, your technical assistance was extremely valuable as well as your support. Tony Paganini, you always kept things exciting, good luck in the completion of your thesis. Rob MacDonald, your work in the lab and on my projects was outstanding. I am sure your career as a physical therapist and researcher will be a successful one.

I would like to thank all my fellow graduate students for their support and commitment to success. I would especially like to acknowledge Drs. Samita Bhattacharya, Jon Feeman, Ormond MacDougald, and Zhawoen Wang for their encouragement, sharing of ideas, and "intellectual discussions", all which greatly enhanced my graduate school experience.

Finally, I would like to thank Sharon Shaft for all she did for me from the very first day of graduate school. Also my heartfelt thanks to Barb Burnett, Bobbi Milar, Marilyn Walker and Shirley Zutaut for their invaluable assistance and incredible support over the years.

TABLE OF CONTENTS

LIST OF TABLES	xii
LIST OF FIGURES	xiii
I. INTRODUCTION AND LITERATURE REVIEW	1
<u>SKELETAL MUSCLE METABOLISM</u>	2
<u>OXIDATIVE PHOSPHORYLATION</u>	9
<u>THEORIES OF CONTROL OF OXIDATIVE PHOSPHORYLATION</u>	11
Inorganic Phosphate (Pi)	15
ADP	17
Cytoplasmic Phosphorylation Potential	20
[ATP]/[ADP]	26
Creatine	27
<u>APPLICATION OF PHOSPHORUS NUCLEAR MAGNETIC</u>	29
<u>RESONANCE STUDIES TO MUSCLE METABOLISM</u>	
³¹ P-NMR Studies Supporting Regulation	33
By Redox Potential	
³¹ P-NMR Studies Supporting ADP Control	34
³¹ P-NMR Studies Supporting Thermodynamic Models	37
<u>THE PHOSPHORYLATION STATE CONTROVERSY</u>	45
<u>SUMMARY</u>	46
<u>RESEARCH OBJECTIVES</u>	48
II. GENERAL MATERIALS AND METHODS	49
<u>PHOSPHORUS NUCLEAR MAGNETIC SPECTROSCOPY (³¹P-NMR)</u>	49
General Principles	49
NMR Probes For Muscle Studies	56
Procedures For The Basic ³¹ P-NMR Pulse	69
Experiment	
Gated ³¹ P-NMR Pulse Experiment	70

<u>MUSCLE PREPARATIONS</u>	71
<i>In situ</i> Soleus Studies	74
Isolated Perfused Muscle Studies	76
III. CONTROL OF RESPIRATION BY PHOSPHORYLATION STATE IN SLOW-TWITCH MUSCLE <i>IN SITU</i>	83
<u>INTRODUCTION</u>	83
<u>MATERIALS AND METHODS</u>	86
Surgical Techniques	86
Experimental Series I/Phosphorus NMR	87
Experimental Series II/Oxygen Consumption	88
<u>RESULTS</u>	89
<u>DISCUSSION</u>	105
IV. EFFECT OF HYPERCAPNIC ACIDOSIS ON THE ATP COST OF CONTRACTIONS IN FAST- AND SLOW-TWITCH MUSCLES	109
<u>INTRODUCTION</u>	109
<u>MATERIALS AND METHODS</u>	112
Surgical Techniques	112
Gated ³¹ P-NMR Experiments	113
<u>RESULTS</u>	114
<u>DISCUSSION</u>	125
V. CONTROL OF RESPIRATION IN SLOW-TWITCH MUSCLE	128
<u>INTRODUCTION</u>	128
<u>MATERIALS AND METHODS</u>	133
Surgical Techniques	133
Experimental Series I/Phosphorus NMR	133
Experimental Series II/Oxygen Consumption	135
<u>RESULTS</u>	135
<u>DISCUSSION</u>	149
VI. SUMMARY AND CONCLUSIONS	153

LIST OF TABLES

Table 1.	Mammalian Skeletal Muscles.	8
Table 2.	PCr time constants.	94
Table 3.	pH, force, oxygen consumption, and blood flow measurements of soleus muscle at rest and during stimulation.	98
Table 4.	Biceps and soleus muscle phosphate levels and contractile properties during hypercapnia and normocapnia.	116
Table 5.	PCr time constants.	139
Table 6.	Phosphate levels, pH and oxygen consumption in soleus muscle during hypercapnia and normocapnia.	140

LIST OF FIGURES

Figure 1.	Schematic of muscle contraction.	5
Figure 2.	Schematic of Oxidative Phosphorylation.	13
Figure 3.	Linear Circuit Model	40
Figure 4.	Representation of the Free Induction Decay (FID) and NMR spectrum	52
Figure 5.	Chemical structure of PCr, ATP, and Pi and the phosphorus NMR spectrum containing the corresponding peak that represents each phosphate signal.	54
Figure 6.	Plexiglas/Lexan probe constructed for animal experiments within a 4.7 Tesla magnet.	59
Figure 7.	Schematic of Helmholtz coil and circuitry of the coil.	61
Figure 8.	Circuit for specially constructed force transducers.	63
Figure 9.	Probe for isolated perfused muscle experiments within a 9.2 Tesla magnet.	66
Figure 10.	Top portion of probe for isolated perfused muscle experiments within a 9.2 Tesla magnet.	68
Figure 11.	Gated ^{31}P -NMR Experimental Protocol.	73
Figure 12.	Isolated perfused muscle experimental setup.	82
Figure 13.	Series of spectra of soleus muscle, control (1 minute), during 3 Hz stimulation (15 minutes), and during recovery (15 minutes).	91

Figure 14.	PCr levels from ³¹ P-NMR spectra of cat soleus muscle acquired during and after 15 minutes of stimulation at 0.5, 1, 2, 3, and 4 Hz.	93
Figure 15.	PCr time constants for stimulation rates of 0.5, 1, 2, 3, and 4 Hz.	97
Figure 16.	Steady-state oxygen consumption vs. product of stimulation rate times mean peak twitch force during soleus muscle stimulation.	100
Figure 17.	Steady-state PCr vs. product of stimulation rate times mean peak twitch force during soleus muscle stimulation.	102
Figure 18.	Relationship between steady-state PCr and oxygen consumption at rest and during stimulation (0.5, 1, 2, 3, 4 Hz).	104
Figure 19.	Spectra acquired at rest and immediately following isometric twitch and tetanic contractions in soleus muscle during normocapnia and hypercapnia.	118
Figure 20.	Spectra acquired at rest and immediately following isometric twitch and tetanic contractions in biceps muscle during normocapnia and hypercapnia.	120
Figure 21.	Energy cost ($\mu\text{mol PCr/g muscle}$) per isometric contraction during normocapnic and hypercapnic perfusion of soleus and biceps muscles.	122
Figure 22.	Energy cost and force production per isometric contraction during normocapnic and hypercapnic perfusion of soleus and biceps muscles.	124
Figure 23.	PCr changes during soleus muscle stimulation and recovery under normocapnic and hypercapnic conditions.	138
Figure 24.	pH changes during 0.25 and 0.5 Hz stimulation of soleus muscle during hypercapnia and normocapnia.	142

- Figure 25. [ADP] versus oxygen consumption at 0.25 Hz and 0.5 Hz during hypercapnia and 0.25 Hz, 0.5 Hz, and 1 Hz during normocapnia. 144
- Figure 26. Steady-state PCr levels versus oxygen consumption of soleus muscle during rest and stimulation at 0.25 and 0.5 Hz during hypercapnia and 0.25, 0.5, and 1 Hz during normocapnia 146
- Figure 27. Cytoplasmic phosphorylation potential versus oxygen consumption of soleus muscle during rest and stimulation at 0.25 and 0.5 Hz during hypercapnia and 0.25 Hz, 0.5 Hz, and 1 Hz during normocapnia. 148

CHAPTER 1

INTRODUCTION AND LITERATURE REVIEW

The pathways of intermediary metabolism and ATP production in muscle and other tissues are known in remarkable detail. However, our understanding of the control mechanisms of these pathways is often surprisingly primitive. This discrepancy between our knowledge of the biochemical machinery, versus our understanding of how this machinery actually works in intact tissues, is perfectly illustrated when considering the control of respiration in skeletal muscle. As outlined below, the potential regulatory mechanisms linking respiratory rate to muscle work were identified by the early 1960's. By 1980, the general mechanisms by which mitochondria synthesize ATP were clear, although some molecular details are still not complete. Nonetheless, the exact signal which links mitochondrial adenosine triphosphate (ATP) synthesis to cytoplasmic adenosine triphosphatase (ATPase) rate in muscle is still a major source of controversy among muscle physiologists. The experiments described in this thesis will help to clarify this issue, at least to the extent that they seem to eliminate one major hypothesis, i.e., that muscle respiration is regulated in a simple

Michaelis/Menton fashion by total cytoplasmic ADP concentration.

The following discussion will: 1) provide a general overview of muscle metabolism; 2) consider in some detail the various proposals for the control of respiration in skeletal muscle, including the adenosine diphosphate (ADP) control hypothesis, and 3) introduce the methods and rationale for the experiments included in this thesis.

SKELETAL MUSCLE METABOLISM

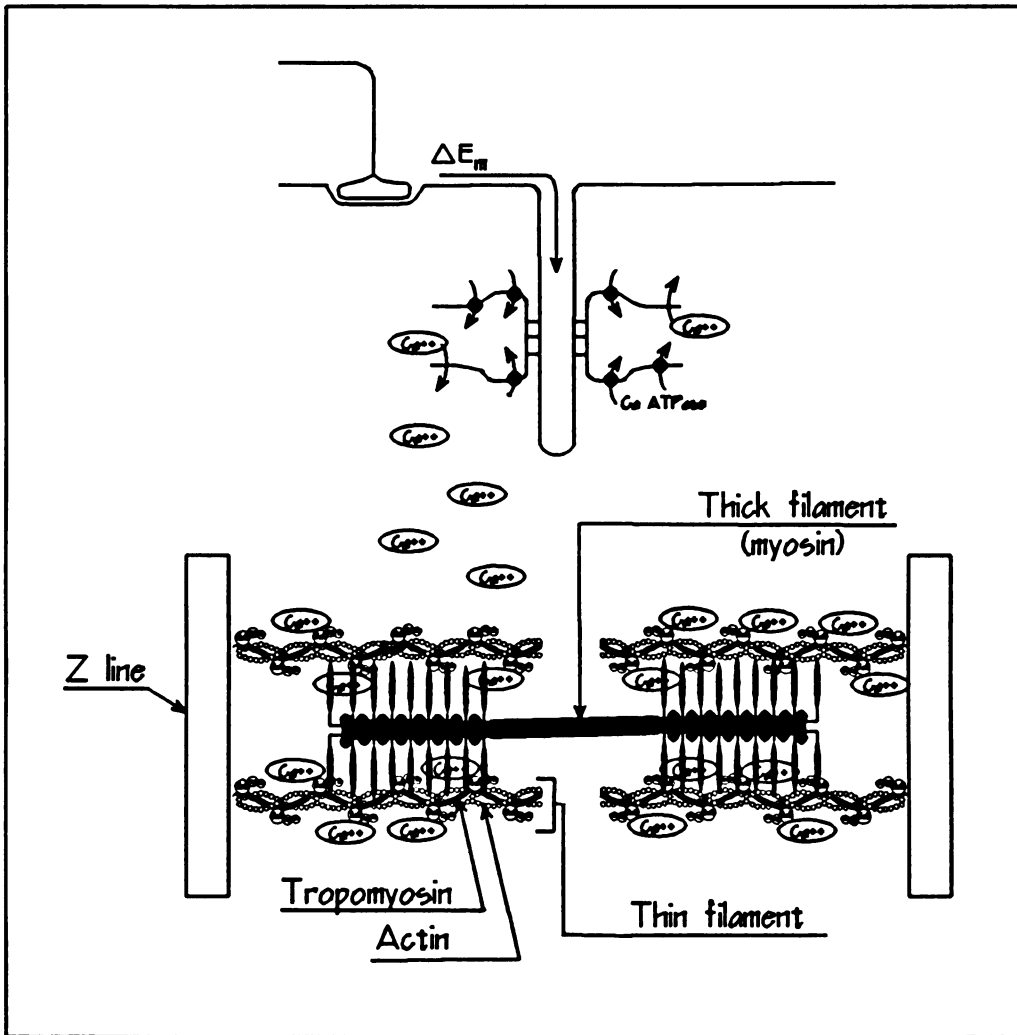
The primary energy utilizing functions of skeletal muscle cells are to maintain cell homeostasis and to perform mechanical work. As in other tissues, cell homeostasis is maintained by several energy utilizing pumps that regulate transmembrane ionic concentrations and intracellular calcium levels (Janis *et al.*, 1987), and by protein synthesis and other basic anabolic reactions. In addition to these basic functions, skeletal muscle performs work following stimulation of the myocyte by a motor neuron. Electrical current travels along t-tubules changing the transmembrane potential. The sarcoplasmic reticulum releases bound stores of calcium which diffuse to contractile proteins, actin and myosin (Hasselbach and Oetliker, 1983; Donaldson and Kerrick, 1975). These proteins overlap and calcium binds to troponin exposing the binding site on actin for myosin. Crossbridges form and

use energy for movement, leading to crossbridge cycling and ultimately muscle contraction [Figure 1] (Cooke, 1990; Huxley and Simmons, 1971; Phillips and Petrofsky, 1983).

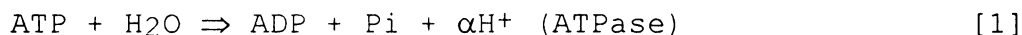
Whether the energy is used for cell homeostasis or crossbridge cycling, ATP is the energy source (Lipmann, 1946, Cain and Davies, 1962). ATPases within the myocyte cleave the terminal phosphate of ATP to release its stored energy. Furthermore, the products of ATP hydrolysis, ADP and inorganic phosphate (Pi), are well known activators of the major ATP synthetic pathways in the cell i.e., glycolysis, and oxidative phosphorylation (Alberty, 1968; Lehninger, 1954). Thus, it seems reasonable to suppose that these products, or some function of them, may provide the feedback signal controlling ATP synthesis. This basic assumption underlies all major theories of respiratory control, at least in skeletal muscle, and is no doubt generally correct. As we will see below, the main controversy is over exactly which product, or combination of products, is operationally the effective controller in intact muscle.

There is a net decrease in chemical potential energy during muscle activity with ATP hydrolysis (Lipmann, 1949; Rall, 1972), yet ATP itself rarely decreases significantly during muscle contraction because it is rapidly rephosphorylated by the creatine kinase reaction [Equation 2]. This reaction has been proven to be near thermodynamic

Figure 1. Schematic of muscle contraction.



equilibrium in intact muscle (McGilvery and Murray, 1974; Lawson and Veech, 1979) and provides access to a phosphate pool for rapid ATP regeneration. Hence, even in the absence of other ATP synthetic reactions, the observed chemical reaction which drives muscle contraction is not net ATP hydrolysis per se, but rather net hydrolysis of PCr to creatine and Pi:





$\beta = (1 - \alpha)$ is 0.4 at pH 7.0 and 0.65 at pH 6.5 (Gilbert et al., 1971; Meyer and Adams, 1990, Adams et al., 1990). The effect is that changes in ATP are effectively buffered by PCr during contraction by nearly instantaneous rephosphorylation of ADP (Bienfait et al., 1975; Mahler, 1985). However, because the level of ADP in muscle at rest is so low (<50 μmol), even an insignificant change in ATP can still result in significant accumulation of ADP. Furthermore, the net reaction does release Pi, so there is a significant change in the free energy of ATP hydrolysis as PCr is depleted:

$$\Delta G = \Delta G^{\circ'} + 2.303 \text{ RT } \log \frac{[\text{ADP}][\text{Pi}][\text{H}^+]}{[\text{ATP}]} \quad [4]$$

$\Delta G^{\circ'} = -30.5 \text{ kJ/mol}$ (Chang, 1981); $R=8.314 \text{ J/K/mol}$.

Thus, muscle contraction and ATP use is accompanied by significant increases in ADP, and Pi and a significant decrease in cytosolic free energy of ATP hydrolysis, even though ATP does not significantly change. Free cytoplasmic ADP is not easy to measure in muscle, because the basal level is low, and because there is a large pool of ADP bound to actin and other proteins which is released during extraction for biochemical assays. Some evidence suggests that chemical measurements of Pi in muscle are inaccurate for similar reasons. However, PCr is easy to measure. As we will see below, non-invasive measurements of PCr by NMR spectroscopy are now commonly used as a general index of muscle energy or "phosphorylation state", and more specifically, can be used to calculate free ADP and the free energy of ATP hydrolysis in muscle.

Finally, before proceeding to the details of various models for respiratory control, it should be noted that mammalian skeletal muscle is not a biochemically homogenous tissue. There are at least three muscle fiber types characterized by different glycolytic, oxidative, and myosin ATPase activities [Table 1] (Close, 1972). Resting Pi levels are higher and PCr and ATP levels are lower in slow-twitch as compared to fast-twitch fibers at rest (Meyer et al., 1985; Meyer et al., 1982; Crow and Kushmerick, 1982). Also, ATPase rates and oxygen consumption rates are lower in slower contracting muscles fibers compared to that of faster contracting fibers at

Table 1

MAMMALIAN SKELETAL MUSCLES

	FAST-TWITCH GLYCOLYTIC	FAST-TWITCH OXIDATIVE- GLYCOLYTIC	SLOW-TWITCH OXIDATIVE
Actomyosin ATPase Activity	High	High	Low
Glycolytic Capacity	High	High	High
Oxidative	Low	High	High

identical twitch rates (Meyer et al., 1985). Velocity of shortening, as the classification implies, is much more rapid in fast-twitch fibers (Claflin and Faulkner, 1985) but slow-twitch fibers are more fatigue resistant (Baldwin and Tipton, 1972). Myosin proteins are distributed differently between the fiber types with high concentrations of Type I in slow muscle fibers and, in contrast, primarily Type IIa and IIb in fast muscle fibers (Close, 1972). These differences must be kept in mind for two reasons: first, it is conceivable that respiration is controlled differently in different fiber types; and second, these differences complicate the interpretation of studies performed on muscles of mixed fiber types.

OXIDATIVE PHOSPHORYLATION

Oxidative metabolism is the major source of ATP produced during muscle stimulation at rates below the maximum aerobic capacity of muscle (Erecinska and Wilson, 1982; Kushmerick, 1983; Mahler, 1985). The following discussion briefly outlines the history and major conclusions of studies of oxidative phosphorylation.

Engelhardt was the first to demonstrate a fluoride-insensitive, cyanide-sensitive respiratory-linked synthesis of ATP from inorganic phosphate distinct from glycolysis in bird erythrocytes in the early 1930's (Engelhardt, 1932). Yet, oxidative phosphorylation did not seem to become



accepted until several years later when Kalckar showed phosphorylation of glucose, glycerol and AMP coupled to respiration (Kalckar, 1937; Kalckar, 1939). Several investigators showed that respiratory-linked phosphorylation is fundamentally different from glycolysis and requires phosphate acceptor (ADP), and Pi (Johnson, 1941; Ochoa, 1940a; Ochoa, 1940b; Belitzer and Tzibakowa, 1939).

The discovery of the reactions of the Kreb's cycle explained the stimulation of respiration which is observed with addition of dicarboxylic acids and demonstrated that NADH, the product of the dehydration of these substrates, is directly oxidized by the respiratory chain. This clearly established involvement of the respiratory chain in oxidative phosphorylation of ADP (Slater, 1981). Lehninger verified this link by demonstrating phosphorylation accompanies passage of electrons from NADH to oxygen in rat liver mitochondria (Lehninger, 1954; Lehninger and Wagner Smith, 1949).

Chance and Williams (1955; 1956) introduced an assay method to measure oxidative phosphorylation in isolated mitochondria and then outlined the sequence of the respiratory chain components. They measured rapid changes in respiration caused by addition of ADP in isolated mitochondria using a special double beam spectrophotometer. They discerned that the sequence in which spectroscopic

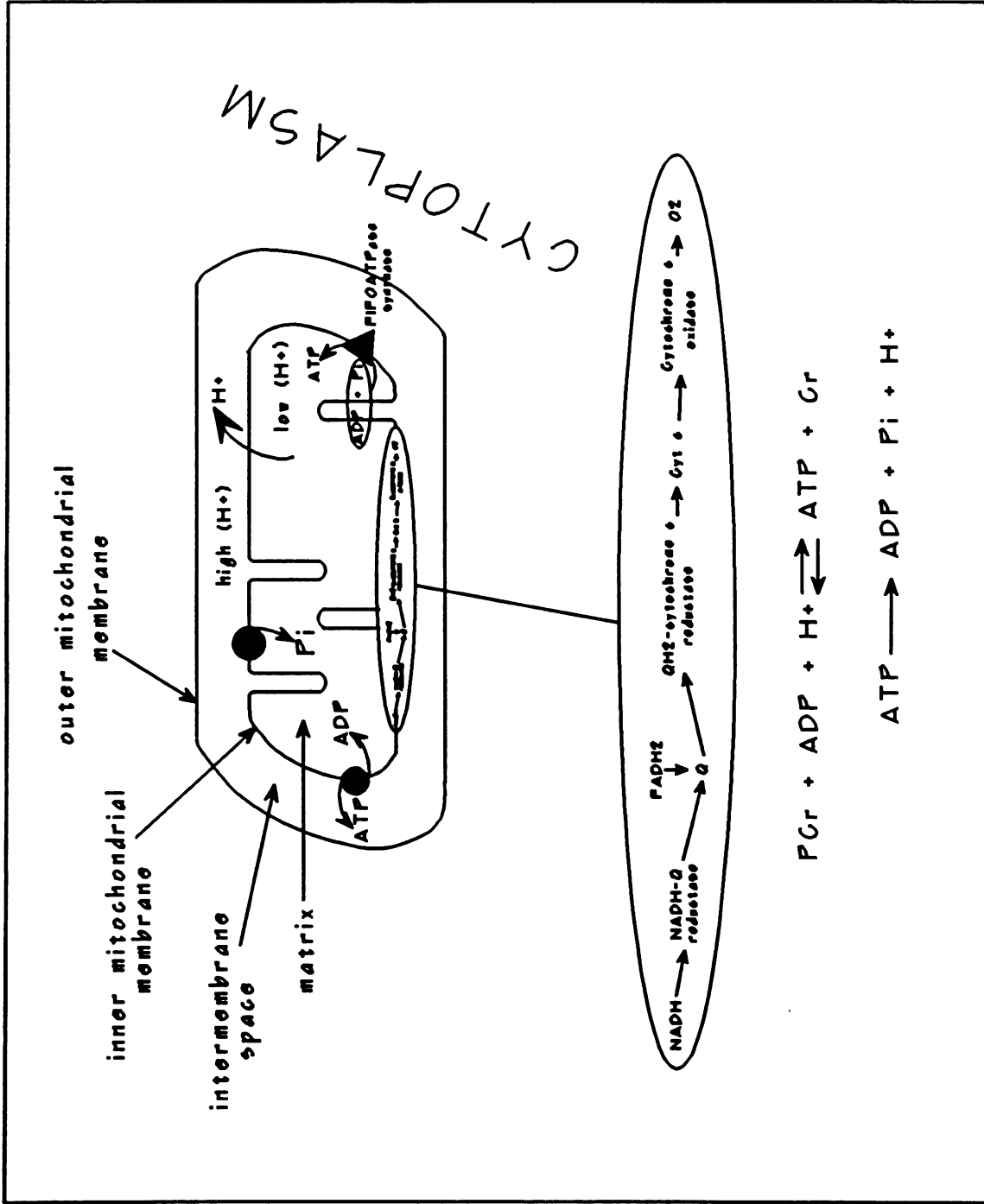
events occur defines the sequence of the chemical redox reactions.

The reactions of oxidative phosphorylation are now well characterized [Figure 2] (Mahler, 1985). The primary respiratory chain substrates are nicotinamide adenine dinucleotide (NADH), and oxygen (O_2). These oxidative reactions are catalyzed by respiratory enzymes of three respiratory complexes that generate an electrochemical gradient of protons across the mitochondrial inner membrane (Senior, 1988). ATP is synthesized from ADP and P_i by F_1F_0 -ATP synthase located within the mitochondrial inner membrane (Mitchell, 1961). Mitchell's "chemiosmotic theory" states that the electrochemical activity difference of hydrogen and hydroxyl ions across the membrane is generated by electron transport, and that the reverse translocation of these ions drives the synthesis of ATP (Mitchell, 1979; Mitchell, 1961). Adenine nucleotide translocase transports ATP and ADP across the mitochondrial inner membrane by an antiport system (Klingenberg, 1980; Klingenberg, 1979).

THEORIES OF CONTROL OF OXIDATIVE PHOSPHORYLATION

In principle, oxidative phosphorylation could be limited by organic substrates (e.g. glucose, lactate), by NADH production, by phosphorylation state (relative concentrations of phosphate metabolites) or by oxygen

Figure 2. Schematic of Oxidative Phosphorylation.



availability (Leigh *et al.*, 1986). This thesis only considers control theories applicable at relatively low respiratory rates, for which organic substrates and oxygen are not limiting in skeletal muscle (Tamura *et al.*, 1989).

In heart muscle, which generally operates at very high respiratory rates, there is some evidence that NADH production may limit respiration (Balaban 1990). From *et al.* (1986), reported a good correlation between NADH/NAD ratio (as measured by surface fluorescence) and respiration rate in intact rat hearts. Katz (1987), suggested that calcium activation of mitochondrial dehydrogenases plays a key role in regulating respiration in the heart. Furthermore, dependence of mitochondrial respiration on the redox ratio was clearly demonstrated in isolated mitochondria (Koretsky and Balaban, 1987; Katz *et al.*, 1988). NAD(P)H fluorescence and oxygen consumption were measured in conditions of various substrate (glutamate, malate, glutamate + malate, pyruvate + malate) concentrations and exogenous ATPase. A linear increase of NAD(P)H was observed associated with a linear increase in oxygen consumption when ADP and Pi were present in excess. When exogenous ATPase was added, oxygen consumption increased proportionately to decreased NAD(P)H. This relationship was linear with all substrates although the slope was substrate dependent. The authors concluded that respiration depends on NAD(P)H levels as well as cytosolic

phosphates, and that pyridine nucleotides may stimulate respiration with increased cellular work in heart muscle.

Despite these results in the heart, most studies conclude that NADH supply does not limit respiration in skeletal muscle. Also, it must be noted that many of the *in vivo* results by Balaban's group in support of NADH control were retracted in a talk by Dr. Balaban at FASEB 1993. Thus, the remaining possibility is that respiration in skeletal muscle is controlled by phosphorylation state, i.e. by the hydrolysis products of ATP, or by some thermodynamic function dependent on these products. There are several specific models which define the relationship between phosphorylation state and respiration. Although there are similarities among them, these models differ in defining the relationships among relative free adenine nucleotide, creatine (Cr) and/or phosphate pools, and oxidative rate. These prominent theories are control by 1) Pi levels, 2) ADP levels, 3) cytosolic phosphorylation potential ($\ln([ATP]/[ADP][Pi][H^+])$), 4) [ATP]/[ADP] ratio, and 5) creatine via the "creatine shuttle".

1. Inorganic Phosphate (Pi)

Johnson (1941) first noted the importance of both Pi and phosphate acceptor as essential reactants of both aerobic and anaerobic breakdown of carbohydrate. In the late forties and early fifties, Lardy and colleagues (1951), demonstrated that availability of either Pi or

phosphate acceptors profoundly effects oxidative rate of several substrates in isolated rat liver mitochondria and also showed that the effects were reversible. Rat liver mitochondria displayed an impressive increase in respiration with availability of phosphate acceptor. Creatine and partially purified creatine kinase provided a phosphate acceptor system that increased respiration 10-fold. In all cases excess phosphate acceptor and enzyme were added. With β -hydroxybutyrate as substrate there was no apparent oxygen consumption until phosphate acceptor systems or dinitrophenol were added (Lardy, 1951; Lardy and Wellmen, 1951).

In summary, Johnson proposed that oxidative rates are limited by rate of hydrolysis of high energy phosphates and their synthesis is coupled to oxidative electron transport. The "P potential" was identified as important in directing "oxidative systems" (Lardy and Wellmen, 1951). They argued that inorganic phosphate is the key factor in respiratory control, although with low sensitivity, since respiration continued at a reduced rate when phosphate was depleted. Because P_i may also be an important factor in control of glycolysis, this scheme was attractive. If P_i regulates both glycolysis and respiration, this would describe a very simple and efficient scheme for metabolic control (Lardy and Wellmen, 1951; Lardy and Maley, 1954; Lardy, 1951; Lynen, 1942; Kingsley-Hickman *et al.*, 1987; Johnson, 1941; Lardy and Wellman, 1953).

2. ADP

Chance and Williams (1956) challenged the idea that phosphate controlled respiration and proposed that ADP was the "physiological substance" responsible for activation of oxidative phosphorylation with stimulation. They developed a rapid assay for oxidative phosphorylation that measured respiration caused by addition of known concentrations of ADP in isolated guinea pig and rat liver mitochondria (Chance and Williams, 1955). In these experiments respiration rate increased rapidly with the addition of exogenous ADP followed by a decrease to a resting state as ADP is exhausted. They estimated that the Michaelis constant for ADP control of mitochondria was 20 - 30 μ m from measurements of deceleration of respiration as a bolus of added ADP was depleted.

Also, in the course of these experiments, they defined the four classic states of respiration. States 2 and 5 were characterized by extremely low rates of oxygen consumption, with state 2 created by lack of organic substrate, and state 5 being created by oxygen deprivation. State 4 is aerobic with excess oxygen and organic substrate, but with no or very low ADP. This is the state which presumably corresponds to the resting state in skeletal muscle. State 3 is the active state with adequate supplies of all substrates. In state 3 a steady-state level of cytochrome c is maintained while ADP varies tremendously.

The respiratory control ratio was defined as the ratio of maximum oxygen consumption in state 3 divided by that in state 4. A wide range of respiratory control ratios were observed, ranging from 6 in ascite tumor cell mitochondria to 65 in guinea pig liver mitochondria. It was concluded that low ratios indicated damaged mitochondria in which electron transport was uncoupled from ATP synthesis, whereas high ratios indicated functionally intact mitochondria (Chance, 1959).

Chance (1959) pointed out that it would be difficult to estimate the respiratory control ratio of mitochondria in intact liver or tumor cells, since this would require experimental control of the total cellular ATPase rate. In contrast, it is easy to vary the work and ATPase rates of skeletal muscle cells by electrical stimulation. Thus, Chance recognized that skeletal muscle is an excellent tissue for studies of respiratory control, and ever since then muscle has been the main focus of his work.

Chance and Connelly (1957) identified ADP as the activator of oxidative phosphorylation in muscle cells following a contraction. They estimated increments of ADP or Pi concentration by measuring oxidation of pyridine nucleotides. Repeated measurements were made on intact muscle and the sensitivity to ADP was less than 0.001 mol/g with a response time of less than 0.1 seconds. They published numerous studies of isolated mitochondria from various sources, including skeletal muscle, all of which

showed similar sensitivity to added ADP, with K_m in the 20 - 50 μM range, which is approximately the ADP level estimated in intact skeletal muscle (Chance, 1959; Chance et al, 1962; Chance, 1965).

Chance and coworkers recognized the possibility that P_i also plays a role in controlling respiration but discounted it on several grounds. First, they reasoned that the level of P_i in resting muscle, as measured by chemical analysis was well above the K_m of mitochondria for P_i (Chance, 1959). Thus, increases in P_i could not account for the large increases in oxygen consumption measured during muscle stimulation. In contrast, they estimated that only 6% of total ADP released with a twitch is required to stimulate respiration half-maximally in muscle (Chance and Williams, 1955). Second, they pointed out that in yeast and ascites tumor cells transition from state 4 to 3 is achieved by addition of glucose is associated with an increase in ADP and no change in P_i (Chance and Maitra, 1963). Finally, in many publications, as mentioned previously, they point out that K_m (20-50 μM) estimated in isolated mitochondria is reasonably close to the levels of ADP in skeletal muscle during moderate exercise.

Since the pioneering work of Chance and coworkers, many other studies of both isolated mitochondria and intact tissues have been interpreted in terms of this simple model of kinetic control of respiration by ADP levels, and this is the only view typically mentioned in standard

biochemistry and physiology texts. Despite the development of the alternative models discussed below, there is little doubt that under some conditions, respiration in isolated mitochondria can be made to behave as predicted by the ADP model. A good illustration of this is the work of Jacobus (1985; 1982) who defended the classical ADP availability model and further contended that neither ATP/ADP ratio nor cytoplasmic phosphorylation potential (see below) correlated with respiration rate. In these experiments, steady-state conditions were established in a solution containing isolated rat liver mitochondria and various amounts of ATP and Pi. Hexokinase, a ADP generating enzyme was added in various amounts to titrate respiratory rates. Only ADP concentrations consistently correlated with respiration rate under all the conditions studied, providing good evidence for ADP regulation of oxidative phosphorylation.

3. Cytoplasmic Phosphorylation Potential

Early on, Klingenberg (1961) argued that respiratory control could not be explained by simply ADP or Pi limitation. He observed respiration to be dependent on [ATP], and reported an ATP-dependent increase in the apparent K_m of oxidative phosphorylation for ADP. He introduced the thermodynamic equilibrium hypothesis, with cytoplasmic phosphorylation potential ($\ln([ATP]/[ADP][Pi])$) (Veech et al., 1979) as the parameter that actually

determines rate of respiration. This theory purports that an approximate thermodynamic equilibrium exists between the pyridine nucleotide pool, the electron transport chain, and high energy phosphate pools.

According to this view, respiratory chain enzymes respond to changes in cytoplasmic phosphorylation potential, generated by various ATPases of the cell. A near equilibrium between the respiratory chain and ATP synthesis would provide an efficient and precise control mechanism for generation of ATP. The best evidence in favor of near equilibrium control of respiration is the observation that the reactions of the respiratory chain are reversible, i.e., that under some conditions ATP hydrolysis by the mitochondrial ATPase can drive reverse flow in the respiratory chain (Lardy and Wellmen, 1951, Klingenberg, 1961).

If equilibrium control models are correct, then the free energy lost by any pair of electrons from reduced pyridine nucleotide (NADH) to cytochrome a_3 should be quantitatively recovered by phosphorylation of 3 ADP molecules. The overall chemical equilibrium reaction is:



and the equilibrium constant of this reaction:

$$K = \frac{[\text{NAD}^+] [\text{a}_3^{+2}]^2 [\text{ATP}]^3}{[\text{NADH}] [\text{a}_3^{+3}]^2 [\text{ADP}]^3 [\text{Pi}]^3} \quad [6]$$

Electron flow generates ATP related to the difference between oxidation-reduction potentials of pyridine nucleotide, $E_h(\text{NAD})$, and cytochrome a_3 , $E_h(\text{a}_3)$. Energy from electrons flowing from NADH to cytochrome a_3 will be equal to three times the free energy of ATP synthesis by the conservation of free energy (Owen and Wilson, 1974). This does not require that phosphorylation potential in the mitochondria and cytoplasm must be identical but only that translocation occurs without significant loss of free energy (Wilson *et al.*, 1974). Thus, thermodynamic theory declares that the free energy's of cytosolic ATP hydrolysis and the oxidation-reduction reaction should be equivalent. Gibb's free energy of ATP hydrolysis is given by:

$$\Delta G = \Delta G^{\circ'} + 2.303RT \log \frac{[\text{ADP}][\text{Pi}][\text{H}^+]}{[\text{ATP}]} \quad [7]$$

($\Delta G^{\circ'} = -30.5 \text{ kJ/mol}$ (Chang, 1981); $R=8.314 \text{ J/K/mol}$.)

Cytosolic phosphorylation potential is derived from this equation and is considered a marker of changes in free energy potential of the adenylate system. The free energy change of oxidation-reduction reactions is given by:

$$\Delta G = -nF\Delta E \quad [8]$$

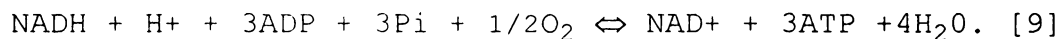
(n =# of electrons transferred per molecule, $F = 96,486.7$ C/mol; ΔE = potential difference between the donor and acceptor redox couples (Chang, 1981)).

Hassinen and Hiltunen (1975) supplied evidence for near-equilibrium between the phosphorylation state of adenine nucleotides and redox state of respiratory carriers using surface fluorometry and spectrophotometry in beating and arrested rat hearts. KCl induced cardiac arrest caused a reduction of fluorescent flavoproteins and nicotinamide nucleotides, oxidation of cytochromes a and c, inhibition of respiration, and increased cytoplasmic phosphorylation potential. The difference between the beating and arrested heart of ΔE of ATP hydrolysis was 21.2 mV comparing favorably with a 23 mV change in ΔE of NAD/NADH and the cytochrome chain. These results demonstrated that cytochromes c and a are in near equilibrium with the state of cytoplasmic adenylates, thus supporting the equilibrium hypothesis of mitochondrial respiratory control in intact myocardial tissue.

The most widely cited studies in favor of a form of near-equilibrium control are those of Wilson and colleagues (Wilson *et al.*, 1974; Erecinska *et al.*, 1974; Holian *et al.*, 1977; Owen and Wilson, 1974; Erecinska *et al.*, 1977). In brief, their conclusions rest on the following series of observations. First, in isolated mitochondria, they found an excellent agreement between the calculated

intramitochondrial free energy potentials of NAD redox reactions and the extramitochondrial free energy of ATP hydrolysis. Second, they found the same agreement in calculated potentials derived from metabolite measurements in intact liver cells. Third, in experiments similar in design to those reported by Jacobus and colleagues (Jacobus and Lehninger, 1973; Jacobus et al., 1982; Jacobus, 1985), they found that only phosphorylation potential consistently correlated with respiration rate. The reason for the discrepancy in results between the studies of Wilson and colleagues and those of Jacobus are difficult to explain, since the experimental designs were quite similar.

Van Der Meer (1978) applied the principles of non-equilibrium thermodynamics to the study of respiratory control. Although formally different than the above equilibrium theories, in general outline the conclusion is similar, that the rate of oxidative phosphorylation ought to depend on the free energy difference between mitochondrial metabolites and cytoplasmic phosphates (Van Der Meer et al., 1980; Van Dam et al., 1980). In these studies, cytosolic phosphorylation potential was measured and NADH/NAD was calculated from lactate/pyruvate and 3- β hydroxybutyrate/acetoacetate ratios in perfused isolated liver cells in steady-state conditions (Van Der Meer et al., 1978). The respiratory chain was considered a "black box" catalyzing the overall reaction :



An affinity term was defined dependent on NADH/NAD , $[\text{ADP}][\text{P}_i]/[\text{ATP}]$, and O_2 . Steady oxygen consumption was found to be linearly dependent on this affinity term and they concluded oxygen consumption is regulated by cytosolic phosphorylation potential, mitochondrial redox potential and partial pressure of oxygen.

A basic prediction of all these thermodynamic models of the control of respiration is that the forward and reverse flux through the mitochondrial ATPase ought to be nearly equal, and both fluxes should be greater than any net flux. This prediction was examined in isolated mitochondria by LaNoue and coworkers (1985). Unidirectional rates were measured by radioactive tracer methods over a range of respiratory rates. At rates near State 4, the fluxes were nearly equal and larger than the net flux. However, as respiration rate was increased toward maximum (State 3), the reverse flux ($\text{ATP} \rightarrow \text{ADP} + \text{P}_i$) decreased. At maximum state 3 rate, the forward flux ($\text{P}_i + \text{ADP} \rightarrow \text{ATP}$) was nearly equal to the net flux. Similar results were obtained by Ugurbil and colleagues in working rat hearts using NMR spin-transfer methods. Based on these studies, it appears that near equilibrium theories of control may apply at relatively low respiratory rates, but not at near maximum rates, when kinetic limitations become dominant.

4. [ATP]/[ADP]

Slater also supported the thermodynamic hypothesis (Bienfait *et al.*, 1975) but later suggested that [ATP]/[ADP] ratio, independent of Pi was the controlling parameter (Slater *et al.*, 1973). This theory is based on the idea that the adenine translocator, which transports ATP and ADP across the mitochondrial membrane, (Klingenberg, 1980; Vignais, 1976), limits respiration (Vignais, 1976; Letko *et al.*, 1980; Kunz *et al.*, 1981; Kuster *et al.*, 1976). In contrast to the thermodynamic theories, this assumes that the translocator is displaced far from equilibrium, although within the mitochondria, the nucleotides may or may not be near equilibrium with the respiratory chain (Kuster *et al.*, 1981; Erecinska and Wilson, 1982; Kunz *et al.*, 1981).

Holian and Wilson (1977) argued against the translocase theory by showing that [Pi] altered respiration rate in isolated mitochondria when the [ATP]/[ADP] remained constant. Oxidative phosphorylation increased by 230 percent with constant [ATP]/[ADP] and a four-fold increase in [Pi], and increases up to 4000 percent were observed with maximum Pi stimulation. Moreover, they studied mitochondria with different respiratory control ratios (RCR). As the RCR decreased the dependence on Pi decreased. Thus they proposed that during isolation of mitochondria translocase could become damaged and only then be rate limiting. Other evidence not supporting the



translocase theory was that the adenylate translocator was observed to be near equilibrium (Kauppinen, 1983).

While there are other studies supporting the nucleotide translocase as the key site of respiratory control (Kunz, 1981, Kuster et al, 1976) it should be noted that in intact skeletal muscle, total cytoplasmic ATP does not significantly change except during the most extreme stimulation regiments. Hence, for our purposes, the ATP/ADP theory essentially reduces to the simple kinetic theory with cytoplasmic ADP as the regulatory parameter, and therefore will not be considered further.

5. Creatine

The creatine shuttle model can also be considered as a variant of the ADP theory (Bessman and Geiger, 1981). Bessman (1966) first introduced this theory based on identification of a specific creatine kinase isozyme located on the inner mitochondrial membrane, clearly distinct from the cytosolic enzyme. Bessman and others conducted an extensive series of tracer studies which showed that creatine can act as a phosphate acceptor in isolated cardiac muscle mitochondria (Jacobus and Lehninger, 1973) and is coupled to oxidative phosphorylation (Saks et al., 1985). They argued that ADP is not freely diffusible in muscle cells, and that the availability of ADP at the mitochondrial inner membrane,

and therefore the rate of respiration, is limited by the diffusion of creatine to the mitochondria.

Mahler (1985) developed a mathematical model of respiratory control based on the creatine shuttle. This model satisfactorily explained the observation that both PCr and oxygen consumption change over a mono-exponential time course after a step change in work rate. Based on the assumption that respiration rate is linearly proportional to mean cytoplasmic creatine levels, Mahler derived the following equation relating changes in oxygen consumption to changes in either creatine or PCr:

$$\Delta Q_{O_2}(t) = -1/\tau\rho \Delta[PCr](t) = 1/\tau\rho \Delta[\text{creatine}](t). \quad [10]$$

[PCr] and [creatine] are total content per unit weight, $\Delta Q_{O_2}(t)$, $\Delta[PCr](t)$, $\Delta[\text{creatine}](t)$ are changes in their respective values from basal levels, τ is the time constant of ΔQ_{O_2} , and ρ is the P/O₂ ratio for oxidative metabolism, expected to be 6 mol/mol (Lemasters, 1984, Crow and Kushmerick, 1982, Chance and Williams, 1955).

The creatine shuttle model has been criticized by several researchers. Meyer (1984) demonstrated that this model is really a special case of the more general phenomenon of facilitated diffusion. Model calculations showed that, although much of the intracellular transport of high energy phosphate in normal muscle must be carried by PCr and creatine, this is simply a consequence of the



fact that ATP hydrolysis and synthesis occur at different places in the cell. Once equilibrium of creatine kinase is acknowledged, this transport effect cannot be offered as evidence that creatine is mechanistically more important than ADP itself.

In addition, several studies have shown that ATP and ADP can diffuse freely between myofibrils and mitochondria without the assistance of the creatine kinase reaction (Yoshizaki et al., 1987; Yoshizaki et al., 1990). Further studies demonstrated that muscle depleted of creatine and PCr by chronic feeding of creatine analogs are capable of normal, or even better than normal, aerobic metabolism (Shoubridge and Radda, 1987; Meyer, 1989).

Taken together these studies demonstrate that creatine is not required for the control of respiration in muscle. Finally, as shown below, the result of Mahler's mathematical analysis can be reproduced beginning with a completely different mechanistic assumption, assuming that cytoplasmic ATP free energy controls respiration (Meyer, 1985).

APPLICATION OF PHOSPHORUS NUCLEAR MAGNETIC RESONANCE STUDIES TO MUSCLE METABOLISM

Hoult (1974) and coworkers published phosphorous Nuclear Magnetic Resonance (^{31}P -NMR) spectra of intact biological tissues, opening the door for study of muscle



metabolism by this uniquely non-invasive technique. They identified peaks corresponding to Pi, ATP, PCr and sugar phosphates in intact rat hindlimb muscle. This was an important discovery for subsequent investigations of skeletal muscle metabolism, because now free levels of high energy phosphates could be measured repeatedly in intact tissue during rest, stimulation, and recovery without disruption of the tissue (Dawson et al., 1980; Taylor et al., 1986; Meyer et al., 1982; Ingwall, 1982)

Among the first results of ^{31}P -NMR studies in skeletal muscle was the recognition that resting metabolite levels in muscle were somewhat different than those measured chemically after tissue extraction (Meyer et al., 1985). Early chemical analysis had given variable results for skeletal muscle PCr, and especially Pi concentrations. The most careful investigators detected lower levels of Pi (Seraydarian et al., 1961), but it wasn't until ^{31}P -NMR spectroscopic results became available that the relatively lower level of Pi (2-3 mM versus 8-10 mM) was generally accepted. The difference between chemical and NMR measurements could be attributed to artifactual hydrolysis of PCr during the extraction procedure in some cases (Meyer et al. 1985) However the possibility that a significant fraction of total Pi in muscle is bound to intracellular proteins, and therefore not visible in high resolution spectra, has not been ruled out. In either case, it is now clear that free, metabolically active Pi in intact muscle,

especially fast-twitch muscle, is less than measured chemically (Meyer *et al.*, 1985; Meyer *et al.*, 1982; Kushmerick and Meyer, 1985).

^{31}P -NMR can investigate the intracellular environment and allow calculation of energetic parameters such as [ADP] or cytoplasmic phosphorylation potential (Meyer *et al.*, 1982). Relative areas are measured and compared to ATP metabolite levels, which remain relatively stable during chemical analysis. Transient metabolic events can be followed using ^{31}P -NMR at rest, and during stimulation and recovery in skeletal muscle. Intracellular creatine kinase enzymes were confirmed to be in chemical equilibrium, in intact muscle, by using NMR spin transfer techniques (Gadian *et al.*, 1981).

A novel feature of ^{31}P -NMR measurements is that they allow non-invasive estimates of intracellular hydrogen ion concentration. Intracellular pH was first measured by ^{31}P -NMR in erythrocytes (Moon and Richards, 1973) and subsequently NMR became an important non-invasive tool to monitor pH changes in cell suspensions (Gillies *et al.*, 1981) and intact tissues (Meyer *et al.*, 1982; Balaban, 1984; Dawson *et al.*, 1980). pH measurement depends on the fact that the resonant frequency (chemical shift) of P_i is sensitive to pH changes within the biological range of pH 6.2-7.4. On the other hand, PCr is insensitive to hydrogen ion changes in this range since its pK_a is 4.5. Thus PCr provides a stable chemical shift reference for muscle

studies. Titration curves are established for phosphate chemical shifts in solutions identical in ionic strength, temperature and metabolite concentration, to the intracellular milieu of skeletal muscle. Although the accuracy of the method depends on independent estimates of such factors, intracellular pH can be measured in intact striated muscle with a very high degree of precision by NMR. Of course, the pH measured depends on the intracellular localization of the phosphate observed. There is good evidence that this is predominantly from the cytoplasmic compartment in muscle tissue (Bailey *et al.*, 1981). Intracellular free magnesium concentration can also be determined by observing the chemical shifts of ATP peaks (Hoult *et al.*, 1974; Gupta and Moore, 1980).

Over the last decade there have been many ^{31}P -NMR studies of skeletal and heart muscle (Meyer *et al.*, 1982; Arnold *et al.*, 1984; Ingwall, 1982; Balaban, 1984; Katz *et al.*, 1987; Argov *et al.*, 1986; Dawson *et al.*, 1977; Jacobus *et al.*, 1977; Sapega *et al.*, 1987; Taylor *et al.*, 1986). Many studies have been performed in humans, and some clinical applications appear promising. Our main interest is in those studies which examine various theories of the control of respiration. Thus, the following sections briefly summarize the major recent ^{31}P -NMR results in support of various theories of respiratory control.

³¹P-NMR Studies Supporting Regulation By Redox Potential

Perhaps the most surprising of the recent NMR results is the observation that changes in respiration rate can occur with no significant change in PCr or pH, and hence no significant change in ADP, Pi or phosphorylation potential. For example, phosphate metabolites were measured over a range of workloads with perfusion solutions containing several different substrates in intact myocardium (From et al., 1986). In glucose perfused hearts, there was no correlation between any of the phosphate metabolites and oxygen consumption. These researchers concluded that neither ADP levels, ATP/ADP ratio or cytoplasmic phosphorylation potential regulate oxidative phosphorylation in the heart, and that carbon substrate delivery may regulate respiration in cardiac tissue.

Similarly, studies by Balaban and coworkers found no change in PCr in dog hearts *in situ* after workload was increased by atrial pacing (Hassinen, 1986; Koretsky and Balaban, 1987; Katz et al., 1987; Balaban, 1990; Heineman and Balaban, 1990; Katz et al., 1988). These results suggest that NADH supply, or some other factor controls respiration in heart muscle. Until very recently, Balaban argued on the basis of fluorescence measurements that NADH/NAD ratio changed in tandem with oxygen consumption under conditions in which PCr was constant. However, these fluorescence measurements were recently found to be faulty, and it now appears that NADH is also constant in hearts

which are not flow-limited. It should be noted that the observation that PCr does not change with change in workload in the heart is not universally accepted (Hak, et al. 1993).

Fortunately for the aims of this thesis, changes in workload are always accompanied by changes in PCr in skeletal muscle. However, there is some evidence that NADH or other factors may play a role in respiratory control in slow-twitch muscle. In a recent study (Kushmerick et al., 1992), respiration appeared to become less dependent on steady-state PCr at higher ATPase rates in isolated perfused slow-twitch, but not fast-twitch muscles. There was also a transient overshoot in PCr and undershoot of Pi after step changes in work rates in the slow-twitch muscle (Kushmerick et al., 1992). This suggests that highly aerobic slow-twitch muscles may function like heart muscle at high respiratory rates, in that phosphorylation state may not be the only metabolic factor for the control of oxidative phosphorylation. The first experimental results described in this thesis will re-examine this issue.

³¹P-NMR Studies Supporting ADP Control

The most popular kinetic model of respiration states that oxidative phosphorylation is limited by ADP availability, and that there should be a simple, Michaelis-Menton dependence of respiratory rate on cytoplasmic [ADP] (Chance and Williams, 1956; Chance et al., 1986; Jacobus et

al., 1982; Leigh *et al.*, 1986; Yoshizaki *et al.*, 1990). For our purposes, creatine shuttle and ATP/ADP ratio hypothesis can be viewed as a variation of this simple kinetic model. Chance outlined a rationale to test this model using ^{31}P -NMR spectroscopy (Chance *et al.*, 1985).

First, Chance defined a transfer function for metabolic control of oxidative phosphorylation by [ADP] as:

$$\frac{V}{V_{\max}} = \frac{1}{1 + K_m/[ADP]} \quad [11]$$

Levels of ADP in muscle cannot be determined by either chemical methods or by ^{31}P -NMR because it is significantly bound to proteins and is in the micromolar range. However, [ADP] can be calculated using the equilibrium of the creatine kinase reaction [Equation 2] using measurements of high energy phosphates and intracellular pH obtained by NMR. (Lawson and Veech, 1979).

$$[ADP] = \frac{[ATP][Cr]}{K_{ck}[PCr][H^+]} \quad [12]$$

Substitution provides

$$\frac{V}{V_{\max}} = \frac{1}{1 + K_m / ([Cr] / [PCr]) ([ATP] / K_{ck} [H^+])} \quad [13]$$

Assuming temperature of 37°C, 1 mM magnesium concentration, pH = 7.1, 5 mM ATP concentration, $K_{ck} = 1.3 \times 10^{-9}$ (Lawson and Veech, 1979), and $K_m = 2 \times 10^{-5}$ M (Chance and Williams, 1956):

$$\frac{V}{V_{\max}} = \frac{1}{1 + (0.52 / ([Cr] / [PCr]))} \quad [14]$$

^{31}P -NMR can detect levels of Pi but not Cr. However, levels of Cr and Pi are approximately equal in resting muscle and during mild exercise (Kushmerick and Meyer, 1985; Meyer *et al.*, 1985; Meyer and Adams, 1990). By simple substitution:

$$\frac{V}{V_{\max}} = \frac{1}{1 + 0.52 / ([Pi] / [PCr])} \quad [15]$$

Thus, the transfer function between work, V/V_{\max} , and the biochemical response, Pi/PCr , is expected to approximate a rectangular hyperbola with "Km" 0.5 to 1 (Chance *et al.*,

1986; Leigh et al., 1986). Many published studies of both animal and human muscle appear to support this analysis (Chance et al., 1986; Nioka et al., 1992; Chance et al., 1981; Chance et al., 1992; Yoshizaki et al., 1987).

Chance and coworkers also used ^{31}P -NMR to re-investigate respiration in isolated mitochondria in order to bridge the gap between previous invasive studies and their more recent studies of intact cells (Gyulai et al., 1985). Substrates and oxygen were added to the suspensions to maintain steady-state respiration and examine phosphates between respiration states 4 and 3. They compared relationships of Pi/PCr ratio, cytoplasmic phosphorylation potential, and free energy of hydrolysis of ATP. Linear relationships were observed with all parameters dependent on ATPase rate. Nonetheless, the authors attributed oxidative control to ADP availability alone, and concluded that the same interpretation could be applied to all of their *in vivo* studies (Arnold et al., 1984; Partain et al., 1984; Chance et al., 1992; Chance et al., 1981; Leigh et al., 1986).

^{31}P -NMR Studies Supporting Thermodynamic Models

Meyer and coworkers published a series of ^{31}P -NMR studies which, in aggregate, seem to support thermodynamic theories of respiratory control (Meyer, 1989; Foley et al., 1991). Interpretation of these studies relies on a circuit analog model of the relation between changes in PCr and

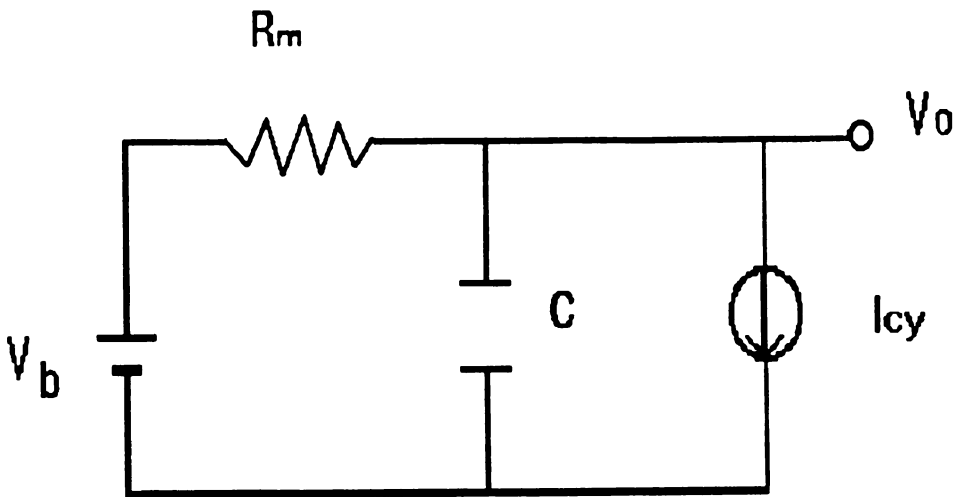
respiration in muscle which is described below (Meyer 1988).

Hill (1940a) was the first to report a simple exponential time course for oxygen consumption during recovery after a single tetanus. Mahler, using a different method of measurement also found oxygen consumption to follow this same pattern (Mahler, 1985). Mahler was surprised to observe this simple response, since it suggested oxidative phosphorylation is limited by a single step that follows an apparent first-order rate law, despite the fact that the scheme of reactions involved are complex. Thus, Mahler derived the model mentioned above by assuming that respiration depends directly on cytoplasmic creatine. Meyer's model is based on an entirely different mechanism, namely thermodynamic control. However, the mathematical result is very similar to Mahler's.

The linear model of the control of respiration (Meyer, 1988) was derived from the principles of non-equilibrium thermodynamics with a direct correlation of respiration rate and phosphorylation potential. The model is depicted by an electrical analog circuit that represents flux through mitochondrial and cytoplasmic ATPases as currents, and the chemical potential energy as voltages [Figure 3]. The creatine kinase reaction is represented by a capacitor, with capacitance proportional to total creatine level, and charge proportional to PCr. A key feature of the model is the demonstration that the phosphorylation of cytoplasmic

Figure 3. Linear Circuit Model.

LINEAR MODEL



I_{cy} ($\text{mol} \cdot \text{g}^{-1} \cdot \text{min}^{-1}$) - cytosolic ATPase rate

V_o ($\text{J} \cdot \text{mol}^{-1}$) - cytosolic free energy of ATP hydrolysis

V_b ($\text{J} \cdot \text{mol}^{-1}$) - mitochondrial free energy of ATP hydrolysis

R_m (J g min mol^{-2}) - a function of the number and properties
of the mitochondria in the cell

I_{rm} ($\text{mol ATP} \cdot \text{g}^{-1} \cdot \text{min} \cdot \text{mol}^{-2}$) - rate of oxidative
phosphorylation

creatine (PCr level or capacitor charge) is directly proportional to cytoplasmic free energy of ATP hydrolysis (V_0) over the observed biological range.

$$(d[\text{PCr}]/dV_0=C) \quad \text{or} \quad (V_0 - K) = 1/C [\text{PCr}] \quad [16]$$

According to this model, step increases in cytoplasmic ATPase rate (I_{cy}) result in decreased cytoplasmic free energy of ATP hydrolysis. This decrease is initially buffered by an exponential decrease in PCr (discharge of the capacitor). The rate of oxidative phosphorylation (I_{rm}) approaches a steady state along the same time course, and assuming that the intramitochondrial potential term (V_b) is constant, this rate is directly proportional to cytoplasmic free energy. Thus, the model incorporates the key element of near-equilibrium thermodynamic models. Mathematical analysis of the circuit model yields a simple linear relationship between steady-state PCr and oxidative rate:

$$QO_2 = -1/(\rho\tau) [\text{PCr}] + (V_b - K)/R_m \rho \quad [17]$$

where, $\rho = P/O_2$ ratio and $\tau = \text{PCr}$ time constant. Thus, the slope of the relation between steady-state oxygen consumption and PCr is

$$dQO_2/d[\text{PCr}] = -1/(\rho\tau). \quad [18]$$

which is identical to Mahler's result. Like Mahler's model, this result provides a method to estimate the P/O₂ ratio in muscle, and therefore, to that extent both models are confirmed by his results. However, unlike Mahler's model, the circuit model also yields a simple physiological interpretation for the time constant of PCr changes. The time constant of the circuit is

$$\tau = R_m \cdot C. \quad [19]$$

C is a simple function of the total creatine content ($C = T_{Cr}/6RT$), and R_m is the measure of the muscle mitochondrial content, such that the maximum respiratory rate is proportional to $1/R_m$. Therefore if total creatine is constant, the time constant of PCr changes should be inversely proportional to muscle mitochondrial content.

In summary, this model predicts that steady-state oxygen consumption should be a linear function of steady-state PCr level for moderate stimulation rates assuming no change in mitochondrial redox potential. The time constant for PCr changes should be independent of stimulation rate and similar at onset of stimulation and during recovery since it depends only on mitochondrial properties and total creatine level. The time constants should be relatively shorter for muscles with increased mitochondria or less total creatine and therefore the slope of the relationship

between oxygen consumption and PCr level should be proportionally increased.

Several predictions of this model were confirmed in rat fast-twitch muscle. First, as predicted by the model (Meyer, 1987), the time constant for PCr changes at onset of stimulation and during recovery were the same, and were independent of stimulation. Second, in muscles depleted of total creatine by feeding the slowly phosphorylated creatine analog, β -guanidinopropionate, the time constant for PCr changes was found to be directly proportional to total creatine content (Meyer, 1989). Third, in a recent study of muscles with increased mitochondrial content induced by exercise training, the time constant for PCr changes was found to be inversely proportional to mitochondrial content (Paganini et al., 1993).

The creatine analog experiments (Meyer, 1982) also coincidentally demonstrated a dependence of recovery metabolism on Pi levels. There was some hydrolysis of the phosphorylated analog during stimulation, which is only slowly rephosphorylated during recovery. Thus, during recovery after stimulation, Pi levels are higher than at rest before stimulation. This extra Pi was associated with increased PCr during recovery after stimulation compared to before. The effect could be mimicked by a computer simulation which assumed respiratory control by phosphorylation potential, by not by models assuming ADP control.

Analogous results were found in rat gastrocnemius muscle acutely depleted of total adenine nucleotide content by intense stimulation and hadacidin administration (blocks resynthesis of adenine nucleotides) (Foley et al., 1991). This procedure also results in extra Pi availability during recovery after stimulation. Calculated ADP in the nucleotide-depleted muscles after recovery was about half that in control muscles, while phosphorylation potential was the same in both groups. Furthermore, during a subsequent mild stimulation, ADP in the nucleotide depleted muscles was similar to that in control muscles at rest. Although oxygen consumption was not measured in this study, it must have been at least 2-3 fold higher during the stimulation, since force was maintained without fatigue, and there was no evidence of lactic acid accumulation. Thus, the results are difficult to reconcile with ADP control models.

Results in slow-twitch skeletal muscle were not so clear. Mitochondrial control by phosphorylation state was not sufficient to explain results in isolated perfused slow-twitch muscles studied by ^{31}P -NMR (Kushmerick et al., 1992). The kinetics of PCr recovery were not first order indicating that neither simple ADP availability nor cytosolic phosphorylation potential could explain respiration in slow-twitch muscle in these experiments.

THE PHOSPHORYLATION STATE CONTROVERSY

Although there is now general agreement that phosphorylation state is important in control of respiration, at least in skeletal muscle under conditions when oxygen and organic substrates are not limiting, the controversy over the specific mechanism rages on. Some papers argue for ADP control, while others (sometimes by the same authors) argue for control by phosphorylation potential. This continuing controversy suggests that these models may not be clearly distinguishable by the simple experiments which have been done. For example, Mahler's analysis of the kinetic theory of control by creatine produced many of the same predictions (i.e. relationships of phosphates and oxygen consumption) as Meyer's analysis based on thermodynamic control models.

Connett (1988a) eloquently analyzed this problem, by quantitatively evaluating the predictions of both models under various conditions. In his calculations, all metabolite levels were normalized to total creatine level since the $[\text{free adenine nucleotide}]/[\text{total creatine}]$ and $[\text{total phosphate}]/[\text{total creatine}]$ are essentially constant over the >20-fold concentration range among tissues. Thus, the results are applicable for many muscle types, ranging from smooth to fast-twitch muscle. He concluded that the ADP and cytosolic phosphorylation potential models can not be distinguished by simple correlative experiments in which steady-state metabolite levels are compared to steady-state

oxygen consumption. These parameters are highly correlated because ADP and phosphorylation potential are both ultimately derived from measurement of PCr. Connett went on to show that discrimination between these models may occur by changing one system variable (pH, total adenine content, % phosphorylation of creatine) independent of changes in stimulation rate in intact tissue. In particular, he showed that the ADP model might be tested by independently altering intracellular pH. This suggestion formed the rationale for the third experiment described in this thesis (Connett, 1988b; Funk *et al.*, 1990; Connett and Honig, 1989; Connett *et al.*, 1990).

SUMMARY

The putative controllers of oxidative phosphorylation within the aerobic capacity of striated muscle are redox potential and phosphorylation state. Evidence in cardiac tissue suggests that redox potential may play an important role. In skeletal muscles most evidence suggests phosphorylation state as the dominant controller. However, despite 40 years of research, the exact mechanism of phosphorylation state control in intact muscle is still not clear.

Chance and Williams introduced the hypothesis based on enzyme kinetics that solely [ADP] concentration was the controlling factor. Models of control by ATP/ADP, or by

creatine, are mechanistically similar, and lead to similar experimental predictions.

Klingenberg first introduced the idea of thermodynamic control, suggesting cytosolic phosphorylation potential ($[ATP]/[ADP][Pi]$) is the critical regulatory signal. Wilson supported this theory and then later expanded the model to include redox potential and oxygen availability. Meyer eventually reduced the thermodynamic model to a circuit analog, which predicts the metabolic behavior of muscle during stimulation at submaximal rates, when organic substrates and oxygen are not limiting.

Thus, the two prominent proposed signaling mechanisms are $[ADP]$ and cytosolic phosphorylation potential. It is possible to test these models by defining steady-state relationships between oxygen consumption and these metabolites while independently varying pH (Connett, 1988a; Connett and Honig, 1989). The primary objective of this dissertation is to test these two competing models for control of respiration by phosphorylation state.

As noted above, there is some evidence that phosphorylation state is not the sole controller of respiration in slow-twitch muscle at higher respiration rates. Therefore the initial focus of this research was to re-investigate this phenomenon in intact slow-twitch muscle. These experiments are discussed in Chapter 3. Chapter 4 describes a study which examines the effect of altered pH on the energy cost of contractions. This was a

prerequisite to design of the final study. Chapter 5 is devoted to testing the two prominent models of the control of respiration following Connett's insight that varying intracellular pH independently of changes in other metabolites may distinguish between these two models.

RESEARCH OBJECTIVES

The objectives of this thesis are to: 1) examine whether steady-state oxidative rate is less dependent on steady-state PCr levels as ATPase rate increases, in slow-twitch muscle *in situ*, as observed in isolated perfused preparations, 2) examine the effects of acidosis on ATP cost of isometric contractions in skeletal muscle, and 3) examine the effects of acidosis on respiratory control during submaximal ATPase rates in slow-twitch muscle.

CHAPTER 2

GENERAL MATERIALS AND METHODS

PHOSPHORUS NUCLEAR MAGNETIC SPECTROSCOPY (³¹P-NMR)

General Principles

There are numerous texts and reviews which describe the physics of NMR spectroscopy, including a few which specifically discuss NMR physics in the context of muscle studies (Meyer et al. 1982; Sepega et al. 1987). The following are a few essential concepts needed for understanding this thesis.

Nuclei with a spin quantum number equal to 1/2, e.g., hydrogen (¹H), fluorine (¹⁹F), and phosphorus (³¹P), acquire a net magnetization when placed in a magnetic field. This net magnetization is initially aligned parallel to the applied field, but its orientation can be changed by applying a pulse of radiofrequency (rf) energy at the appropriate frequency. This frequency (ν) depends directly on the field strength (B), and on a characteristic specific to the nuclei, the gyromagnetic ratio (γ):

$$\nu = \gamma B / 2\pi. \quad [20]$$

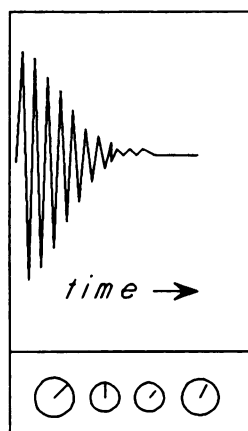
Following the rf pulse, the net magnetization will precess about the main field axis at a specific resonance frequency, and this precession generates a signal that can be detected by a receiver coil tuned to that frequency. The acquired electrical signal, or free induction decay (FID), contains information on both the amplitude and relative resonance frequencies of the nuclei in the sample. The NMR spectrum, is a plot of amplitude versus frequency, which is obtained by computing the Fast-Fourier transform of the rf-demodulated, digitized FID [Figure 4].

Each NMR sensitive nucleus is excited by and resonates at a different frequency dependent on its molecular environment and the magnetic field strength. Thus, metabolites containing these nuclei can be differentiated in a NMR spectrum since the nuclei resonate at different frequencies. For example, phosphorus nuclei of Pi, PCr and the three phosphates of ATP resonate at different frequencies because each phosphate has different chemical bonds, and therefore is in a different magnetic environment [Figure 5]. Since these frequencies also depend on magnetic field strength, a unit of parts per million (ppm) is used to standardize frequencies, also termed chemical shifts, from different strength magnets.

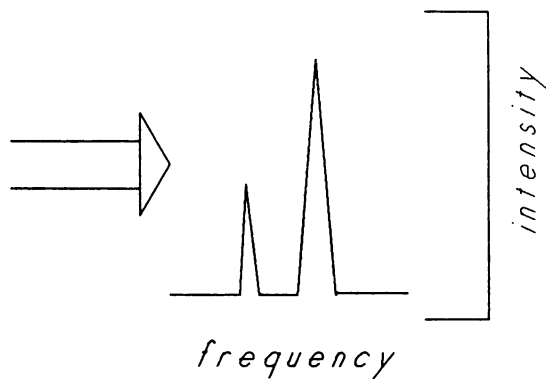
The area of a specific peak in an NMR spectrum is directly proportional to the number of nuclei under ideal conditions. However, nuclei must receive a maximal pulse, (90° pulse width) at the frequency specific to the

Figure 4. Representation of the Free Induction Decay (FID) and NMR spectrum. The NMR spectrum is the plot of signal intensity versus frequency and is obtained by computing the Fourier transform of the digitized FID.

Fourier Transformation

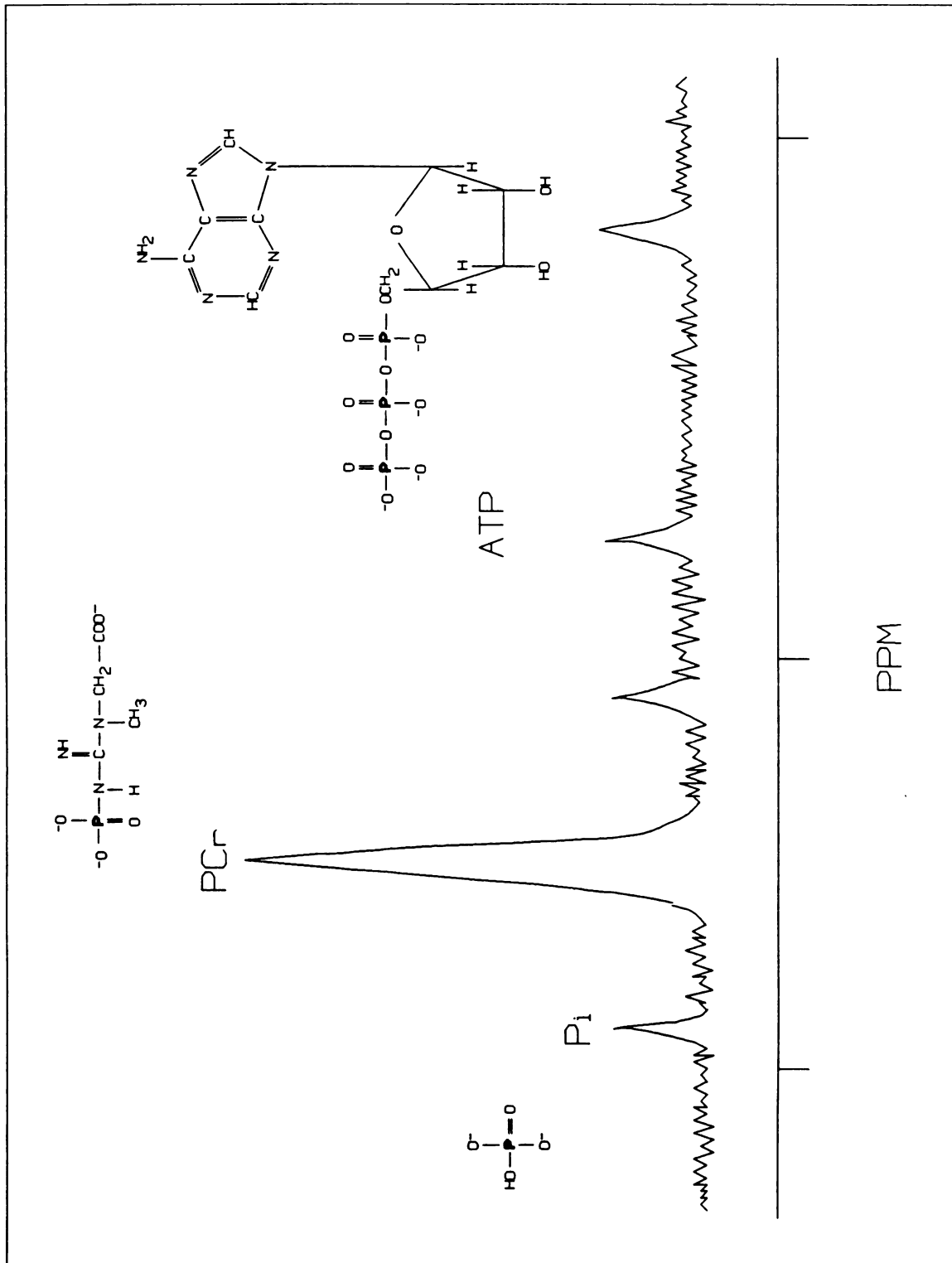


FID



Spectrum

Figure 5. Chemical structure of PCr, ATP and Pi and the phosphorus NMR spectrum containing the corresponding peak that represents each phosphate signal.



nucleus, and be allowed to relax completely back to the original orientation to detect a maximum signal on the next pulse. This relaxation (characterized by a time constant, T_1) typically takes 10-15 s for phosphorus nuclei in biological tissues. If a submaximal pulse is given ($<90^\circ$) or only partial relaxation of the nuclei occur, only a fraction of the signal is observed and saturation of the signal occurs. Molecular interactions affect relaxation times and therefore nuclei of different molecules relax at different rates. This may cause variable signal saturation unless the delay between scans is long enough to allow all nuclei to fully relax.

Unfortunately, multiple FID's or "scans" typically must be acquired and averaged together to achieve a reasonable signal to noise ratio because the sensitivity of NMR is relatively low. The signal to noise ratio increases with the square root of the number of acquired scans. For example, to acquire 16 scans with 15 s between scans (to allow full relaxation) would take 4 minutes. However, if repeated scans are applied too closely together, only partial relaxation will occur between scans and the peaks become partially saturated. This is one of the major technical problems in quantitative *in vivo* NMR studies.

Some of our experiments required less than one minute time resolution, therefore we used a method developed to reduce the saturation effects, yet also improve time

resolution. The NMR signal can be maximized even with a reduction in time between scans (termed relaxation delay) by giving a shorter pulse width ($\sim 60^\circ$). Some saturation still occurs, therefore, we optimized our parameters to obtain the best S/N ratio for primary signal of interest, the PCr peak. When quantitative comparisons between different peak areas were required, we corrected for saturation effects by comparing peak areas in fully-relaxed (15 s pulse interval) and saturated (1 - 3 s interval) spectra of resting muscle.

NMR Probes For Muscle Studies

An NMR study of muscle requires a strong homogenous magnetic field, a radio-frequency transmitter and receiver, and apparatus to measure physiological parameters such as temperature and muscle force. The experiment must be done in the magnet, and therefore, commercial apparatus that contains magnetic materials cannot be used because they would destroy the homogeneity of the magnetic field. Furthermore, any wires to or from recorders or stimulators must be filtered to prevent other rf signals (TV or radio stations) from entering the magnet. Standard chemistry NMR "probes" supplied with NMR equipment do not contain enough space for this extra apparatus. Finally, because the experiments require the best possible S/N ratio, it is worthwhile to construct rf coils specifically tailored to

match the muscle's size and geometry. For these reasons, the experiments in this thesis required construction of NMR probes specifically designed for these studies, which are described below.

In situ cat experiments. A Plexiglas®/Lexan® probe was designed and built for these experiments [Figure 6]. One half of a Plexiglas® tube was used as a cradle to hold the animal. A hollow base along the entire length of the cradle provided a protected area to run the cables for the stimulating wires, force transducer and temperature probe. A 2 cm helmholtz coil was built from 16 gauge copper wire and the rf circuitry [Figure 7] was contained in an aluminum box placed within a holder attached to the sides of the cradle. The circuit could be tuned with the probe inside the magnet. An adjustable knee mount held the joint in place and stabilized the surface temperature probe and platinum bipolar electrode. A non-magnetic force transducer was built with four semi-conductor strain gauges (120 ohms, BLH electronics) arranged in Wheatstone bridge configuration [Figure 8], attached to an aluminum cantilever beam. The deflection of the aluminum beam changed the resistance in the strain gauges, and the voltage output of the bridge was amplified and recorded (Gould Model RS3200 amplifier) outside the magnet. The force transducer was mounted on a movable Plexiglas® base so that the muscle length could be adjusted. An aluminum

Figure 6. Plexiglas/Lexan Probe constructed for animal experiments within in a 4.7 Tesla magnet. Force and temperature measurements can be made, stimulating wires allow muscle stimulation, and the helmholtz coil transmits and receives the NMR signal.

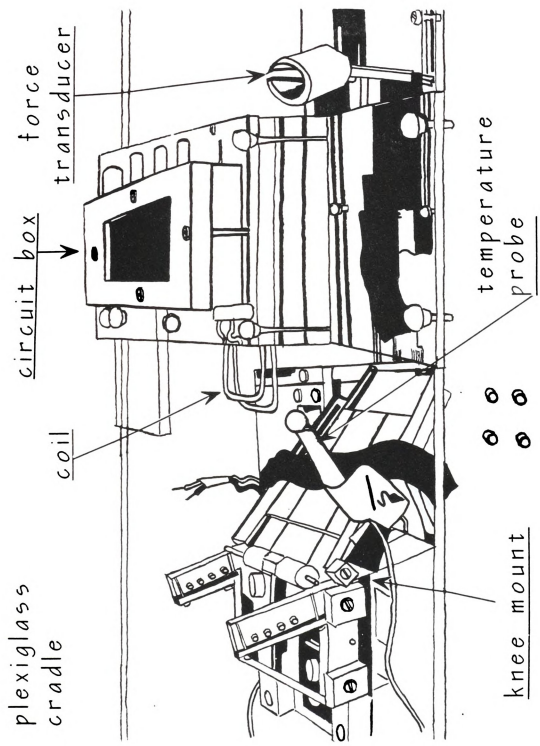
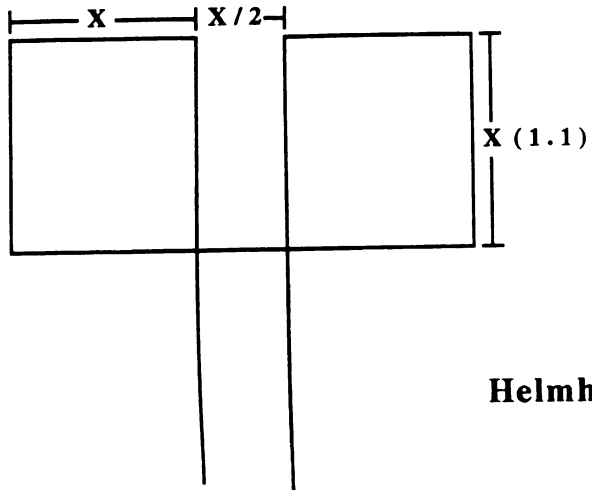
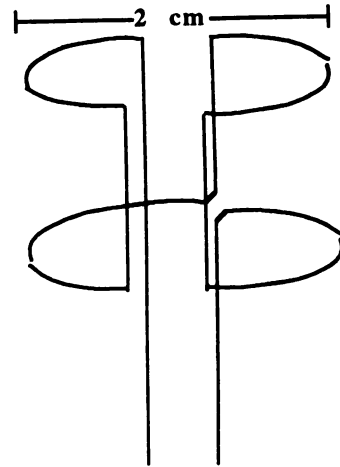


Figure 7. (A) and (B) Schematic of Helmholtz coil and (C) circuitry of the coil.

A



B



Helmholtz Coil

C

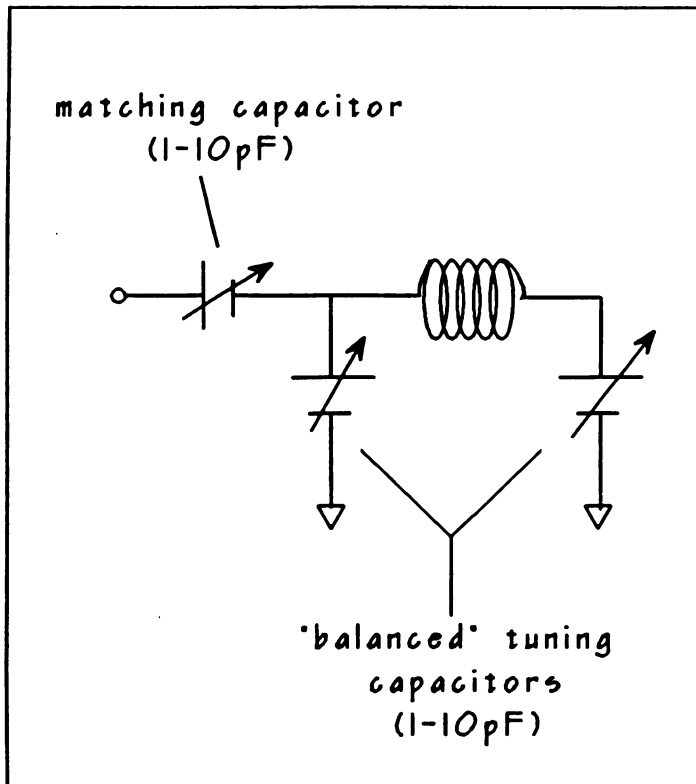
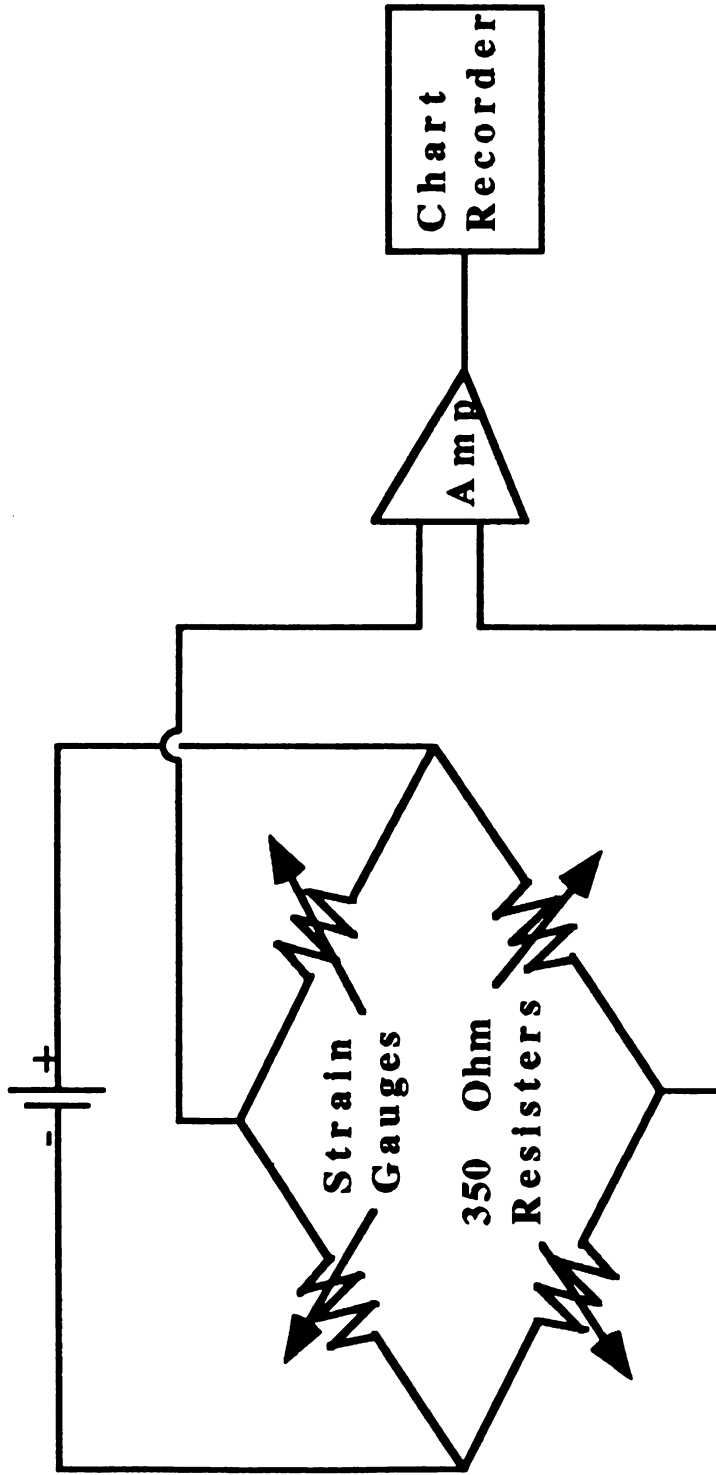


Figure 8. Circuit for specially constructed force transducers.



Wheatson Bridge

door for the magnet bore was built and embedded with radio frequency chokes for all wires running through the probe to reduce rf interference from outside the magnet.

Isolated perfused muscle studies. A probe previously built in our lab was modified for the isolated muscle experiments [Figures 9 and 10]. The probe case was constructed from aluminum. A 2 cm helmholtz coil [Figure 7] was mounted on the top portion of the probe with the capacitors directly underneath. The wires of the completed circuit ran down the length of the probe to a connector. Brass rods were positioned so that the circuit could be tuned with the probe within the magnet. An upper muscle mount was built from Delrin® (non-magnetic polymer) with a threaded brass rod to allow changes in muscle length. The muscle was attached to specially built force transducers directly below the muscle. The force transducers were built from four microfoil strain gauges (350 ohms, BLH electronics) arranged in a Wheatstone bridge configuration, [Figure 8] and were mounted on either Delrin® or brass beams. In some experiments a stiff nylon "weed eater" line was tied to the muscle tendon and extended to a commercial force transducer positioned outside of the magnet. All force transducers were calibrated by hanging weights (100 g - 5 kg) and recording the output. A linear response was observed within this range. Two platinum electrodes were

Figure 9. Probe for isolated perfused muscle experiments within a 9.2 Tesla magnet.

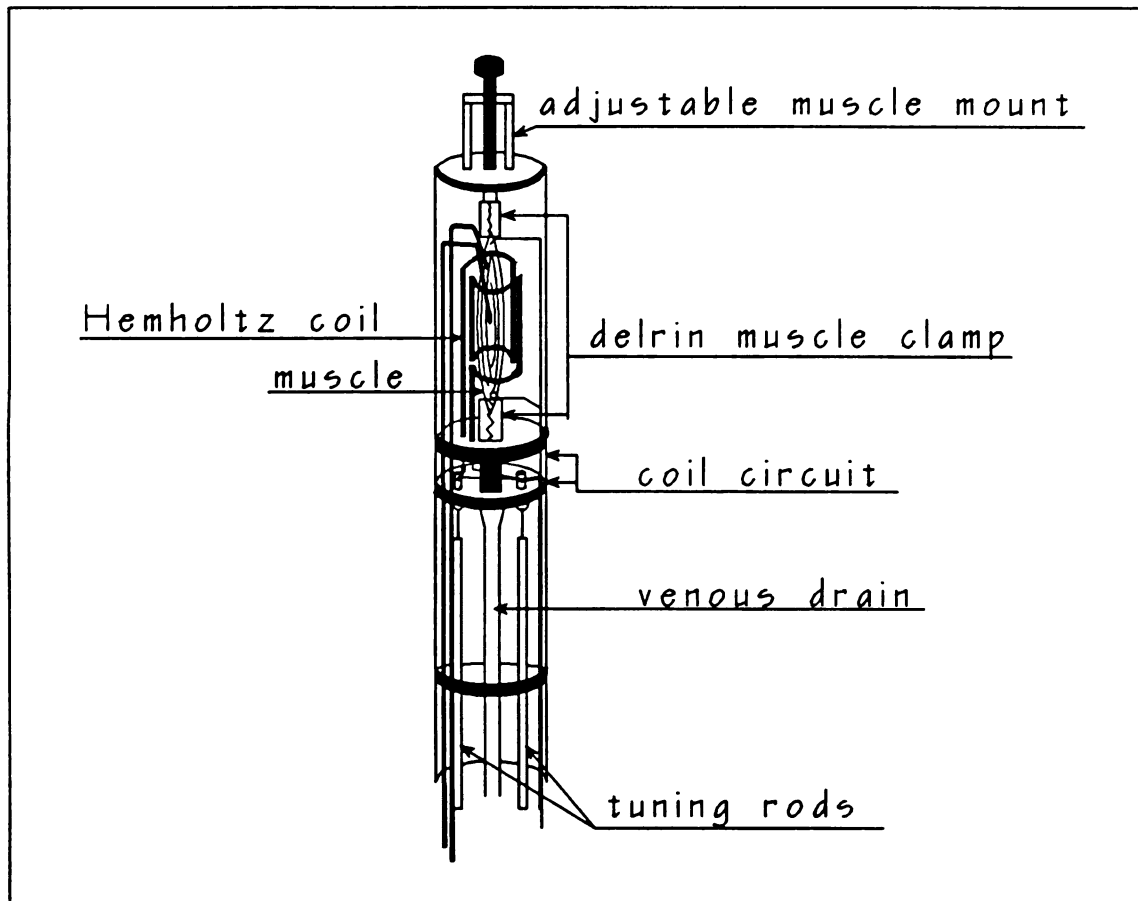
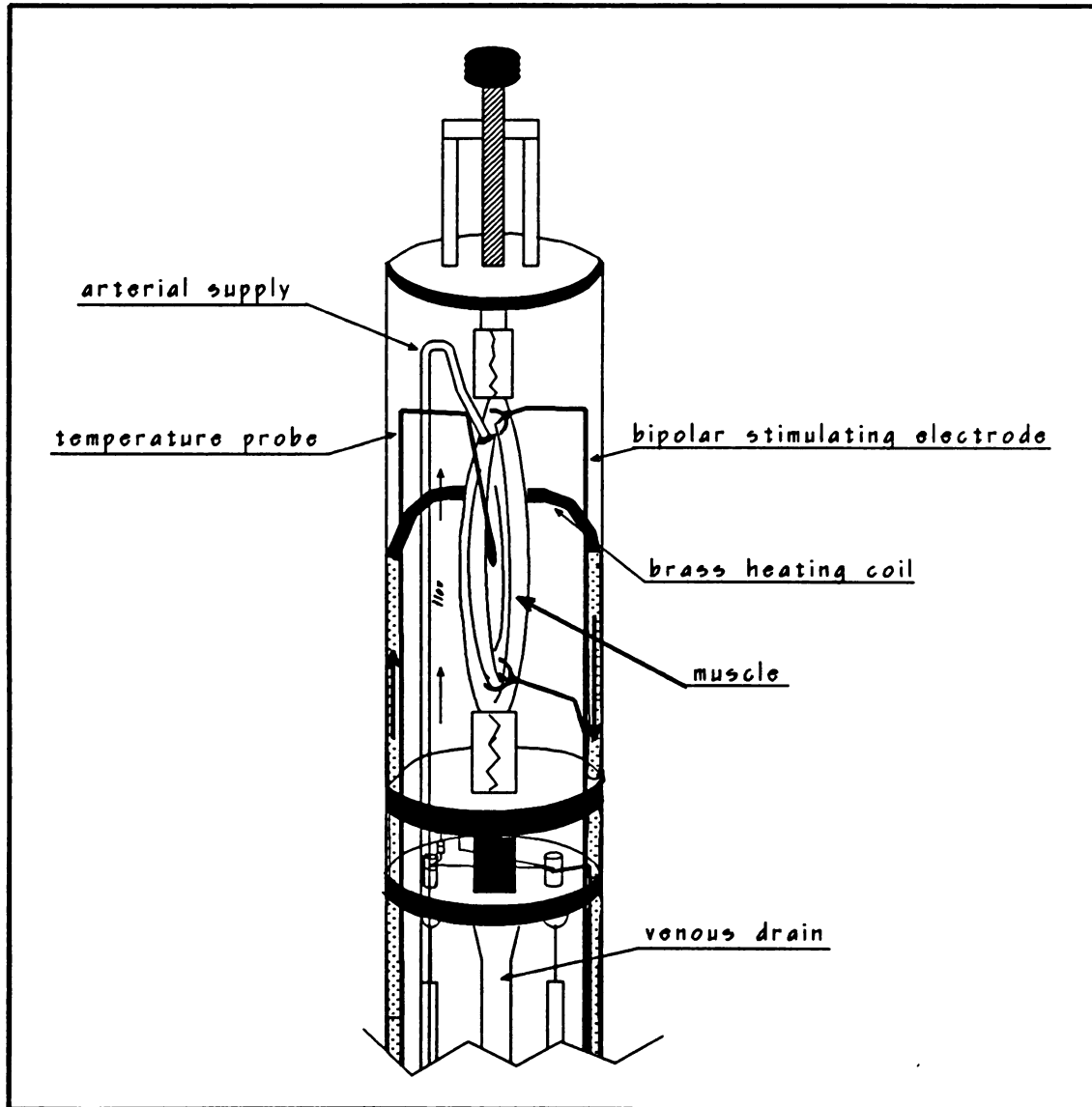


Figure 10. Top portion of probe for isolated perfused muscle experiments within a 9.2 Tesla magnet.



mounted to allow direct stimulation of the muscles at the proximal and distal tendons. A thermistor was placed near the surface of the muscle for recording temperature (YSI Model 73A) recorded the surrounding temperature. All wires were connected to radio frequency chokes embedded in an aluminum plate located at the bottom portion of the probe. The remainder of the cylinder was constructed to house perfusion lines and tubing for the copper heating coils located directly behind the muscle.

Procedures For The Basic ^{31}P -NMR Pulse Experiment

The magnetic field strength was either 4.7 Tesla (*in situ* cat experiments) or 9.4 Tesla (isolated perfused muscle experiments). In both experiments a helmholtz coil served as both a transmitter and receiver specific for the phosphorus frequency. The phosphorus frequency was dependent on the spectrometer used (81 MHz at 4.7 Tesla, 162 MHz at 9.4 Tesla).

At the beginning of each experiment, the proton NMR signal (200 MHz at 4.7 Tesla, 400 MHz at 9.4 Tesla) from muscle water was monitored while adjusting the magnetic field homogeneity, a procedure known as "shimming". This procedure takes between 10 and 30 minutes, and is important, since if the magnetic field is as homogenous as possible across the sample, then the spectral peaks are narrowed, and the peak signal to noise (S/N) ratio is

correspondingly enhanced. The proton signal from muscle water was used rather than the phosphorus signal because of its relatively high abundance and sensitivity, which enables high S/N FID's in a single scan.

Next, a fully relaxed (15 s pulse interval, 90° pulse width) spectrum was acquired from resting muscle. Typically 32-64 scan spectra were acquired, requiring 8-16 min. As noted above, these fully relaxed spectra allowed for direct quantitative comparisons of metabolite levels, and can be used to calculate saturation corrections for other spectra acquired under saturating conditions. For most protocols, the spectrometer's computer was then programmed to acquire a series of from 32-64 spectra, each averaged over a 15 to 60 second time interval. At the beginning of the third time block, muscle stimulation was initiated. The stimulation was turned off after 20 min, after the 32nd block was finished. Thus about half the spectra were recorded during recovery after stimulation.

Gated ^{31}P -NMR Pulse Experiment

Using the above protocol, metabolic events can be monitored with a time resolution of about 15-60 seconds, depending on the S/N ratio. For some experiments time resolution below 1 s was necessary. Gated NMR can accomplish this time resolution by acquiring each FID signal at precise time points relative to a contraction,

storing the data, allowing the muscle to recover, and then repeating the sequence, while averaging the FID's acquired at each time point (Adams *et al.*, 1990; Foley and Meyer, 1992). The effective time resolution of this method is limited only by the acquisition time of a single FID, or typically 140 ms in our experiments.

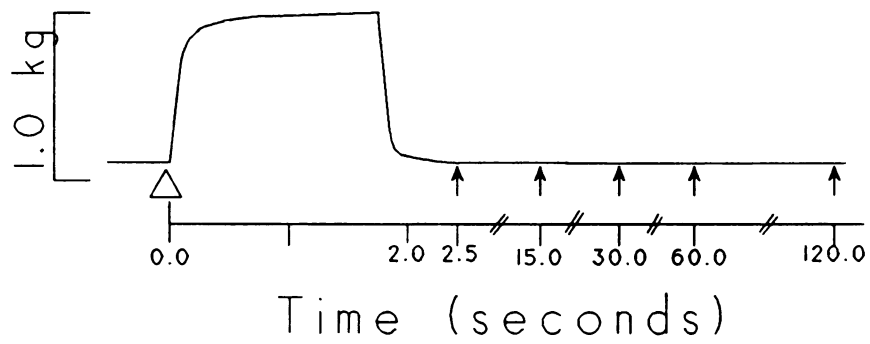
This method was used for the experiments described in Chapter 4, in which the effect of acidosis on the ATP cost of contractions was measured. Data was acquired at specific time points before and following either a short burst of twitches or a single tetanus [Figure 11]. The cycle was repeated several times and the data from each specific time point was averaged until an adequate S/N ratio was achieved. The difference between metabolite concentrations immediately before and after the contraction yields the changes associated with contraction.

MUSCLE PREPARATIONS

The advantage of intact tissue is that it allows monitoring of intracellular metabolites continuously in animals and humans (Arnold *et al.*, 1984). Perfused tissue studies allow environmental manipulation by the investigator. Both preparations are limited by tissue heterogeneity and the fact that the signal is averaged over cell populations and time. It is important to assess organ

Figure 11. Gated ^{31}P -NMR Experimental protocol. Pulses are given at each time point, the first given immediately after contraction. The signal is temporarily stored and after several repetitions, signals at each time point are averaged.

GATED NMR PROTOCOL



↑ - *radio frequency pulses*
△ - *spectrometer triggers
isometric contraction*

metabolic stability, in addition to assessment of metabolite levels obtained by NMR (Balaban, 1984).

In Situ Soleus Studies

Surgical techniques. Cats (4-5 kg) were anesthetized with ketamine chloride (15 mg/kg) subcutaneously, and sodium pentobarbital (30 mg/kg) intravenously. The carotid artery was cannulated to monitor arterial pressure and obtain blood samples. The animal was ventilated and hemodynamically stable throughout the experiments. Rectal temperature was maintained at 37°C by a heating pad placed underneath the animal. Supplemental fluids and anesthetic were given intravenously as needed during the entire experiment.

The calf muscle group (gastrocnemius, plantaris and soleus) was exposed by dissecting away the skin and outer fascia. All tendons were dissected from the calcaneus. The soleus tendon was dissected free from gastrocnemius tendons and ligated. The muscles surrounding the soleus were carefully reflected away. The femoral artery branch that supplied the soleus also had sub-branches that supplied the gastrocnemius and several anterior compartment muscles. The branches not directly supplying the soleus muscle were double ligated and severed. The venous branches paralleled the arterial configuration and were also ligated and cut. The proximal insertion remained

intact and the muscle was perfused by the animal's circulation. The proximal joint was stabilized by a tungsten pin inserted in the bone and fixed to a Lexan® support. The distal tendon was attached to a force transducer. The soleus motor nerve was isolated, severed distally, and placed in the bipolar platinum electrode for muscle stimulation. Muscle temperature was monitored by a surface probe placed on the exterior surface of the muscle and maintained within a physiological range (35°-37°C). The muscle was bathed in mineral oil and wrapped in Parafilm®. The muscle was stretched to optimal length and maximally stimulated (5-10V, 1 ms duration) with a Grass stimulator generating isometric twitches. Taken together, these procedures required around 5 hours from the time the animal was anesthetized until the first spectrum was acquired.

Additional surgery was required for oxygen consumption experiments. The venous branch that normally drains the blood supply of anterior compartment muscles, was ligated and cannulated (PE 90 tubing) for blood sampling. The proximal femoral venous branch was clamped during sampling so blood flowing from the soleus muscle could be collected in an air tight Hamilton® (Hospex) syringe from the cannula. Arterial blood samples were taken from the carotid artery before and after each stimulation period.

Isolated Perfused Muscle Studies

Isolated perfused cat soleus and biceps muscles preparations (Kushmerick and Meyer, 1985; Meyer et al., 1985) enable study of the contractile and metabolic properties of muscle contraction with greater control of experimental parameters, at the cost of considerably greater surgical preparation. Cat biceps (>70% fast glycolytic, >25% fast-oxidative glycolytic) and soleus (>95% slow oxidative fibers) muscles are relatively homogenous in cell fiber type thus reducing the complication of energetic parameters being attributed to different fiber types within the muscle rather than metabolic changes within the myocyte.

Surgical procedures. Cats (4-5 kg) were anesthetized with ketamine chloride (15 mg/kg) subcutaneously, and sodium pentobarbital (30 mg/kg) intravenously in all experiments. The animal was ventilated throughout the surgery. Rectal temperature was maintained at 37°C by a heating pad placed underneath the animal. Supplemental fluids and anesthetic were given intravenously as needed during muscle isolation of either the soleus or biceps muscle.

Soleus Isolation: Surgical procedures were similar to those previously described (see *In situ* Muscle Preparations section) with some modifications. The calf muscle group was exposed and the soleus tendon was dissected free from

the calcaneus and all other tendons and ligated with fishing line. The muscles surrounding the soleus were carefully reflected away. All arterial and venous branches not supplying or draining the soleus were double ligated and severed. The femoral artery was isolated anteriorly to allow cannulation with PE 50 tubing. The vein was also isolated and cannulated with PE 90 tubing only in experiments in which oxygen consumption was measured. The soleus nerve was cut and cauterized. The muscle was entirely isolated, except for its proximal insertion on the tibia. This bone was cut and the soleus muscle was removed from the animal. Braided, nylon fishing line (25 lb. test) was secured around the bone and used to attach the muscle to the upper muscle mount. In this case, the entire procedure, from anesthetizing the animal to acquisition of the first spectrum, typically took 6-8 hours.

Biceps Isolation: The forelimb muscle groups were exposed by removal of skin and outer fascia. Several muscles comprised a layer covering the biceps muscle and were cauterized and reflected away. The distal tendon was isolated and severed from its radial insertion. The tendon was ligated with fishing line. The fascia surrounding the biceps was carefully drawn away exposing the surrounding vessels. The biceps is supplied and drained by several arterial and venous branches located primarily on the

proximal and distal portions of the muscle. These branches stem from an artery and vein running parallel to the muscle. All branches not supplying the biceps were double ligated and severed. All nerves were cut and cauterized. The muscle was isolated, and the proximal tendon insertion was severed from the bone and also ligated with fishing line. The proximal tendon was attached to the upper muscle mount.

Both muscles (soleus and biceps) were bathed in mineral oil and surrounded by a plastic tube (3M transparency film PP2200). The distal tendon was attached to a force transducer. Platinum electrodes were placed on the proximal and distal portions of the muscle for stimulation. Temperature was monitored by a surface probe placed on the exterior surface of the muscle and maintained within a physiological range (35-37°C). The muscle was stretched to optimal length and maximally stimulated (10-50V, 1 ms duration) with a Grass stimulator.

Perfusion solution. Kreb's Heneleit solutions (KHS) were prepared for blood washing and final perfusion solutions a day prior to the NMR experiments (storage 4°C). The final perfusion solution was prepared the day of the experiment.

KHS Preparation: Solutions were prepared for use at either 37°C or 20°C for perfusion solutions or blood washing, respectively. The solutions contained NaCl (116

mM), KCl (4.6 mM), KH_2PO_4 (1.16 mM), NaHCO_3 (24 mM), $\text{CaCl}_2 \cdot 2\text{H}_2\text{O}$ (2.5 mM), $\text{MgSO}_4 \cdot 7\text{H}_2\text{O}$ (1.16 mM), to mimic physiological conditions and gentamycin sulfate (30 mg/L) to prevent bacterial growth. All solutions were bubbled with 95% O_2 and 5% CO_2 and filtered (Fisher 0.2 μm clay filters). For KHS (37°C) glucose (5 mM) and sodium pyruvate (0.15 mM) were added to provide substrates, as well as papaverine HCl (10 mg/L) to prevent vasoconstriction.. Phenylphosphonate (PPA) was brought to physiological pH with sodium hydroxide and added to the KHS (37°C) solution (PPA 10-15 mM final concentration). PPA is used for an extracellular volume and pH marker, since it has been shown not to cross the muscle cell membrane, and its NMR chemical shift is sensitive to pH within the physiological range (Kushmerick et al., 1982).

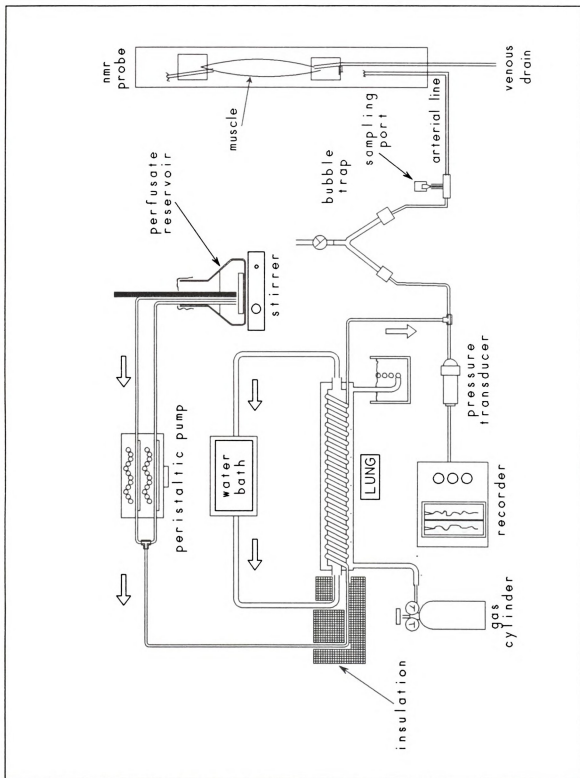
Red Blood Cell Preparation (Blood Washing): Packed sheep red blood cells (400 ml, Lampire Biological Labs) were divided evenly into six 250 ml polycarbonate centrifuge bottles. The bottles were then filled with 0.9% filtered saline solution for rinsing. The cells were then spun at 1800 RPM (refrigerated centrifuge) for 10 minutes at 10°C and the supernatant aspirated. This procedure was repeated 3 times with saline solution and 3 times with KHS (20°C).

Perfusion Solution Preparation: The final perfusate consisted of filtered 3.5% bovine serum albumin, 12 - 15%

washed red blood cells and 85% KHS (37°) (Meyer et al., 1985). Perfusate was mixed every hour in 60 ml batches of filtered KHS solution and albumin, and washed erythrocytes.

Perfusion Set-Up: The perfusate was gently stirred in a round bottom beaker and peristaltically pumped at 0.2 - 0.4 ml/min/g muscle through a brass artificial lung, a bubble trap, and then to the muscle [Figure 12]. Silastic® tubing was used throughout the lung to allow gas diffusion. All remaining tubing was Tygon® (gas impermeable) to prevent gas equilibration with room air.

Figure 12. Isolated perfused muscle experimental set up.



CHAPTER 3
CONTROL OF RESPIRATION BY PHOSPHORYLATION STATE IN
SLOW-TWITCH MUSCLE *INSITU*.

INTRODUCTION

There is a balance between energy production and utilization in skeletal muscle cells indicating metabolic control. ATP and PCr provide chemical potential energy for energy requiring processes (Kushmerick, 1983). The primary source of ATP at rest and during mild stimulation is oxidative phosphorylation. There is considerable controversy over the exact signal which links the rate of oxidative phosphorylation to the rate of ATP utilization in muscle. The major candidates for this control are phosphorylation state (relative concentrations of adenine nucleotides, phosphocreatine, and Pi), redox state (ratio of NADH and NAD⁺), and oxygen delivery (Balaban, 1990).

Metabolic control may be different in distinct skeletal muscle types, since the different fiber types have diverse metabolic characteristics. Slow-twitch fibers have a higher mitochondrial content, lower glycolytic capacity and lower actomyosin activity than fast-twitch fibers, as well as lower resting levels of PCr and ATP and higher Pi (Lawrie, 1953; Meyer *et al.*, 1985). The time course for

PCr changes is faster and oxygen consumption is lower at identical twitch rates in slow-twitch fibers than in fast-twitch fibers. On the other hand, mitochondrial structure is similar between muscle types, and although slow-twitch muscles have a higher aerobic capacity than fast-twitch muscles, when corrected for mitochondrial content, the values of maximal oxygen consumption are equivalent (Hoppeler *et al.*, 1987).

Most studies of respiratory control in mammalian muscle have been conducted on human muscles of mixed fiber type, or on animal muscles with predominantly fast-twitch fibers. These studies almost unanimously agree that changes in phosphorylation state can account for changes in respiration, although there is still disagreement on whether this dependence is due to control of respiration by ADP, or by phosphorylation potential (Foley *et al.*, 1991; Meyer, 1988; Meyer, 1989; Meyer *et al.*, 1986; Meyer *et al.*, 1985; Kushmerick *et al.*, 1992; Nioka *et al.*, 1992). In contrast, studies of heart muscle indicate that changes in respiratory rate can occur with no change in phosphorylation state (From *et al.*, 1986; Katz *et al.*, 1987; Hassinen, 1986; Balaban, 1990; Heineman and Balaban, 1990; Katz *et al.*, 1988). This indicates that some other controlling mechanism, possibly redox potential, must be at play in the heart.

Mammalian slow-twitch muscle has characteristics of both heart and fast-twitch muscles from the metabolic point

of view. Like cardiac muscle, slow-twitch muscle is almost totally dependent on aerobic metabolism for ATP production, and contraction is rapidly reduced if blood flow or oxygen supply is eliminated (Meyer and Terjung, 1980). On the other hand, like other skeletal muscles, it is not spontaneously active, can be tetanized, and is not sensitive to extracellular calcium changes (Crow and Kushmerick, 1982). In view of this, it seems reasonable that if there is a mechanism for respiratory control independent of phosphorylation state in heart muscle, this mechanism should be evident to some extent in slow-twitch muscle.

A recently published study of perfused cat soleus muscle suggested control of respiration in slow-twitch muscle was similar to that in heart (Kushmerick et al., 1992). Although there was a roughly linear relationship between PCr and oxygen consumption at relatively low stimulation rates, as stimulation rate was increased, steady-state PCr changed less dramatically. Furthermore, during recovery after stimulation, PCr recovered to values above those observed before stimulation. These observations are not consistent with control by a single factor such as phosphorylation state.

The purpose of this study was to examine the relationship between phosphorylation state and oxygen consumption in cat soleus muscle *in situ*. One series of experiments monitored PCr, ATP, Pi and pH noninvasively

during submaximal stimulation in intact soleus muscles using ^{31}P -NMR. Another series measured oxygen consumption during steady-state conditions at identical stimulation rates. The results do not confirm the previous study of perfused cat soleus muscle, and suggest that phosphorylation state is the dominant regulator of respiration in slow-, as well as fast-twitch muscle.

MATERIALS AND METHODS

Surgical Techniques

Cats (4-5 kg) were anesthetized with ketamine chloride (15 mg/kg) subcutaneously, and sodium pentobarbital (30 mg/kg) intravenously. The carotid artery was cannulated to monitor arterial pressure and obtain blood samples. The animal was ventilated and hemodynamically stable throughout the experiments. Mean arterial blood pressure was 115 ± 4 mmHg (mean \pm SE, $n=12$). Rectal temperature was maintained at 37°C with a heating pad placed underneath the animal. Supplemental fluids and anesthetic were given intravenously as needed.

The soleus muscle was isolated as described previously (see Chapter 2). In brief, muscle groups surrounding the soleus were gently reflected away. The soleus tendon was dissected free from the calcaneus and all other tendons and ligated. The soleus blood circulation was isolated. The branches not directly supplying or draining the soleus

muscle were double ligated and severed. The proximal insertion remained intact and the muscle was perfused by the animal's circulation. The proximal joint was stabilized by a tungsten pin inserted in the bone and fixed to a Lexan® support. The distal tendon was attached to a force transducer. The soleus motor nerve was isolated, ligated, and placed in a bipolar platinum electrode for muscle stimulation. Muscle temperature was monitored by a thermistor placed on the exterior surface of the muscle and maintained within a physiological range (35°-37°C). The muscle was stretched to optimal length and maximally stimulated (5-10V, 1 ms duration) with a Grass® stimulator at 0.5, 1, 2, 3, and 4 Hz, (order randomized) for 15 minutes. These stimulation rates were selected because preliminary experiments indicated that they maintained a metabolic and mechanical steady-state.

Experimental Series I/Phosphorous NMR

Cats (n=6) were placed in a Plexiglas®/Lexan® probe constructed for this project [Figure 6]. The soleus muscle was positioned within in a 2 cm diameter Helmholtz coil. The tendon was attached to a non-magnetic force transducer for isometric force measurements. The probe was placed within a GE Omega 4.7 Tesla magnet. The circuit was tuned to 81 MHz and the magnetic field shimmed on protons of muscle water. Control spectra were acquired (pulse width = 90°, rd = 15 s, ns = 8) at the beginning of each experiment

and between stimulation bouts. Sixty-two phosphorus spectra (pulse width = 60°, rd = 1.87 s, ns = 8) were continuously acquired during stimulation and recovery. The muscle recovered completely between stimulation bouts, as indicated by restoration of phosphate metabolites and force to control levels.

FID's were zero-filled to 4K data points and multiplied by an exponential corresponding to 15 Hz line broadening. Peak integrals were computed after baseline correction and Fourier transformation. Steady-state PCr levels were determined by averaging the PCr integral of 20 spectra acquired during the final 10 minutes of stimulation and by calculating a percentage from control spectrum immediately prior to stimulation. Percentage values were multiplied by 12.7 moles PCr/gram wet weight muscle (Meyer *et al.*, 1985). Exponential time constants for PCr changes were computed by non-linear least squares fit. Intracellular pH was estimated from the chemical shift of the inorganic phosphate peak (Moon and Richards, 1973).

Experimental Series II/Oxygen Consumption

In addition to the surgical techniques described above cats (n=6) underwent the following surgical procedures. The femoral venous branch, that normally drains the blood supply of anterior compartment muscles, was ligated and cannulated for blood sampling. Arterial blood samples were

taken from the carotid artery before and after each stimulation period. The distal tendon was connected to a commercial force transducer (Grass instruments). For each stimulation period (same frequencies and duration as above) three successive venous blood samples were taken during the final 10 minutes of stimulation. This was during the metabolic and mechanical steady-state as determined by PCr levels and force measurements of ^{31}P -NMR experiments. Blood flow measurements were taken by collecting venous effluent for 15 seconds. Blood oxygen content was measured by a LexO₂Con Oxygen Analyzer (Lexington Instruments). Oxygen consumption was calculated by multiplying (arterial - venous) oxygen content differences by blood flow and dividing by the muscle wet weight.

Results

Figure 13 shows a series of ^{31}P -NMR spectra for a cat soleus muscle *in situ* during 15 minutes of stimulation (2 Hz) and recovery. Each spectrum is the sum of two 15 s spectra. There is an exponential decline of PCr to a steady-state level and a corresponding increase in Pi during stimulation. Both metabolites recovered to pre-stimulation levels, but there was no overshoot of PCr and undershoot of Pi during recovery ($p > 0.05$). ATP levels were constant during stimulation and recovery. Figure 14 shows the mean PCr changes at stimulation rates of 0.5, 1, 2, 3,

FIGURE 13. Series of spectra of soleus muscle, control (1 minute), during 3 Hz stimulation (15 minutes), and during recovery (15 minutes). Each spectrum is an average of 16 scans (60 pulse width, $rd = 1.62$ s).

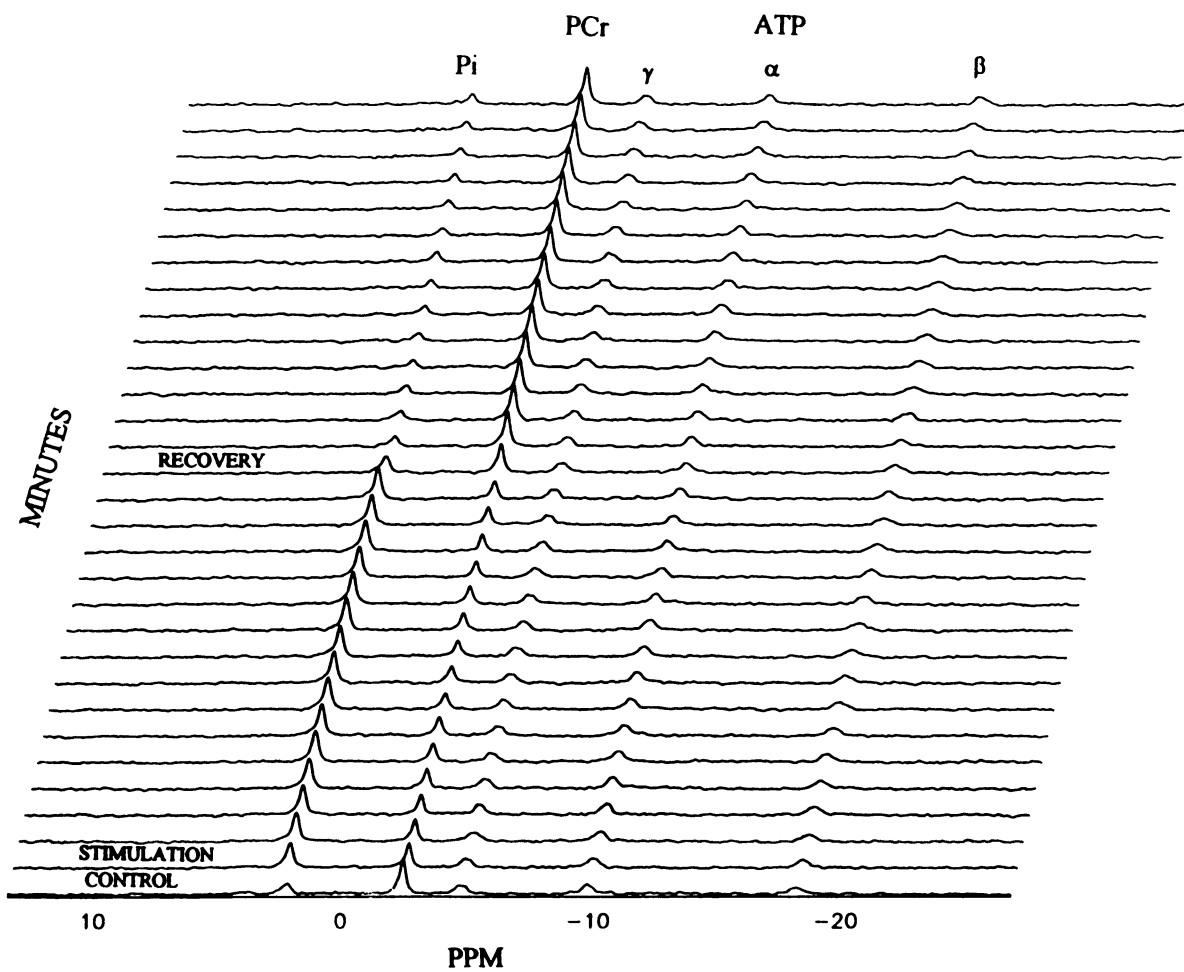


Figure 14. PCr levels from ^{31}P -NMR spectra of cat soleus muscle acquired during and after 15 minutes of stimulation at 0.5, 1, 2, 3, and 4 Hz. Exponential lines were computed assuming a single time constant (0.83 min) and 95% recovery of signal intensity.

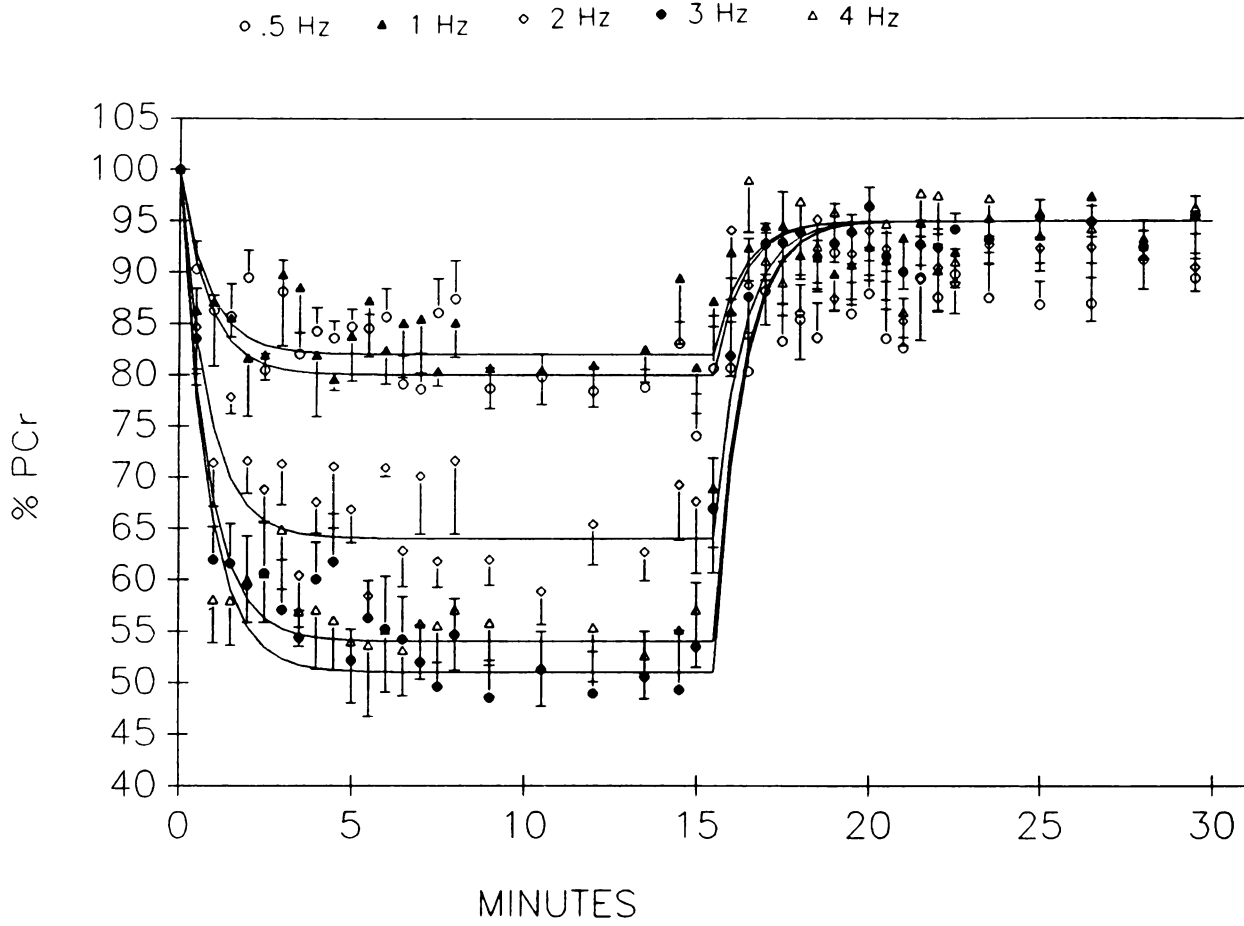


TABLE 2

PCr time constants

Onset stimulation	0.85 ± 0.8
Recovery	0.83 ± 0.1

(Values are means \pm SE given in minutes; onset n=16, recovery n=17).

and 4 Hz. Steady-state PCr levels (mean over last 10 min) decreased with increases in stimulation rate. The overall mean time constant for PCr changes was 0.83 ± 0.07 minutes [Table 2].

The time constant of PCr changes was independent of stimulation rate, as shown in Figure 15, and similar at onset of stimulation versus during recovery [Table 2].

Table 3 summarizes intracellular pH, oxygen consumption and twitch force data at rest and in the steady-state during repetitive stimulation. Resting oxygen consumption was 0.185 ± 0.04 $\mu\text{mol O}_2/\text{min/g}$ and blood flow was $0.075 \pm .007$ $\text{ml}/\text{min}/\text{g}$ at 37°C [Table 3], comparable to previous studies of intact (Bockman, 1983) and perfused soleus muscles (Meyer et al., 1985). Intracellular pH was not different from control values during steady-state stimulation. Steady-state peak force decreased with an increase in stimulation rate. Oxygen consumption and PCr levels were proportional to the product of peak force and stimulation rate [Figure 16, 17]. Steady state oxygen consumption was a linear function of steady-state PCr levels, ($r = 0.965$) with slope = -0.15857 , and y - intercept = 3.432 [Figure 18].

Figure 15. PCr time constants for stimulation rates of 0.5, 1, 2, 3, and 4 Hz.

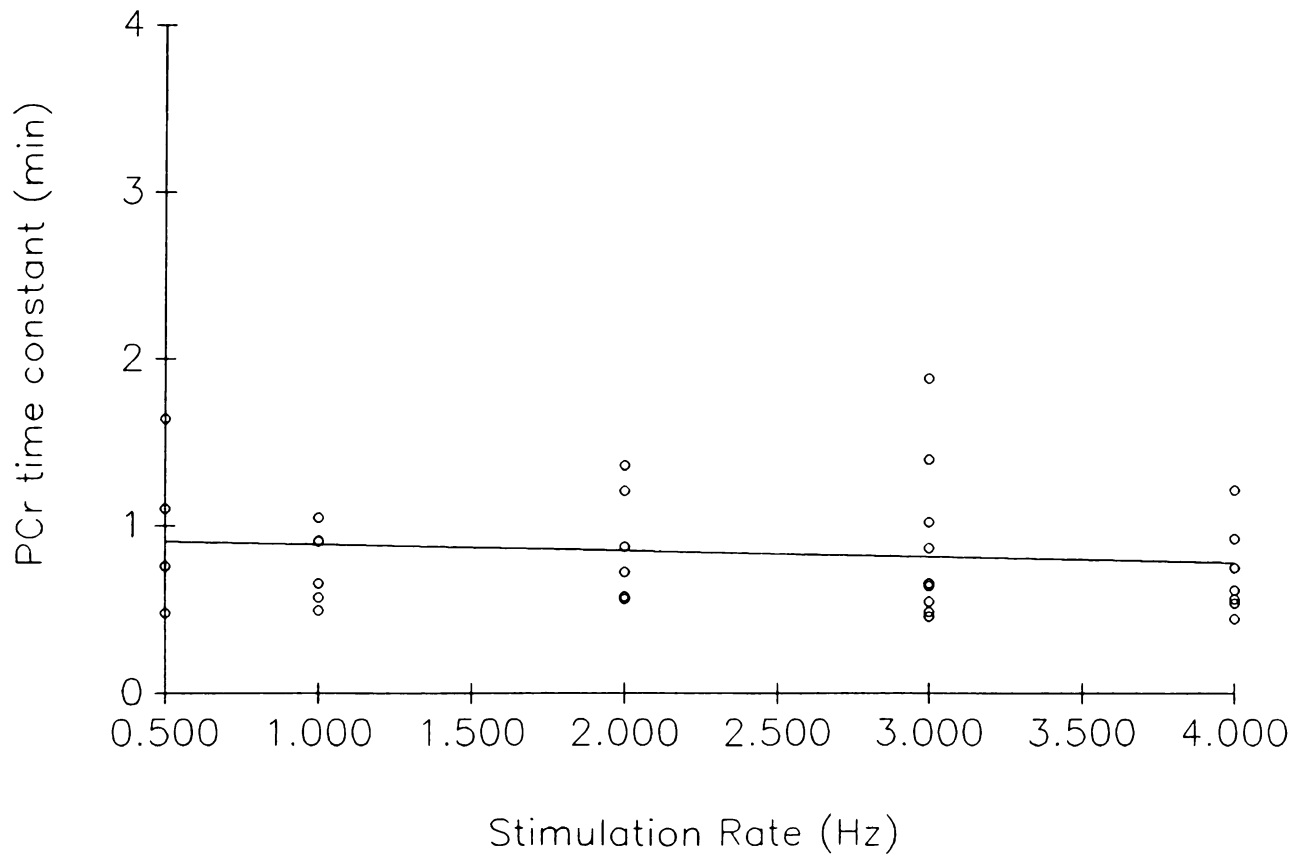


TABLE 3

Hz	0.0	0.5	1	2	3	4
pH	7.05	7.07	7.09	7.05	7.08	7.09
	± 0.04	± 0.02	± 0.05	± 0.04	± 0.02	± 0.03
Force		94	95	95	87	79
%control		± 2.0	± 2.8	± 4.5	± 2.6	± 2.0
VO ₂	0.185	0.365	0.567	0.780	1.11	1.15
$\mu\text{mol}/\text{min}/\text{g}$	± 0.04	± 0.07	± 0.10	± 0.16	± 0.10	± 0.09
Blood Flow	0.075	0.930	0.114	0.121	0.160	0.160
ml/min/g	± 0.007	± 0.015	± 0.021	± 0.025	± 0.027	± 0.033

(Values are means \pm SE.)

Figure 16. Steady-state oxygen consumption vs. product of stimulation rate times mean peak twitch force (percent of initial i.e., first twitch of each stimulation series) during soleus muscle stimulation ($r = 0.98$).

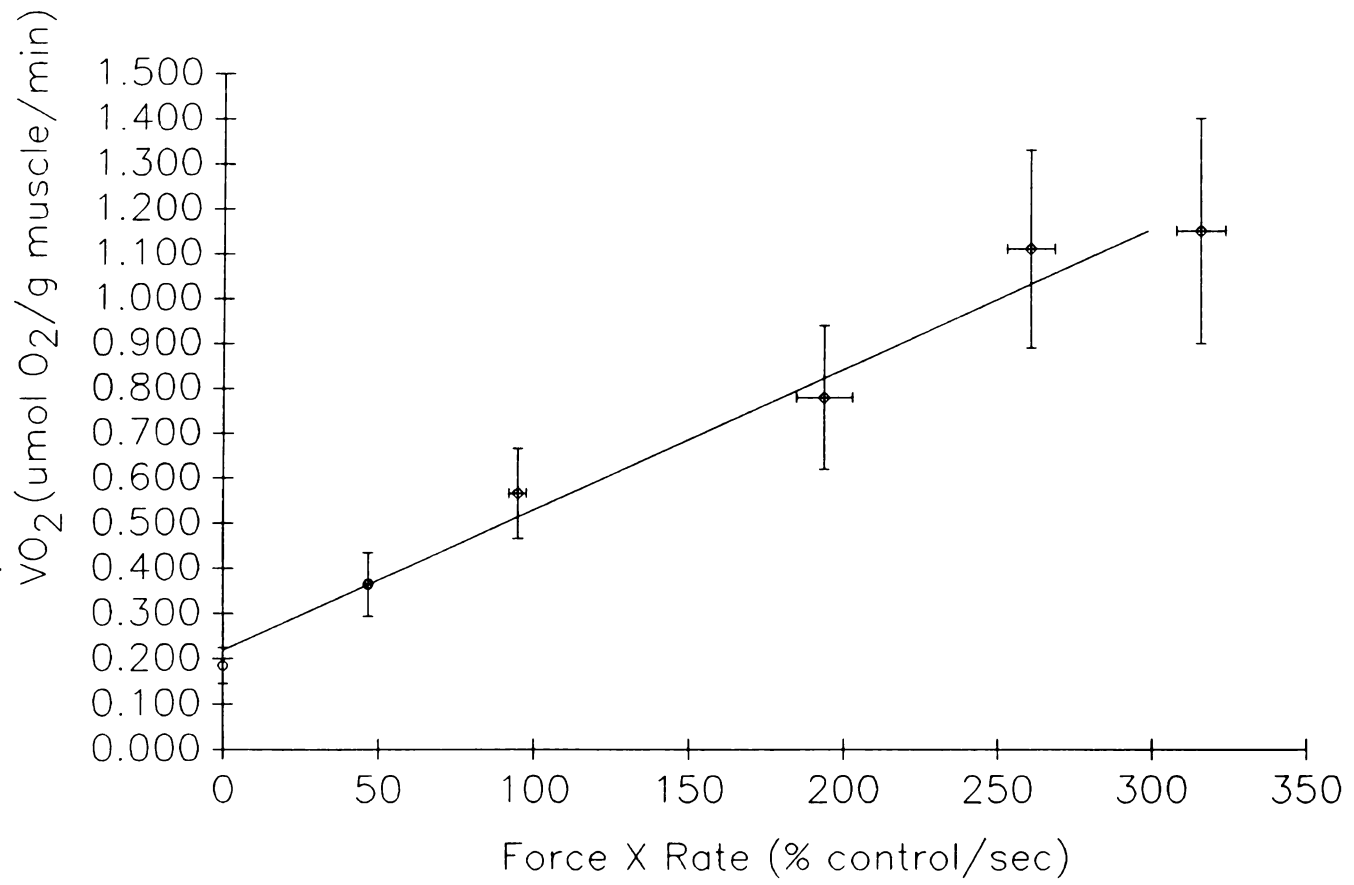


Figure 17. Steady-state PCr vs. product of stimulation rate times mean peak twitch force (percent of initial i.e., first twitch of each stimulation series) during soleus muscle stimulation ($r = 0.96$).

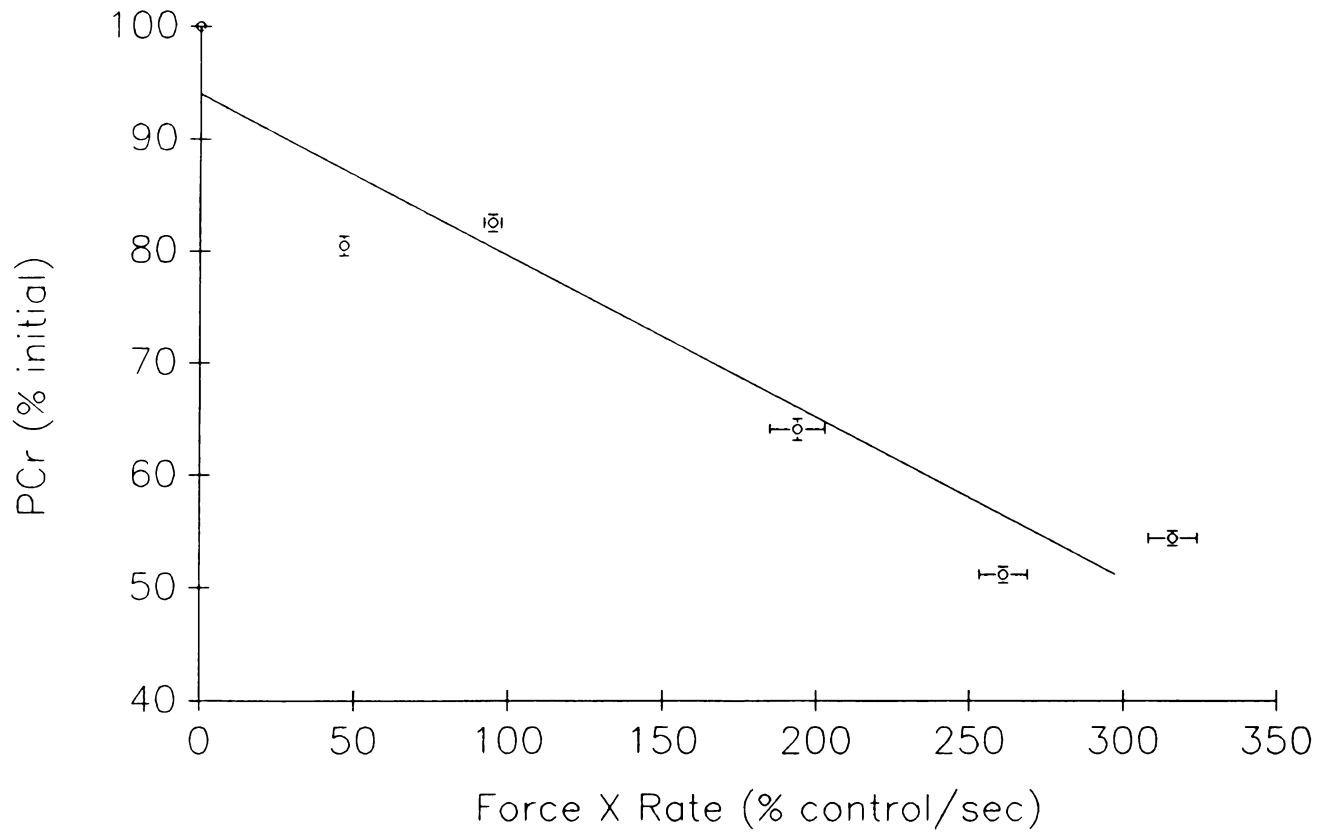
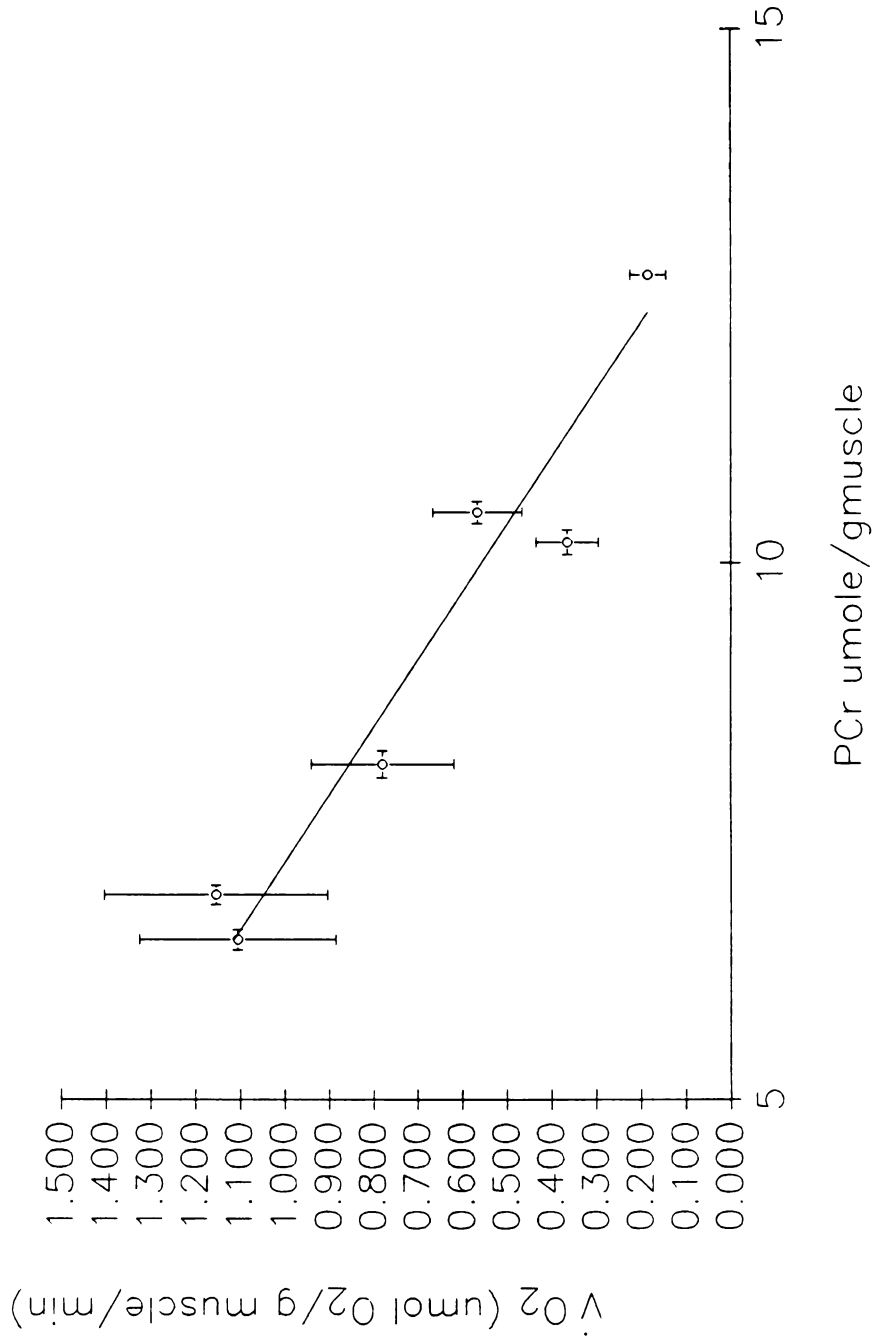


Figure 18. Relationship between steady-state PCr and oxygen consumption at rest and during stimulation (0.5, 1, 2, 3, 4 Hz). PCr levels are from figure 15, assuming an initial PCr value of 12.7 mol/g muscle (Meyer et al., 1985). Values for oxygen consumption are from Table 3 (Slope = -0.15857, y intercept = 3.432, r = 0.97).



DISCUSSION

Our study shows oxygen consumption is a linear function of steady-state PCr, for moderate ATPase rates of slow-twitch muscle *in situ*. These results are not consistent with a previous study of isolated perfused slow-twitch muscle, in which respiration rate was observed to become less dependent on steady-state PCr at higher ATPase rates (Kushmerick *et al.*, 1992). The difference may be because blood flow became limited at the higher stimulation rates in that study. Limited blood flow might result in increased lactate/pyruvate ratio, and hence increased redox potential, which could persist during the recovery period, and drive PCr to a higher level compared to before stimulation. Alternatively, the lower temperature (30°C) at which that study was conducted may also contribute to the difference between results. In any case, our results suggests that changes in phosphorylation state are sufficient to explain respiratory control in slow-twitch muscle. However, our results do not distinguish between control by ADP versus by phosphorylation potential ($\ln[\text{ATP}]/[\text{ADP}][\text{Pi}]$).

There was a balance between power output and energy production, which depended both on respiratory control, and on the control of twitch force. Oxygen consumption values did not increase linearly with stimulation but were proportional to steady-state force times stimulation rate. Yet, steady-state isometric twitch force decreased as

twitch rate increased. This decrease is not analogous to the fatigue which is observed during more intense or ischemic stimulation, because it was not associated with acidosis, and because, a steady-state of twitch force was rapidly achieved, and then maintained for many minutes of stimulation. These observations suggest that there is a rate dependent mechanism modulating calcium release during twitch stimulation of slow-twitch muscle. The details of this mechanism are obscure, but deserve further investigation.

Near-equilibrium thermodynamic models of control of respiration predict that oxidative rate should be dependent on the difference between the cytoplasmic free energy of ATP hydrolysis and an intramitochondrial energy term related to redox potential (Erecinska and Wilson, 1982). If the redox potential remains constant, respiration rate should depend linearly on cytosolic phosphorylation potential over a submaximal range of respiratory rates. This basic hypothesis has been incorporated into an electrical analog model of the relation between PCr changes and respiration in skeletal muscle (Meyer, 1988). This model predicts that steady-state respiration should be linearly dependent on PCr levels during stimulation at rates within the maximum aerobic capacity of the muscle. The slope of this steady state relation is $d\dot{Q}O_2/d[PCr] = -1/(\rho\tau)$, with $\rho = P/O_2$, and $\tau =$ apparent time constant for PCr changes. The model also predicts that the time

constant for PCr changes at the onset of stimulation and during recovery should be the same, and both should be independent of stimulation rate. Also, these PCr time constants should be relatively shorter in muscles with higher mitochondrial content and/or lower total creatine levels.

The results of this study are basically consistent with the predictions of this model. First, steady-state oxygen consumption was a linear function of PCr levels [Figure 18]. The P/O_2 ratio was estimated to be 7.9 by applying the equation above using the slope of the relationship between steady-state PCr levels and oxygen consumption (Figure 18) and the mean time constant for PCr changes (0.83 min). This value is reasonably close to the expected value of 6 (Lemasters, 1984). Second, the PCr time constant was independent of stimulation rate, and not significantly different between the onset of stimulation and during recovery. Third, as expected from the higher mitochondrial content and the lower total creatine content of slow-twitch compared to fast-twitch muscle, the mean time constant (0.83 min) was less than that observed in rat fast-twitch muscle (1.4 min) (Kushmerick and Meyer, 1985; Foley et al., 1991). Thus, these results are consistent with the linear model, and therefore are consistent with respiration rate controlled by phosphorylation potential. However, as pointed out by Connett, these results do not rule out metabolic control by ADP availability.

In summary, we found no evidence for a non-phosphorylation state mechanism for respiratory control in cat soleus muscle *in situ*. We conclude that respiratory control in slow-twitch muscle is fundamentally the same as in fast-twitch muscle being primarily controlled by phosphorylation state.

CHAPTER 4

EFFECT OF HYPERCAPNIC ACIDOSIS ON THE ATP COST OF
CONTRACTIONS IN FAST- AND SLOW-TWITCH MUSCLESINTRODUCTION

Although there is general agreement that respiration is controlled by cytoplasmic phosphorylation state within maximum aerobic capacity in skeletal muscle, the specific controlling parameter is not clear (Mahler, 1985; Meyer, 1989; Meyer *et al.*, 1986; Chance *et al.*, 1986). The two most likely candidates are cytoplasmic ADP concentration and cytoplasmic phosphorylation potential. These two hypotheses are difficult to distinguish by simple correlative experiments because both ADP and cytoplasmic phosphorylation potential change in tandem during muscle stimulation. Connett has shown that study of contracting muscles during experimentally induced acidosis could, in principle, distinguish between control by ADP versus phosphorylation potential (Connett, 1988a; Connett, 1988b). However, a potential obstacle to the design of such a study is the possibility that acidosis alters the utilization of ATP, as well as ATP synthesis. For example, if acidosis profoundly inhibits cross-bridge cycling, it would be difficult to increase respiratory rate by muscle stimulation in acidic muscles.

Acidosis has long been reputed to have a significant role in muscle fatigue (Curtin *et al.*, 1988; Lannergren and Westerblad, 1989; Dawson *et al.*, 1980; Chance *et al.*, 1985; Miller *et al.*, 1988; Westerblad and Lannergren, 1988). Fatigue is the decline of force observed during repeated contraction of skeletal muscle at power outputs above those which can be maintained by aerobic metabolism. It is well known that fatigue is associated with decreased ATP utilization (Close, 1972; Dawson *et al.*, 1978; Terjung *et al.*, 1985; Dawson *et al.*, 1980). Skinned muscle fiber studies suggest that decreased intracellular pH is an important cause of muscle fatigue (Cooke *et al.*, 1988). Lowered pH decreased the calcium sensitivity of the contractile apparatus, (Fabiato and Fabiato, 1978; Donaldson and Hermansen, 1978), the peak force during maximum calcium stimulation, and the rate of cross-bridge cycling and shortening velocity (Chase and Kushmerick, 1992; Cooke *et al.*, 1988; Godt and Nosek, 1989; Metzger and Moss, 1987). If these effects occurred in intact muscle (Hultman *et al.*, 1985), the result could be profound fatigue and a decrease in ATP use during contraction under acidic contractions.

On the other hand, studies of intact muscles do not consistently show a good correlation between acidosis and fatigue. In particular, Adams (1991) found little effect of hypercapnic acidosis on peak isometric tetanic force in cat skeletal muscles, although peak twitch force and the

rates of force development and relaxation were reduced. Unfortunately, these results do not prove that ATP utilization is not sensitive to acidosis, since the actual rate of cross bridge cycling or shortening velocity was not measured. Thus, it is possible that the economy of isometric force development is increased by acidosis, so that less ATP is required to maintain isometric force.

The economy of muscle contraction, the relationship between isometric mechanical response and energetic cost, varies among animals as well as between fiber types. The frog sartorius muscle is 40 times less economical than tortoise skeletal muscle and 100 times less economical than mammalian smooth muscle. The energy cost of mouse fast-twitch muscle was measured to be from 50-300% greater than slow-twitch muscle depending on duration of the stimulation (Crow and Kushmerick, 1982; Close, 1972; Rall, 1972).

There are several chemical reactions that contribute to the energy cost of muscle contraction (Rall, 1972; Kushmerick, 1983; Kushmerick *et al.*, 1969; Bienfait *et al.*, 1975). Energy release during steady-state contraction is primarily determined by actomyosin ATPase (70%) at the crossbridges, and Ca^{2+} ATPase (30%) at the sarcoplasmic reticulum. There is a direct relationship between actomyosin ATPase rate and maximum velocity of shortening (Nakamaru and Schwartz, 1972). A change in hydrogen ion concentration may alter ATPase activity and affect the energy cost of contraction.

The purpose of this study was to directly measure the effect of hypercapnic acidosis on ATP utilization during isometric contractions of perfused cat fast- and slow-twitch muscles. This information was a prerequisite to the design of the following study (Chapter 5), since that study required selection of a range of stimulation rates which would result in similar rates of ATP utilization during normocapnia and hypercapnia. ATP utilization was observed during acidosis with gated ^{31}P -NMR (Foley and Meyer, 1992; Adams et al., 1990) in isolated cats soleus and biceps muscles. The results show that the ATP cost of tetanic contractions is reduced in proportion to the reduction in force. Thus, the intrinsic rate of cross-bridge cycling and the economy of force development appear to not be sensitive to changes in pH over the range studied (pH 6.6 - 7.1).

MATERIAL AND METHODS

Surgical Techniques

Cats were anesthetized with ketamine subcutaneously and pentobarbital intravenously. A tracheotomy was performed to allow controlled ventilation. Either the soleus or biceps muscle was vascularly isolated and excised, as previously described (Chapter 2). The artery supplying the muscle was cannulated and perfused at $0.2\text{-}0.4\text{ ml min}^{-1}\text{ g}^{-1}$ (perfusion pressure 80 - 100 Torr) with a 15%

suspension of sheep red blood cells in bicarbonate-buffered Krebs-Henseleit solution. Perfusate was equilibrated with either 5% CO₂-95% O₂ (normocapnia) or 70% CO₂-30% O₂ (hypercapnia) at 37°C in a Silastic® tube oxygenator. The isolated muscle was placed within a 2 cm Helmholtz coil mounted in a custom made 7.4 cm diameter probe. Both tendons were secured by custom built Delrin® clamps. Platinum wire electrodes were securely placed on each end of the muscle and isometric force recorded as described previously. Supramaximal isometric twitch contractions of soleus (1 Hz, 10 s) and biceps (2 Hz, 10 s) were induced by a square wave pulse of a Grass stimulator (20-50 V). Tetanic contractions of soleus and biceps were given at 30 Hz for 2 s and 100 Hz for 1 s, respectively. Each stimulation protocol was administered at normocapnia and during hypercapnia.

Gated ³¹P-NMR Experiments

Spectra of isolated perfused muscles were acquired at 162 MHz on a Bruker AM400 wide bore spectrometer. Control spectra (90° pulse, 15 s interval, ns = 1, 4, 8 or 16 scans) were acquired prior to each stimulation series and during the time interval of gas equilibration. The gated protocol (see Chapter 3) was implemented, with the first scan acquired 0.5 s after the end of the tetanus or burst of twitches, and with 6 successive scans following at

intervals of 15, 30, 45, 60, 120, and 240 s. The 240 s scan served as the pre-contraction spectrum.

FID's were zero-filled to 4K data points and multiplied by an exponential corresponding to 15-25 Hz line broadening before Fourier transformation. Control spectra were integrated and PCr/ATP ratios were determined during normal and low pH. Spectrum 7 (240 s) represented control levels of phosphates and was compared directly to spectrum 1 acquired 0.5 s immediately following contraction. The percent decrease in PCr was calculated and converted to μ mol ATP/g muscle by multiplying the ratio of PCr/ATP in the control spectra, and by the content of ATP measured chemically in previous studies (5.03 μ mol/g for soleus, 8.9 μ mol/g biceps, Meyer *et al*, 1985). Intracellular pH was estimated from the chemical shift of the inorganic phosphate peak (Moon and Richards, 1973). Extracellular pH was determined from the chemical shift of the PPA peak (Meyer *et al.*, 1985).

RESULTS

Table 4 shows the extracellular and intracellular pH, PCr/ATP ratios, and contractile characteristics in both muscles during normocapnic and hypercapnic perfusion. The results are basically the same as reported previously (Adams *et al.* 1991). Intracellular pH decreased from 7.2 to 6.6 in both muscles. There was no significant decrease

in PCr/ATP ratios in either muscle during hypercapnia as compared to normocapnia. There was also no significant effect of hypercapnia on peak tetanic force, but peak twitch force decreased by about half in both the soleus and biceps muscles. There was a significant increase in relaxation time after tetanic contractions in both muscles, and a slower rise time in the soleus muscle only with acidosis.

Representative gated phosphorus spectra are shown in Figures 19 and 20 in soleus and biceps muscles, respectively, before and after isometric contractions, during normocapnia and hypercapnia. Figure 21 summarizes the calculated change in PCr associated with twitch and tetanic contractions in the two muscle types under both pH conditions. There was a reduction in PCr levels and corresponding increase in Pi during contraction in both muscles. There was no significant difference in PCr changes associated with the tetanic contractions in either muscle type. On the other hand, there was a significant decrease in PCr cost of twitch contractions in the biceps, and a similar trend was evident in the soleus. Thus, the effects of acidosis are roughly proportional to the effects on isometric force in both muscle types [Figure 22].

TABLE 4

	BICEPS		SOLEUS	
	normo- capnia	hyper- capnia	normo- capnia	hyper- capnia
[PCr]/[ATP]	3.55 ±0.51	3.64 ±0.58	2.94 ±0.49 _(n=12)	3.0 ±0.60 _(n=12)
pH _{ic}	7.19 ±0.02	6.56 ±0.05*	7.15 ±0.06	6.57 ±0.06*
pH _{ec}	7.52 ±0.03	7.74 ±0.04*	7.51 ±0.04	6.78 ±0.07*
TWITCH				
rise time ms	28 ±3	26 ±1	103 ±10	102 ±10
relax time ms	23 ±4	22 ±2	124 ±6	195 ±30
peak force g/g	188 ±33	99 ±14*	93.2 ±12	48.7 ±15*
TETANIC				
rise time ms	82 ±5	114 ±10*	380 ±29	530 ±56*
relax time ms	37±	90	129	259
peak force g/g	5 738 ±96	±14* 620 ±82	±14 323 ±39	±40* 270 ±36

(Values are means ± SE, n=7 unless noted otherwise.)

*Significant difference between normocapnia and hypercapnia by paired Student's t-test (p<0.05).

Figure 19. Spectra acquired at rest and immediately following isometric twitch and tetanic contractions in soleus muscle during normocapnia (pH = 7.2) and hypercapnia (pH = 6.6). (A) twitch, pH = 7.2, (B) twitch, pH = 6.6, (C) tetanus, pH = 7.2, (D) tetanus, pH = 6.6.

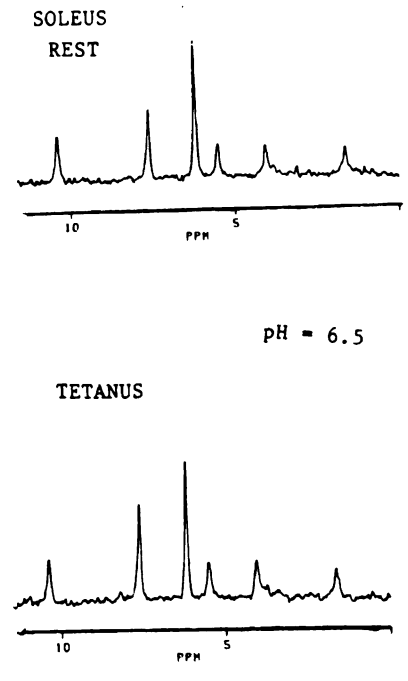
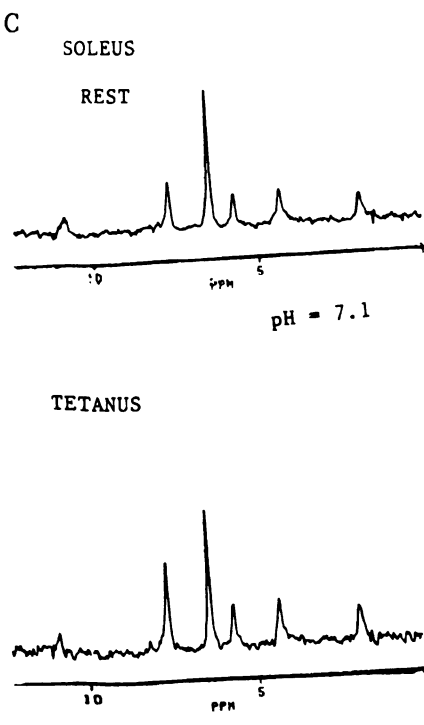
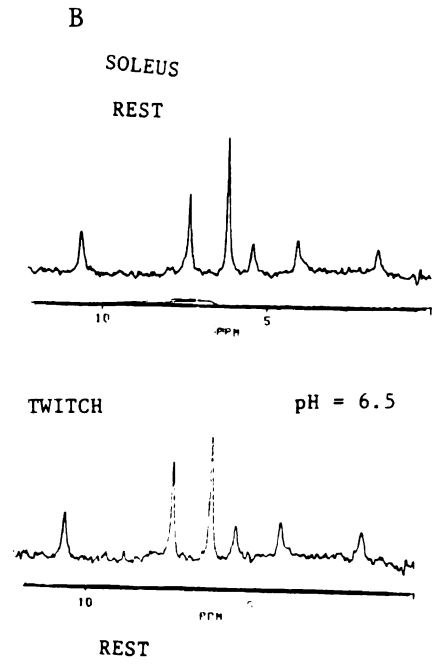
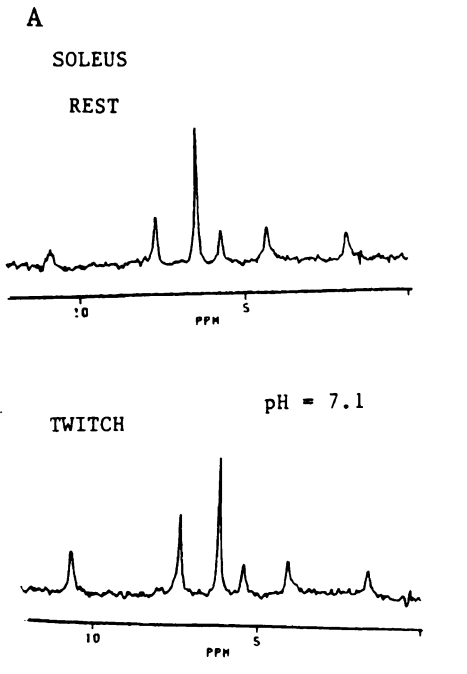


Figure 20. Spectra acquired at rest and immediately following isometric twitch and tetanic contractions in biceps muscle during normocapnia (pH = 7.1) and hypercapnia (pH = 6.5). (A) twitch, pH = 7.1, (B) twitch, pH = 6.5, (C) tetanus, pH = 7.1, (D) tetanus, pH = 6.5.

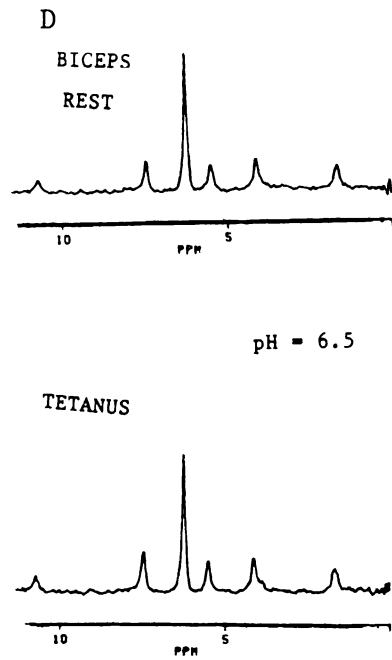
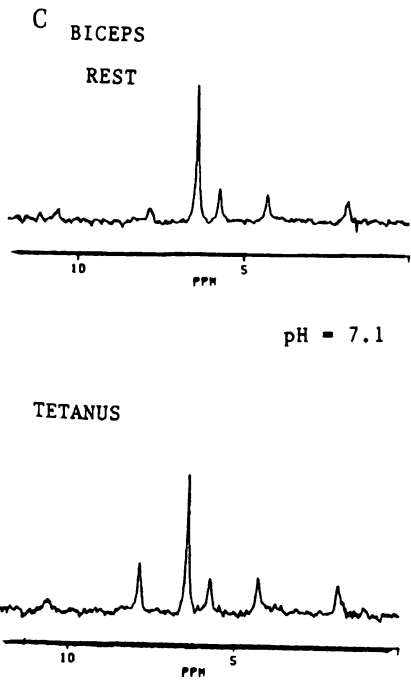
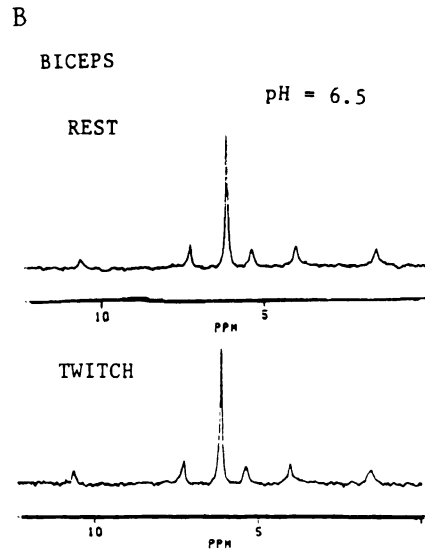
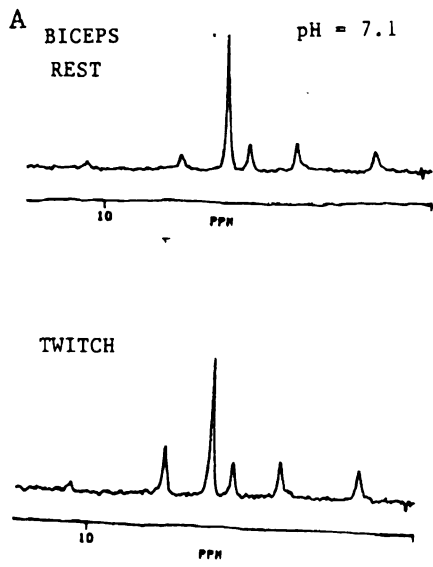


Figure 21. Energy cost ($\mu\text{mol PCr/g}$ muscle) per isometric contraction (tetanus or 10 twitches) during normocapnic (5% CO_2 -95% O_2) and hypercapnic (70% CO_2 -30% O_2) perfusion of soleus and biceps muscles.

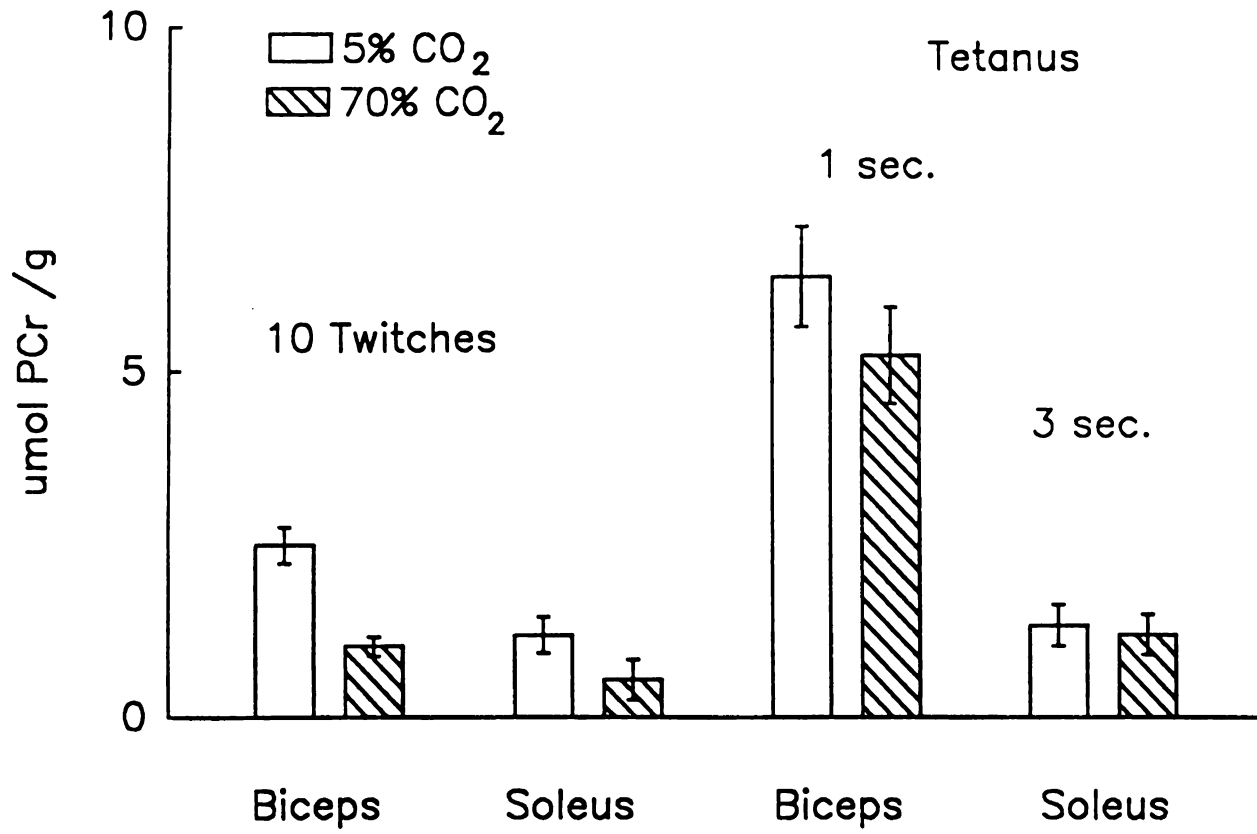
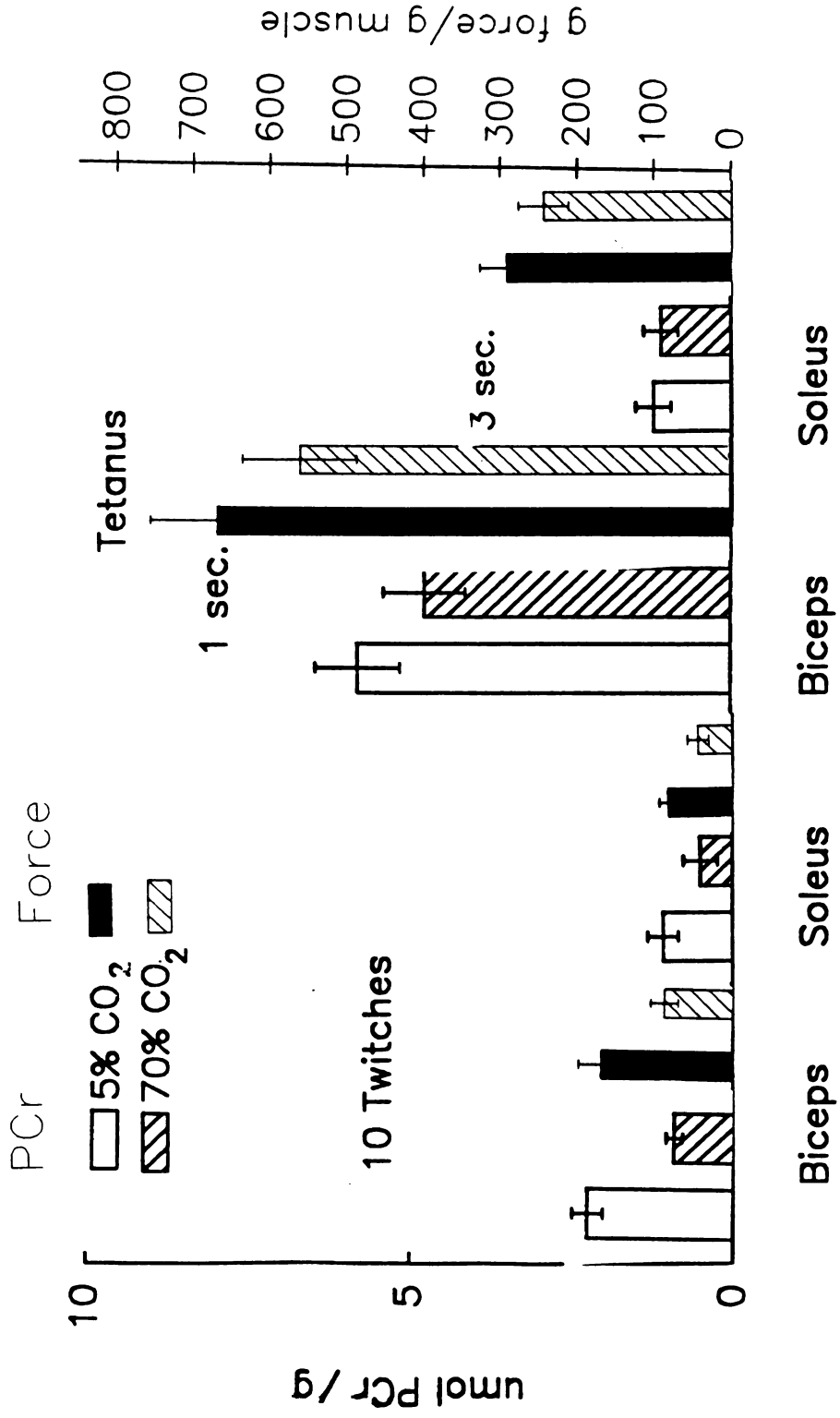


Figure 22. Energy cost (mol PCr/g muscle) and force production per isometric contraction (tetanus or 10 twitches) during normocapnic (5% CO₂-95% O₂) and hypercapnic (70% CO₂-30% O₂) perfusion of soleus and biceps muscles.



DISCUSSION

In this study we estimated the ATP cost of isometric contractions from the change in PCr in spectra acquired immediately before and after the contractions. This assumes that glycolysis and aerobic metabolism make no significant contribution to ATP production during the brief time of a single tetanus or a short burst of twitches. This assumption has been validated in rat hindlimb muscle (Foley and Meyer, 1993). The PCr cost of contractions measured by gated NMR was the same as that calculated by others from steady-state oxygen consumption measurements. Similarly, PCr cost of contractions measured chemically in mouse muscles was the same as that calculated from recovery oxygen consumption after the contractions (Crow and Kushmerick, 1982).

As expected from many previous studies, we found that the ATP cost of both twitch and tetanic contractions under normocapnic conditions was less in slow-twitch than in fast-twitch muscle. These measurements include both the ATP cost of calcium cycling and force development (i.e. internal shortening), as well as the cost of isometric force maintenance. However, it appears that the greatest difference between the muscle types is in the cost of force maintenance. The cost of twitch contractions was only about two-fold higher in biceps compared to soleus muscle. In contrast, the ATP cost of a 3 s tetanus in soleus muscle was less than 1/3 the ATP cost of a 1 s tetanus in the

fast-twitch biceps muscle. Thus, the economy of isometric force maintenance is at least 4-fold higher in soleus compared to biceps muscle. This indicates that isometric force is not necessarily a good measure of energy consumption during contraction, at least between different muscle types. Thus, although a previous study (Adams et al. 1990) had shown that intracellular acidosis did not decrease tetanic force, it was still possible that acidosis altered the economy of contractions.

In fact, this study shows that acidosis has little effect on the economy of force maintenance in either muscle type. Acidosis had no effect on the ATP cost of tetanic contractions, nor on the peak tetanic force. Furthermore, although acidosis did cause a decrease in the ATP cost of twitch contractions, this decrease occurred in proportion to the decrease in peak twitch force. Therefore, we conclude that acidosis, at least to pH 6.6, has no significant effect on the rate of cross-bridge cycling in intact muscle. In contrast to the results obtained in skinned fibers, this suggests that the maximum velocity of shortening would also not be significantly compromised by acidosis in intact skeletal muscle. The reason for this discrepancy between results in skinned fibers versus intact muscle is not clear. One possibility is that the effect of acidosis is temperature dependent. Skinned fiber studies are typically conducted at 25°C, whereas these studies were conducted at physiological temperature. Alternatively, it

may be that acidosis has an effect on the spacing of actin and myosin filaments in skinned fibers which does not occur in intact muscle fibers.

Although we find no evidence supporting that acidosis alters rates of cross-bridge cycling during contractions, it is clear that acidosis does directly alter both calcium release and sequestration processes in intact muscle. This is consistent with a number of previous studies which suggest that acidosis alters the kinetics of calcium release channels and the Ca^{++} ATPase pump in sarcoplasmic reticulum (Hasselbach and Oetliker, 1983).

In summary, the results of this study suggest that intracellular acidosis down to pH 6.6 has no significant effect on the intrinsic ATP cost of contractions (i.e. ATP cost/force) in either fast- or slow-twitch muscle. Although twitch force is reduced by acidosis, the ATP cost of a twitch decreases in proportion to twitch force.

CHAPTER 5

CONTROL OF RESPIRATION IN SLOW-TWITCH MUSCLE.

INTRODUCTION

There is overwhelming evidence that the recruitment of mitochondrial ATP production in skeletal muscle is primarily controlled by levels of cytoplasmic phosphate metabolites or "phosphorylation state". However, the specific mechanism of this control is still controversial. The two most frequently cited hypotheses are 1) simple kinetic control by cytoplasmic ADP concentration and 2) thermodynamic control by cytoplasmic free energy of ATP hydrolysis.

In an elegant analysis, Connett showed that these two hypotheses would be difficult to distinguish by simple correlative experiments in intact muscle, because the predictions of both models are similar (Connett, 1988b; Gyulai *et al.*, 1985; Connett *et al.*, 1990). For example, both predict that there should be roughly a linear decrease in PCr as stimulation rate is increased, at least over the submaximal range below 50-60% of the muscles maximum oxygen consumption. However, Connett also suggested that these models could be tested by examining the rate of respiration while experimentally manipulating one of the system variables independent of stimulation rate. In particular, it should be possible to test the ADP hypothesis by

manipulating intracellular pH independently of changes in other metabolites (Connett, 1988a).

There are distinct predictions of the two models with acidosis. The kinetic model predicts that oxygen consumption should depend on total ADP concentration in a simple Michelis-Menton fashion, with a K_m of 20 - 50 μm :

$$\frac{QO_2}{QO_{2\text{max}}} = \frac{1}{1 + K_m/[ADP]}$$

Assuming that the creatine kinase reaction is near equilibrium, then the relationship between ADP and PCr depends on pH:

$$QO_2 \propto [ADP] = \frac{[ATP][Cr]}{K_{ck}[PCr][H^+]}$$

Thus, according to this view, if hydrogen ions are independently increased, but the rate of respiration is held constant, then PCr must decrease to maintain the same ADP concentrations. Alternatively, if pH is decreased, and PCr and ATP are observed not to change (as is the case in resting muscle, see Chapter 4), then ADP, and hence oxygen consumption should decrease. More generally, this model predicts that acidosis should always result in relatively

decreased steady-state PCr compared to non-acidic muscles respiring at the same rate.

Thermodynamic models predict that respiration should be proportional to the difference between the cytoplasmic free energy of ATP hydrolysis, and an intramitochondrial energy term, which depends on oxygen and intramitochondrial NADH/NAD ratio. Assuming the latter are constant then:

$$QO_2 = \Delta G^{\circ}_{ATP} - RT \ln \frac{[ATP]}{[ADP][Pi][H^+]} - \Delta G_{mito}$$

or,

$$QO_2 \propto \ln \frac{[ATP]}{[ADP][Pi][H^+]^{\alpha}}$$

where $\alpha = 0.63$ at pH 7, and 0.34 at pH 6.5. This logarithmic term includes the dependence of ATP free energy on pH, which, however, can be factored out:

$$QO_2 \propto \ln \frac{[ATP]}{[ADP][Pi]} + \ln 1/[H]^{\alpha}$$

Thus, the thermodynamic model predicts that oxygen consumption should be linearly dependent on cytoplasmic phosphorylation potential. In addition, the slope of the relationship should be the same under both normal and acidic conditions, although the y-intercept should decrease

with an increase in hydrogen ion concentration. Note, however, if the pH change is not confined to the cytoplasm, the exact extent of the y-intercept change cannot be predicted from the above, since a change in ΔG_{mito} would also change the y-intercept. Meyer's linear model is basically consistent with this prediction, since [PCr] is directly proportional to $\ln [\text{ATP}]/[\text{ADP}][\text{Pi}]$, even though the model does not specifically include the effect of changes in pH.

The above predictions (and Connett's analysis) assume that acidosis has no direct effect on mitochondrial enzymes. In fact, there is evidence that acidosis decreases the maximum state 3 respiratory rate of isolated mitochondria (Westerblad and Lannergren, 1988, Tobin et al., 1972; Chang and Mergner, 1973). If the same effect occurs in intact muscle, then both models predict that the regulatory signal should change to a greater extent at the same absolute rate of respiration during acidic stimulation, as compared to during normal stimulation. This would be predicted since the absolute respiratory rate would correspond to a greater percentage of the maximum rate. For the ADP control model, this would require even higher ADP, and hence lower PCr, at any respiration rate under acidic compared to control conditions. For the thermodynamic model, the slope of the relationship between respiratory rate and phosphorylation potential should change in proportion to the change in maximum respiratory

rate. This can be easily seen from the linear model because the slope ($-1/\rho\tau$) of the relationship between PCr and oxygen consumption is dependent on R_m (with $\tau = R_m C$), and $1/R_m$ is proportional to the maximum mitochondrial capacity, the slope would be expected to change in proportion to the difference in mitochondrial capacity. Therefore, the relationship between cytoplasmic phosphorylation potential and oxygen consumption would be linear, with a change in slope proportional to the decrease in mitochondrial capacity.

The purpose of this study was to test the above predictions by examining the effect of hypercapnic acidosis on the relationship between PCr, ADP, and phosphorylation potential versus respiratory rate in intact cat soleus muscle at rest and during moderate stimulation. Intracellular pH was decreased by changing the gas content of the perfusate in isolated perfused cat soleus muscles (Adams et al., 1991). Metabolite concentrations (PCr, Pi, ATP, and pH) were measured by ^{31}P -NMR and oxidative rates were calculated from oxygen consumption measurements in the slow-twitch muscles. Although interpretation of the study was complicated by the observation that acidosis decreased the maximum aerobic capacity of muscle, the results are clearly not consistent with the simple ADP model of respiratory control, but do remain consistent with thermodynamic models.

MATERIALS AND METHODS.

Surgical Techniques

Adult cats were anesthetized with ketamine chloride (15 mg/kg) subcutaneously and sodium pentobarbital intravenously (30 mg/kg) and artificially ventilated. The soleus muscle was isolated and excised as previously described (Chapter 2). In brief, muscle groups surrounding the soleus were carefully dissected and gently drawn away. Soleus muscle blood supply was isolated by ligating and severing the supplying arteries and draining veins. The artery supplying the soleus was cannulated (PE 50) and perfused at $0.2 - 0.4 \text{ ml min}^{-1} \text{ g}^{-1}$, 80 - 100 Torr, with a 20% suspension of sheep red blood cells in bicarbonate-buffered Krebs-Henseleit solution. Perfusate was equilibrated with either 5% CO_2 -95% O_2 or 70% CO_2 -30% O_2 at 37°C in a Silastic® tube oxygenator. The muscle was stretched to optimal length for maximum isometric twitch force development. Muscles were stimulated by a supramaximal square wave pulses (10-50V, 1 ms) applied from a Grass stimulator.

Experimental Series I/Phosphorous NMR

The isolated soleus was placed within a 2 cm Helmholtz coil within a custom made 7.4 cm diameter probe. The proximal bone and distal tendon were secured by custom built Delrin® clamps. The distal clamp was attached to a strain gauge force transducer. Platinum wire electrodes

were securely placed on each end of the muscle for direct stimulation. Muscle temperature was monitored by a thermistor and maintained at 37°C.

Phosphorus NMR spectra of isolated perfused soleus muscles were acquired at 162 MHz on a Bruker AM400 wide bore spectrometer. In all experiments, the circuit was tuned with the muscle in place, and field homogeneity shimmed on the proton signal from muscle water. Fully relaxed spectra were acquired at rest under normocapnic and hypercapnic conditions (90° pulse width, 15 s rd, 16 or 32 scans). Spectra (90° pulse, 8 scans, 15 s rd, 22 spectra or 60° pulse, 32 scans, 1.67 s rd, 42 spectra) were acquired continuously during stimulation and recovery in both conditions. Each muscle was stimulated at two rates during normocapnia and hypercapnia (0.25, 0.5, or 1 Hz).

FID's were zero filled to 4K data points and multiplied by an exponential corresponding to 15-30 Hz line broadening. Peak integrals were computed after baseline correction and Fourier transformation. Steady-state PCr levels were determined by averaging the PCr integral of spectra acquired during the final 10 minutes of stimulation and by calculating a percentage relative to a spectrum acquired immediately prior to stimulation. PCr/ATP ratios were determined by calculating the ratio of integrals of PCr and ATP peaks and averaging from each muscle. Exponential time constants were computed by non-linear least squares fit.

Experimental Series II/Oxygen Consumption

In addition to the above surgical procedures the femoral vein branch draining the soleus was cannulated (PE 90) to obtain blood samples. Arterial blood samples were taken from a sampling port before and after each stimulation period. During stimulation successive venous blood samples were taken in the final 10 minutes of stimulation to ensure steady-state conditions. Blood flow was controlled by a peristaltic pump. Oxygen content was measured by a Lexcon Oxygen Analyzer (Lexington Instruments). Oxygen consumption was calculated by multiplying arterial minus venous oxygen content differences by flow and dividing by the muscle wet weight. The proximal bone was secured to a Plexiglas® mount and the distal tendon was attached to a commercial force transducer. Platinum electrodes were placed on each end of the muscle and each muscle was stimulated at two rates during normocapnia and hypercapnia (0.25, 0.5, 0.75, 1 or 2 Hz).

RESULTS

Figure 23 shows the PCr changes at stimulation rates of 0.25 and 0.5 Hz of one soleus muscle during normocapnia and hypercapnia. PCr levels decreased with increased stimulation rate under both conditions. PCr levels reached a lower steady-state at the same twitch rate during

normocapnia as compared to hypercapnia. The average time constant during normocapnia was 3.4 ± 0.33 minutes and during hypercapnia was 7.66 ± 1.0 minutes [Table 5]. The time constant of PCr changes was similar at onset of stimulation and during recovery within each condition.

Table 6 summarizes intracellular and extracellular pH and oxygen consumption at rest and during stimulation. Resting oxygen consumption was 0.098 ± 0.008 $\mu\text{mol O}_2/\text{min/g}$ wet weight during normocapnia and 0.103 ± 0.013 $\mu\text{mol O}_2/\text{min/g}$ wet weight during hypercapnia. Resting intracellular pH was 7.16 ± 0.06 during normocapnia and 6.6 ± 0.08 during hypercapnia. Intracellular pH was not significantly different from initial pH during the last 5-10 minutes of stimulation at either pH. However, there was a transient alkalinization during the first ten minutes stimulation at pH 6.6 [Figure 24] that is was not observed at normal pH.

There was not a consistent dependence of oxygen consumption on calculated [ADP] concentration during normocapnia and hypercapnia [Figure 25]. There was a linear dependence of steady-state oxygen consumption on steady-state PCr levels [Figure 26] during normocapnia (slope = -0.11, $r = 0.97$) and hypercapnia (slope = -0.04, $r = 0.99$). There was a linear relationship between $\ln[\text{ATP}]/[\text{ADP}][\text{Pi}][\text{H}^+]$ at pH 7.2 (slope = -0.78, $r = 0.97$, y-intercept = 10.4) and pH (6.6 slope = -0.26, y-intercept = 2.5), $r = 0.99$) [Figure 27].

Figure 23. PCr changes during soleus muscle stimulation (0.25 and 0.5 Hz) and recovery under normocapnic (open circles) and hypercapnic (closed circles) conditions.

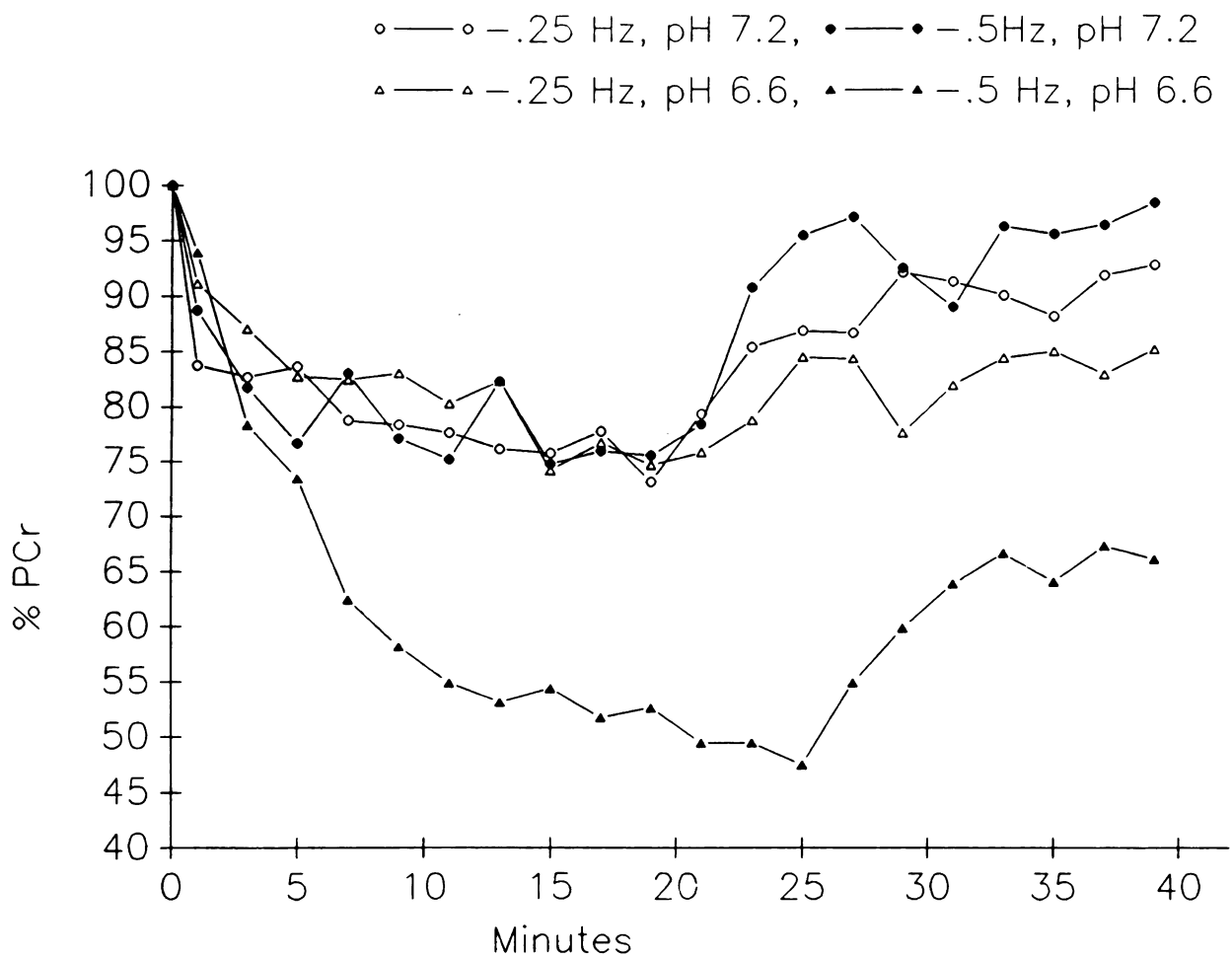


TABLE 5

PCr time constants
(minutes)

	<u>Normocapnia</u>	<u>Hypercapnia</u>
onset	3.23±0.5	7.73±0.95*
stimulation	(n=9)	(n=7)
recovery	3.56±0.44	7.58±2.0*
	(n=7)	(n=7)

Values are mean SE, * significantly different from normocapnia (p<0.05).

TABLE 6

	NORMOCAPNIA					HYPERCAPNIA			
HZ	0	0.25	0.5	1	2	0	0.25	0.5	1
<u>PCr</u>	2.94					3.0			
<u>ATP</u>	±0.14					±0.17			
<u>pH_{ic}</u>	7.16	7.19	7.18	7.17		6.6	6.55	6.57	
	±0.02	±0.02	±0.03	±0.04		±0.04*	±0.03*	±0.03*	
<u>pH_{ec}</u>	7.5					6.74			
	±0.03					±0.06*			
<u>QO₂</u>	0.098	0.295	0.464	0.585	0.848	0.102	0.205	0.26	0.189
<u>μmol/ min/g</u>	±0.01	±0.04	±0.08	±0.07	±0.2	±0.01	±0.05	±0.01	±0.08

(Values are mean ± SE, * significantly different from normocapnia at the same stimulation rate (p<0.05)).

Figure 24. pH changes during 0.25 and 0.5 Hz stimulation of soleus muscle during normocapnia (N=pH 7.2) and hypercapnia (A=pH 6.6). 0.5 Hz at pH = 7.2 (filled circles); 0.25 Hz at pH = 7.2 (open circles); 0.5 Hz, pH = 6.6 (closed triangles); 0.25 Hz, pH = 6.6 (open triangles).

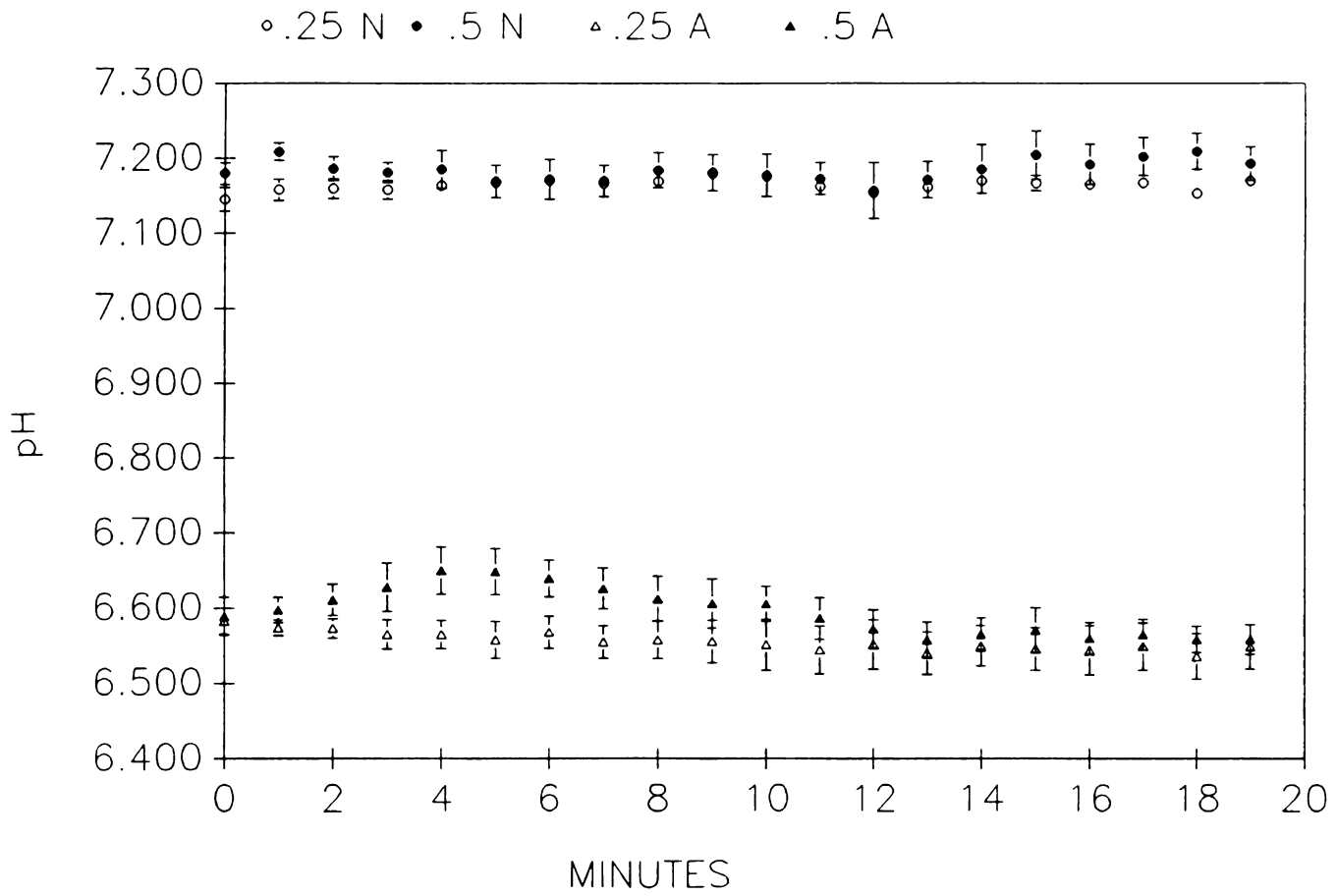


Figure 25. [ADP] versus oxygen consumption at 0.25 and 0.5 Hz during hypercapnia and 0.25, 0.5 and 1 Hz during normocapnia. Calculated [ADP] from creatine kinase equilibrium assuming apparent $K_{eq} = 1.66$. At rest [ATP] = 5.03 mM, total Cr = 24.4 mM, and Pi = 10.1 mM from chemical analysis of perfused muscles (Meyer et al., 1985). pH = 6.6 (filled circles); pH = 7.2 (open circles).

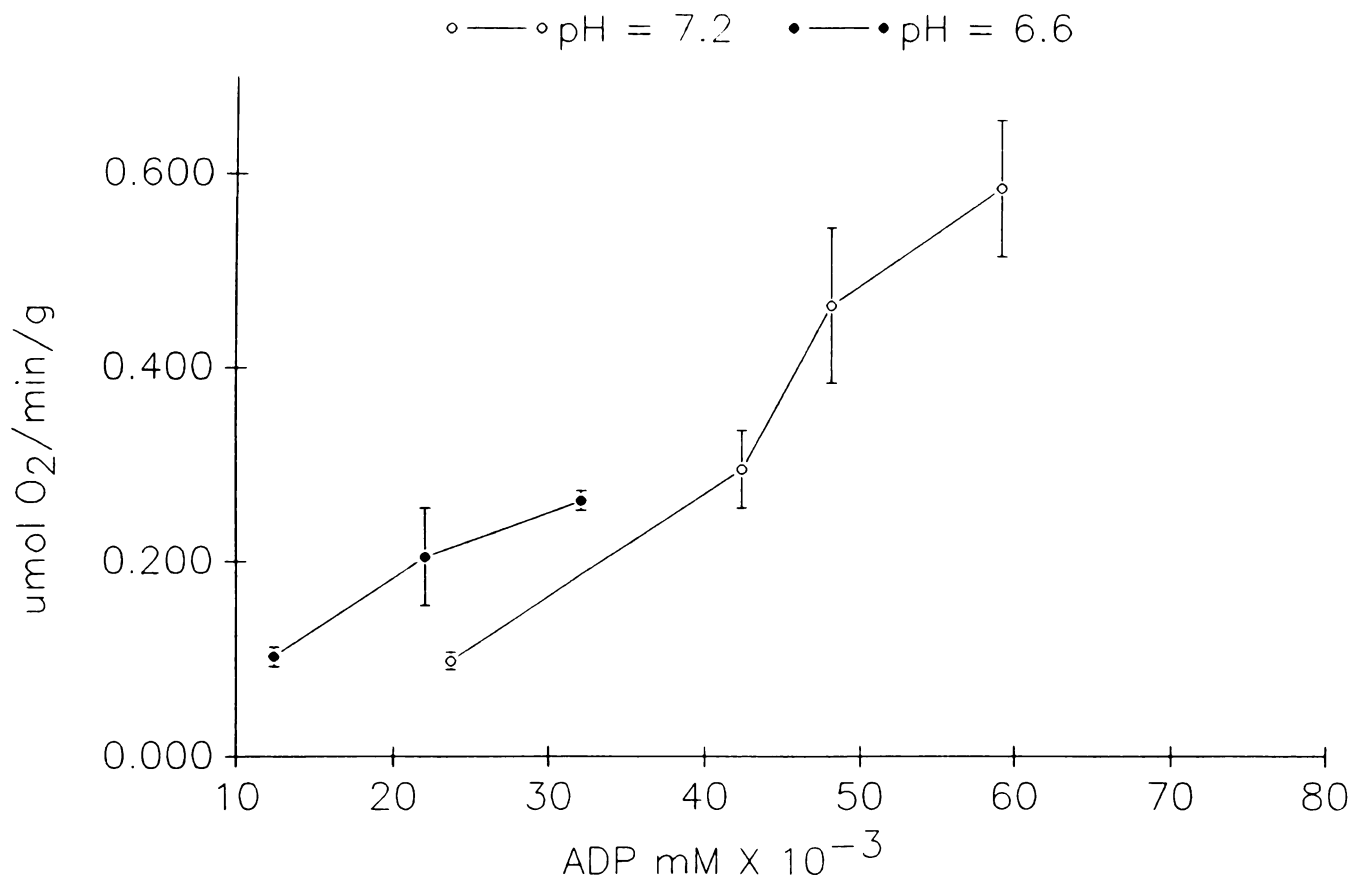


Figure 26. Steady-state PCr levels versus oxygen consumption of soleus muscle during rest and stimulation at 0.25 and 0.5 Hz during hypercapnia (pH = 6.6) and 0.25, 0.5, and 1 Hz during normocapnia (pH = 7.2). pH = 6.6 (filled circles, $r = 0.99$); pH = 7.2 (open circles, $r = 0.97$) .

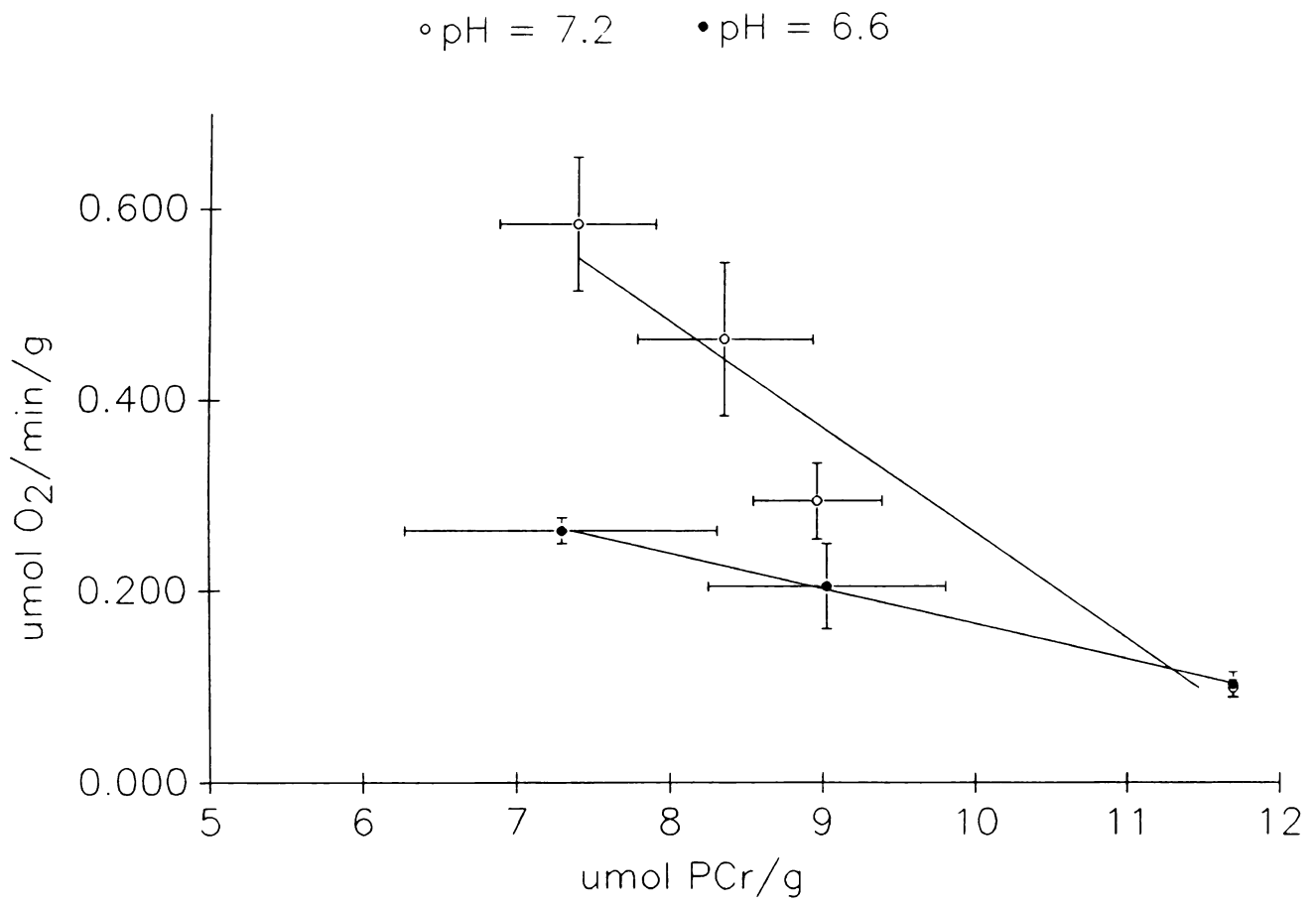
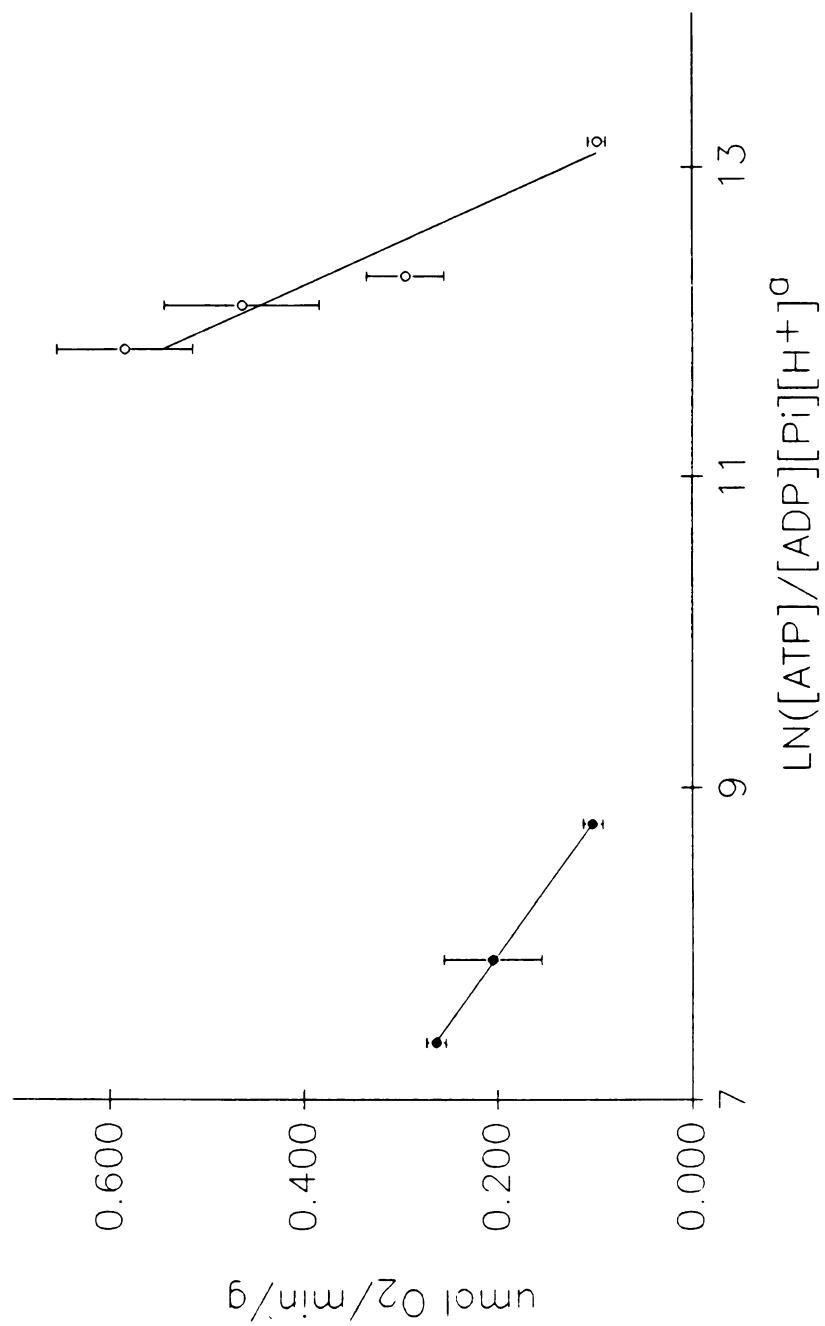


Figure 27. Steady-state cytoplasmic phosphorylation potential versus oxygen consumption of soleus muscle during rest and stimulation at 0.25 and 0.5 Hz during hypercapnia and 0.25, 0.5 and 1 Hz during normocapnia. Calculated [ADP] from creatine kinase equilibrium assuming apparent $K_{eq} = 1.66$. At rest [ATP] = 5.03 mM, total Cr = 24.4 mM, and Pi = 10.1 mM from chemical analysis of perfused muscles (Meyer et al., 1985). pH = 7.2 (open circles, $r = 0.97$); pH = 6.6 (closed circles, $r = 0.99$).

◦ pH = 7.2 • pH = 6.6



Discussion

Several studies of isolated mitochondria suggest that decreased pH results in decreased maximum oxygen consumption (Westerblad and Lannergren, 1988; Tobin et al., 1972; Chang and Mergner, 1973). Two features of our results appear to confirm that acidosis has the same effect on maximum oxygen consumption in intact skeletal muscle. First, in our study the time constants for PCr changes during the onset of stimulation and during recovery were 2-fold longer during acidosis. Because the time constant for PCr changes is inversely proportional to maximum aerobic capacity, this suggests that maximum aerobic capacity was decreased by 2-fold. Second, direct measurements of oxygen consumption showed that it did not significantly increase above $0.189 \mu\text{mol}/\text{min}/\text{g}$ during acidosis, but reached at least $0.848 \mu\text{mol}/\text{min}/\text{g}$ under normal pH conditions.

Our results are not consistent with a recent study by Nioka, et al (1992), which did not find a reduction in maximum oxygen consumption during acidosis in intact muscle. They not only found the V_{max} of oxidative phosphorylation to be similar between normal and low pH stimulation, but also found a dependence of respiration on cytoplasmic [ADP] in intact skeletal muscle. They observed a dependence of work (proportional to oxygen consumption) on [ADP] in a Michaelis-Menton fashion with an estimated K_m of $26 \mu\text{M}$, *in vivo*. One of their assumptions was that an increase in proton concentration will result in a decrease

in PCr levels. Results from our studies (Table 6, see also Chapter 4) do not confirm this assumption since at rest, during normocapnia and hypercapnia, the PCr, ATP, and Pi concentrations are similar. They also use the tension-time integral to estimate oxygen consumption, but used submaximal voltages during stimulation so the fraction of fibers that were actually contracting is obscure, and this may have affected their results. Also, they induced hypercapnia by ventilating the animal with 20% CO₂ for several hours, which most likely introduced several physiological alterations that may also have complicated the results of the experiment.

Our results are not compatible with the simple kinetic ADP theory of respiratory control. At rest, with an experimentally imposed increase in hydrogen ion concentration, you would expect either a lower oxygen consumption rate (if PCr was constant) or a decrease in PCr levels (if oxygen consumption was constant). We did not observe a significant difference in PCr levels or oxygen consumption rate at rest between normal and low pH conditions. Also, at any given respiration rate during stimulation, you would expect lower PCr levels and correspondingly a higher [ADP]. Furthermore, because the maximum oxidative rate was reduced, ADP should have been even higher than predicted from the pH change alone. In fact, we observed lower cytoplasmic [ADP] at similar oxidative rates during acidic stimulation. These results

are difficult to reconcile with control of respiration by total cytoplasmic ADP.

Our data is consistent with linear models of the control of respiration with cytoplasmic phosphorylation potential as the signal for oxidative phosphorylation. The time constants were similar during stimulation and recovery at each pH, consistent with predictions of the linear model proposed by Meyer. Steady-state oxygen consumption was linearly related to steady-state PCr levels at both pH values, although the slope during acidosis was reduced over 2-fold. This decrease in slope would be expected since the mitochondrial capacity was reduced by over 50% during hypercapnia.

The relationship between cytoplasmic phosphorylation potential and oxygen consumption was also linear with a significant reduction in y-intercept and slope during acidosis. These results are consistent with the predictions for thermodynamic models, as again, the slope change can be attributed to the decreased mitochondrial capacity. The reduction of y-intercept was expected due to the increase in hydrogen ion concentration, although the exact attenuation cannot be determined because the free energy potential within the mitochondrial may also change with acidosis.

The reduction of mitochondrial capacity in intact skeletal muscle tissue with acidosis also has implications for the controversy about the role of acidity in fatigue.

Taken together with the observation of no reduction in maximal force production, our observation that the maximum aerobic capacity is decreased, suggests that the correlation seen between acidosis and fatigue in human studies may be due to the restriction of ATP supply rather than a direct inhibition at the crossbridges.

Another interesting feature of our results is the transient alkalinization during the initial stages of stimulation during acidosis. Transient alkalinization at the beginning of contraction has been contributed to the net consumption of protons by PCr hydrolysis (see Equation 3, chapter 1). Because the stoichiometric coefficient increases as pH decreases you would expect a larger transient alkalinization at lower pH. This is exactly what we observed, confirming that the net alkalinization at the beginning of contraction is due to the effect of PCr hydrolysis.

In summary our study eliminates total cytoplasmic ADP level as the primary regulator of respiration but does remain consistent with thermodynamic theories of control of respiration with cytoplasmic phosphorylation as the signal for stimulation of oxidative phosphorylation

CHAPTER 6

SUMMARY AND CONCLUSIONS

The primary focus of this research was to distinguish between the two prominent models of the control of oxidative phosphorylation. The kinetic model of respiration states that oxidative phosphorylation is limited by ADP availability and should follow a Michaelis-Menton dependence of respiratory rate of cytoplasmic [ADP]. Thermodynamic models of the control of respiration argue that the mitochondria is regulated by cytosolic phosphorylation potential. Correlative experiments relating phosphate changes and oxygen consumption coincide satisfactorily with both theories. Yet, by manipulating intracellular pH the theories can be distinguished.

In fast-twitch muscle, several studies have confirmed that phosphorylation state, i.e. one of the primary models, controls respiration. Yet, in slow-twitch muscle some studies suggest control by substrate availability. Our initial experiments focused on whether slow-twitch muscle was regulated by phosphorylation state. Our results support that phosphorylation state regulates respiration in slow-twitch muscle *in situ* although it did not specifically distinguish between the two primary models.

The remainder of the research focused on distinguishing between the two models of the control of respiration by changing the intracellular concentration of hydrogen ion. Previous studies indicated that the relaxation times of isometric contractions were reduced but that maximal force was not attenuated. This suggested that energy cost may be different with twitch contractions during acidosis and therefore it was important to explore this energetic parameter in order to design our experiments to test the two models of the control of respiration during acidosis. We then implemented experiments to determine the energy cost of contraction of fast-and slow-twitch muscle during acidosis. Our data showed that energy cost of contraction was reduced during acidosis during twitch contractions but not during tetanus in both muscle types.

The reduction of energy cost in skeletal muscle could be attributed to several factors. The velocity of contraction could be reduced, the reactions involved in contraction inhibited, or calcium cycling attenuated. Although the energy cost could be attributed to force reduction with twitch contractions, maximal force output was not inhibited. This would suggest that acidosis is not exerting its effects on the crossbridge itself but possibly on calcium handling. Previous studies with ATP depletion have shown a reduction in energy cost without a reduction in force. This energy cost may also be attributable to an affect on calcium handling. This hypothesis could be

tested by designing experiments that stimulate the muscle fibers while stretched beyond the length of crossbridge attachment. The muscle would not be able to develop force but enzymes involved in calcium cycling would be activated. By measuring energy cost during normal and acidic conditions this hypothesis could be addressed. Additional studies could be designed to directly measure the velocity of contraction during acidosis.

The final series of experiments were then designed to test the control of oxidative phosphorylation at rates within the maximum aerobic capacity of slow-twitch skeletal muscle. Our data supports the control of respiration by cytosolic phosphorylation potential, a direct prediction of thermodynamic models since respiration is directly dependent on cytosolic phosphorylation state at various pH values. In contrast, our data is not consistent with the simple kinetic theory of control of respiration since there was not a consistent dependence of respiration on [ADP] during acidosis.

There was also a reduction in maximal oxygen consumption with low pH. Several studies have implicated acidosis as an important player in fatigue by exerting effects directly on the crossbridges. Again, when considered with the absence of maximal force reduction this would imply that acidosis may not directly affect the crossbridge but limit the amount of ATP available for muscle contraction during fatigue. This limitation of the

mitochondria may also be due to inhibition of calcium kinetics. Unfortunately, a precise measurement of intracellular calcium fluxes in intact muscles is not currently available. Further study of these questions is warranted.

In summary, we conclude that the control of respiration is regulated by cytosolic phosphorylation potential and not by ADP availability in skeletal muscle.

LIST OF REFERENCES

- Adams, G.R., J.M. Foley, and R.A. Meyer. Muscle buffer capacity estimated from pH changes during rest-to-work transitions. J. Appl. Physiol. 69(3): 968-972, 1990.
- Adams, G.R., M.J. Fisher, and R.A. Meyer. Hypercapnic acidosis and increased H₂PO₄⁻ concentration do not decrease force in cat skeletal muscle. Am. J. Physiol. 260: C805-C812, 1991.
- Alberty, R.A. Effect of pH and metal ion concentration on the equilibrium hydrolysis of adenosine triphosphate to adenosine diphosphate. J. Biol. Chem. 243(7): 1337-1343, 1968.
- Allen, D.G. and C.H. Orchard. The effects of changes of pH on intracellular calcium transients in mammalian cardiac muscle. J. Physiol. (Lond.) 335: 555-567, 1983.
- Argov, Z., W.J. Bank, J. Maris, S. Eleff, N.G. Kennaway, D. Phil, R.E. Olson, and B. Chance. Treatment of mitochondrial myopathy due to complex III deficiency with vitamins K₃ and C:A ³¹P-NMR follow-up study. Ann. Neurol. 19: 598-602, 1986.
- Arnold, D.L., P.M. Matthews, and G.K. Radda. Metabolic recovery after exercise and the assessment of mitochondrial function in vivo in human skeletal muscle by means of ³¹P NMR. Magn. Reson. Med. 1: 307-315, 1984.
- Bailey, I.A., S.R. Williams, G.K. Radda, and D.G. Gadian. Activity of phosphorylase in total global ischaemia in the rat heart. Biochem. J. 196: 171-178, 1981.
- Balaban, R.S. The application of nuclear magnetic resonance to the study of cellular physiology. Am. J. Physiol. 246: C10-C19, 1984.
- Balaban, R.S. Regulation of oxidative phosphorylation in the mammalian cell. Am. J. Physiol. 258: C377-C389, 1990.
- Baldwin, K.M. and C.M. Tipton. Work and metabolic patterns of fast and slow twitch skeletal muscle contracting in situ. Pflugers Arch. 334: 345-356, 1972.

Belitzer, V.A. and E.T. Tzibakowa. . Biokhimiya 4(5): 516-535, 1939.

Bessman, S.P. and A. Fonyo. The possible role of the mitochondrial bound creatine kinase in regulation of mitochondrial respiration. Biochem. Biophys. Res. Comm. 22: 597-602, 1966.

Bessman, S.P. and P.J. Geiger. Transport of energy in muscle: the phosphorylcreatine shuttle. Science 211: 448-452, 1981.

Bienfait, H.F., J.M.C. Jacobs, and E.C. Slater. Mitochondrial oxygen affinity as a function of redox and phosphate potentials. Biochim. Biophys. Acta 376: 446-457, 1975.

Blanchard, E.M. and R.J. Solaro. Inhibition of the activation and troponin calcium binding of dog cardiac myofibrils by acidic pH. Circ. Res. 55: 382-391, 1984.

Bockman, E.L., J.E. McKenzie, and J.L. Ferguson. Resting blood flow and oxygen consumption in soleus and gracilis muscles of cats. Am. J. Physiol. 239: H516-H524, 1980.

Bockman, E.L. Blood flow and oxygen consumption in active soleus and gracilis muscles in cats. Am. J. Physiol. 244: H546-H551, 1983.

Bolitho Donaldson, S.K. and L. Hermansen. Differential, direct effects of H^+ and Ca^{2+} -activated force of skinned fibers from the soleus, cardiac and adductor magnus muscles of rabbits. Pflugers Arch. 376: 55-65, 1978.

Burton, A.C. The properties of the steady state compared to those of equilibrium as shown in characteristic biological behavior. Pflugers Arch. 327-349, 1.

Cain, D.F. and R.E. Davies. Breakdown of adenosine triphosphate during a single contraction of working muscle. Biochem. Biophys. Res. Comm. 8: 361-366, 1962.

Chance, B. The response of mitochondria to muscular contraction. Annals New York Academy of Sciences: 477-489, 1965.

Chance, B., S. Eleff, jr. Leigh, J.S., D. Sokolow, and A. Sapega. Mitochondrial regulation of phosphocreatine/inorganic phosphate ratios in exercising human muscle: A gated ^{31}P NMR study. Proc. Natl. Acad. Sci. USA 78(11): 6714-6718, 1981.

Chance, B., J.S. Leigh, B.J. Clark, J. Maris, J. Kent, S. Nioka, and D. Smith. Control of oxidative metabolism and oxygen delivery in human skeletal muscle: A steady-state analysis of the work/energy cost transfer function. Proc. Natl. Acad. Sci. USA 82: 8384-8388, 1985.

Chance, B., J.S. Leigh, J. Kent, and K. McCully. Metabolic control principles and ^{31}P NMR. Federation Proc. 45: 2915-2920, 1986.

Chance, B., A. Waterland, and A. Tanaka. Mitochondrial function in normal and genetically altered cells and tissues. Annals New York Academy of Sciences 360-373, 1992.

Chance, B. and C.M. Connelly. A method for the estimation of the increase in concentration of adenosine diphosphate in muscle sarcosomes following a contraction. Nature 179: 1235-1237, 1957.

Chance, B. and H. Conrad. Acid-linked functions of intermediates in oxidative phosphorylation. Nature 234(6): 1568-1570, 1959.

Chance, B. and P.K. Maitra. Determination of the intracellular phosphate potential of ascites cells by reversed electron transfer. Annals New York Academy of Sciences 307-332, 1.

Chance, B. and G.R. Williams. A simple and rapid assay of oxidative phosphorylation. Nature 175: 1120-1121, 1955.

Chance, B. and G.R. Williams. The respiratory chain and oxidative phosphorylation. In: Adv. Enzymol. Relat. Subj. Biochem. 17, 1956: p. 65-134.

Chang, R. Physical Chemistry with Applications to Biological Systems. Macmillan Publishing Co., Inc., Lond, 1981.

Chang, S.H. and W.J. Mergner. The effect of hydrogen ion concentration on mitochondrial respiration, oxidative phosphorylation, and morphology. Lab. Invest. 28: 380, 1973. (Abstract)

Chase, P.B. and M.J. Kushmerick. Effects of pH on contraction of rabbit fast and slow skeletal muscle fibers. Biophys. J. 53: 935-946, 1992.

Claflin, D.R. and J.A. Faulkner. Shortening velocity extrapolated to zero load and unloaded shortening velocity of whole rat skeletal muscle. J. Physiol. (Lond.) 359: 357-363, 1985.

Close, R.I. Dynamic properties of mammalian skeletal muscles. Physiol. Rev. 52: 129-196, 1972.

Connett, R.J. Analysis of metabolic control: new insights using scaled creatine kinase model. Am. J. Physiol. 254: R949-R959, 1988a.

Connett, R.J. The cytosolic redox is coupled to VO_2 . A working hypothesis. Adv. Exp. Med. Biol. 222: 133-142, 1988b.

Connett, R.J., C.R. Honig, E.J. Gayeski, and G.A. Brooks. Defining hypoxia: a systems view of VO_2 , glycolysis, energetics, and intracellular PO_2 . J. Appl. Physiol. 68(3): 933-842, 1990.

Connett, R.J. and C.R. Honig. Regulation of VO_2 in red muscle: do current biochemical hypotheses fit in vivo data? Am. J. Physiol. 256: R898-R906, 1989.

Cooke, R., K. Franks, G.B. Luciani, and E. Pate. The inhibition of rabbit skeletal muscle contraction by hydrogen ions and phosphate. J. Physiol. 395: 77-97, 1988.

Cooke, R. Force generation in muscle. Cell 2: 62-66, 1990.

Cooke, R. and E. Pate. The effects of ADP and phosphate on the contraction of muscle fibers. Biophys. J. 48: 789-798, 1985.

Crow, M.T and M.J. Kushmerick. Chemical energetics of slow- and fast-twitch muscles of the mouse. J. Gen. Physiol. 79: 147-166, 1982.

Curtin, N.A., K. Kometani, and R.C. Woledge. Effect of intracellular pH on force and heat production in isometric contraction of frog muscle fibres. J. Physiol. (Lond.) 396: 93-104, 1988.

Dawson, M.J., D.G. Gadian, and D.R. Wilkie. Contraction and recovery of living muscles studied by ^{31}P nuclear magnetic resonance. J. Physiol. (Lond.) 267: 703-735, 1977.

Dawson, M.J., D.G. Gadian, and D.R. Wilkie. Muscular fatigue investigated by phosphorus nuclear magnetic resonance. Nature 274: 861-866, 1978.

Dawson, M.J., D.G. Gadian, and D.R. Wilkie. Mechanical relaxation rate and metabolism studied in fatiguing muscle by phosphorus nuclear magnetic resonance. J. Physiol. (Lond.) 299: 465-484, 1980.

Dawson, M.J. The relation between muscle contraction and metabolism: studies by ^{31}P -nuclear magnetic resonance spectroscopy. Adv. Exp. Med. Biol. 226: 433-448, 1988.

Donaldson, S.K.B. and L. Hermansen. Differential, direct effects of H^+ on Ca^{2+} -activated force of skinned fibers from soleus, cardiac and adductor magnus muscles of rabbits. Pflugers Arch. 376: 55-65, 1978.

Donaldson, S.K.B. and W.G.L. Kerrick. Characterization of the effects of Mg^{2+} on Ca^{2+} and Sr^{2+} activated tension generation of skinned skeletal muscle fibers. J. Gen. Physiol. 66: 427-444, 1975.

Engelhardt, W.A. . Biochem. Z. 251: 343-368, 1932.

Erecinska, M., R.L. Veech, and D.F. Wilson. Thermodynamic relationships between the oxidation-reduction reactions and the ATP synthesis in suspensions of isolated pigeon heart mitochondria. Arch. Biochem. Biophys. 160: 412-421, 1974.

Erecinska, M., M. Stubbs, Y. Miyata, C.M. Ditre, and D.F. Wilson. Regulation of cellular metabolism by intracellular phosphate. Biochim. Biophys. Acta 462: 20-35, 1977.

Erecinska, M. and D.F. Wilson. Homeostatic regulation of cellular energy metabolism. TIBS 219-223, 1978.

Erecinska, M. and D.F. Wilson. Regulation of cellular energy metabolism. J. Membrane Biol. 70: 1-14, 1982.

Fabiato, A. and F. Fabiato. Effects of pH on the myofilaments and the sarcoplasmic reticulum of skinned cells from cardiac and skeletal muscles. J. Physiol. (Lond.) 276: 233-255, 1978.

Foley, J.M., S.J. Harkema, and R.A. Meyer. Decreased ATP cost of isometric contractions in ATP-depleted rat fast-twitch muscle. Am. J. Physiol. 261: C872-C881, 1991.

Foley, J.M. and R.A. Meyer. Energy cost of twitch and tetanic contractions of rat muscle estimated in situ by gated ^{31}P NMR. NMR Biomed 5: 1992.

From, A.H.L., M.A. Petein, S.P. Michurski, S.D. Zimmer, and K. Ugurbil. ^{31}P -NMR studies of respiratory regulation in the intact myocardium. FEBS Letters 206(2): 257-261, 1986.

Funk, C.I., Jr. Clark, A., and R.J. Connett. A simple model of aerobic metabolism: applications to work transitions in muscle. Am. J. Physiol. 258: C995-C1005, 1990.

Gadian, D.G., G.K. Radda, T.R. Brown, E.M. Chance, M.J. Dawson, and D.R. Wilkie. The activity of creatine kinase in frog skeletal muscle studied by saturation-transfer nuclear magnetic resonance. Biochem. J. 194: 215-228, 1981.

Gilbert, C., K.M. Kretzschmar, D.R. Wilkie, and R.C. Woledge. Chemical change and energy output during muscular contraction. J. Physiol. (Lond.) 218: 163-193, 1971.

Gillies, R.J., K. Ugurbil, J.A. Den Hollander, and R.G. Shulman. ^{31}P NMR studies of intracellular pH and phosphate metabolism during cell division cycle of *Saccharomyces cerevisiae*. Proc. Natl. Acad. Sci. USA 78(4): 2125-2129, 1981.

Godt, R.E., and T.M. Nosek. Changes of intracellular milieu with fatigue or hypoxia depress contraction of skinned rabbit skeletal and cardiac muscle. J. Physiol. (Lond.) 412: 155-180, 1989.

Goodman, M.N. and J.M. Lowenstein. The purine nucleotide cycle: Studies of ammonia production by skeletal muscles in situ and in perfused preparations. J. Biol. Chem. 252: 5054-5060, 1977.

Gupta, R.K. and R.D. Moore. ^{31}P NMR studies of intracellular free Mg^{2+} in intact frog skeletal muscle. J. Biol. Chem. 255(9): 3987-3993, 1980.

Gyulai, L., Z. Roth, jr. Leigh, J.S., and B. Chance. Bioenergetic studies of mitochondrial oxidative phosphorylation using ^{31}P phosphorus NMR. J. Biol. Chem. 260(7): 3947-3954, 1985.

Hasselbach, W. and H. Oetliker. Energetics and electrogenicity of the sarcoplasmic reticulum calcium pump. Ann. Rev. Physiol. 45: 325-339, 1983.

Hassinen, I.E. and K. Hiltunen. Respiratory control in isolated perfused rat heart. Role of the equilibrium relations between the mitochondrial electron carriers and the adenylate system. Biochim. Biophys. Acta 408: 319-330, 1975.

Hassinen, I.E., Mitochondrial respiratory control in the myocardium. Biochim. Biophys. Acta 853: 135-151, 1986.

Heineman, F.W. and R.S. Balaban. Phosphorus-31 nuclear magnetic resonance analysis of transient changes of canine myocardial metabolism in vivo. J. Clin. Invest. 85: 1990.

Hill, D.K. The time course of oxygen consumption of stimulated frog's muscle. J. Physiol. (Lond.) 98: 207-227, 1940a.

Hill, D.K. The time course of evolution of oxidative recovery heat of frog's muscle. J. Physiol. (Lond.) 98: 454-459, 1940b.

Holian, A., C.S. Owen, and D.F. Wilson. Control of respiration in isolated mitochondria: Quantitative evaluation of the dependence of respiratory rates on [ATP], [ADP], and [Pi]. Arch. Biochem. Biophys. 181: 164-171, 1977.

Hoppeler, H., O. Hudlicka, and E. Uhlmann. Relationship between mitochondria and oxygen consumption in isolated cat muscles. J. Physiol. 385: 661-675, 1987.

Hoult, D.I., J.W. Busby, D.G. Gadian, G.K. Radda, N.E. Richards, and P.J. Seeley. Observation of tissue metabolites using ^{31}P nuclear magnetic resonance. Nature 252(22): 285-287, 1974.

Hultman, E., S.D. Canale, and H. Sjöholm. Effect of induced metabolic acidosis on intracellular pH, buffer capacity and contraction force of human skeletal muscle. Clin. Sci. 69: 505-510, 1985.

Huxley, A.F., and R.M. Simmons,. Proposed mechanism of force generation in striated muscle. Nature 233: 533-538, 1971.

Ingwall, J.S. Phosphorus nuclear magnetic resonance spectroscopy of cardiac and skeletal muscles. Am. J. Physiol. 242: H729-H744, 1982.

Jacobus, W.E., R.W. Moreadith, and K.M. Vandegaer. Mitochondrial respiratory control. J. Biol. Chem. 257(5): 2397-2402, 1982.

Jacobus, W.E. and A.L. Lehninger. Creatine kinase of rat heart mitochondria. J. Biol. Chem. 248(13): 4803-4810, 1973.

Jacobus, W.E., G.J. Taylor IV,, D.P. Hollis,, and R.L. Nunnally,. Phosphorus nuclear magnetic resonance of perfused working rat hearts. Nature 265: 756-758, 1977.

Jacobus, W.E., Respiratory control and the integration of heart high-energy phosphate metabolism by mitochondrial creatine kinase. Ann. Rev. Physiol. 47: 707-725, 1985.

Janis, R.A., P.J. Silver, and D.J. Triggle. Drug action and cellular calcium regulation. Adv. Drug Res. 16: 309-339, 1987.

Johnson, M.J. The role of aerobic phosphorylation in the pasteur effect. Science 94(2435): 200-202, 1941.

Kalckar, H. . Enzymologia 2: 47-52, 1937.

Kalckar, H. . Biochem. J. 33: 631-641, 1939.

Katz, L.A., A.P. Koretsky, and R.S. Balaban. Respiratory control in the glucose perfused heart a ³¹P NMR and NADH fluoorescence study. FEBS Letters 221{2}: 270-276, 1987.

Katz, L.A., P. Koretsky, and R.S. Balaban. Activation of dehydrogenase activity and cardiac respiration: a ³¹P-NMR study. Am. J. Physiol. 255(Heart Circ.24): H185-H188, 1988.

Kauppinen, R. Proton electrochemical potential of the inner mitochondrial membrane in isolated perfused rat hearts, as measured by exogenous probes. Biochim. Biophys. Acta 725: 131-137, 1983.

Kentish, J.C., and S. Palmer,. Calcium binding to isolated bovine cardiac and rabbit skeletal troponin-C is affected by pH but not by caffeine or inorganic phosphate. J. Physiol. (Lond.): 160P, 1.

Kentish, J.C., and R.J. Solaro,. Differential pH sensitivity of Ca^{2+} -activated force production in myofibrils from adult and neonatal rat hearts. FASEB 39P, 1987. (Abstract)

Kingsley-Hickman, P.B.,, E.Y. Sako,, P. Mohanakrishnan,, P.M.L. Robitaille,, A.H.L. From,, J.E. Foker,, and K. Ugurbil,. ^{31}P NMR studies of ATP synthesis and hydrolysis kinetics in the intact myocardium. Biochem. 26: 7501-7510, 1987.

Klingenberg, M. Zur reversibilitat der oxydativen phosphorylierung. Biochemis. Zeit. 335: 263-272, 1961.

Klingenberg, M. The ADP, ATP shuttle of the mitochondrion. TIBS 249-252, 1979.

Klingenberg, M. The ADP-ATP translocation in mitochondria, a membrane potential controlled transport. J. Membrane Biol. 56: 97-105, 1980.

Koretsky, A.P. and R.S. Balaban. Changes in pyridine nucleotide levels alter oxygen consumption and extramitochondrial phosphates in isolated mitochondria: a ^{31}P -NMR and NAD(P)H fluorescence study. Arch. Biochem. Biophys. 893: 398-408, 1987.

Kunz, W., R. Bohnensack, G. Bohme, U. Kuster, G. Letko, and P. Schonfeld. Relations between extramitochondrial and intramitochondrial adenine nucleotide systems. Arch. Biochem. Biophys. 209(1): 219-229, 1981.

Kushmerick, M.J., R.E. Larson, and R.E. Davies. The chemical energetics of muscle contraction I. activation heat, heat of shortening and ATP utilization for activation-relaxation processes. : 293-333, 1969.

Kushmerick, M.J., Energetics of muscle contraction. In: Handbook of physiology, 1983: p. 189-234.

Kushmerick, M.J., R.A. Meyer, and T.R. Brown. Regulation of oxygen consumption in fast- and slow-twitch muscle. Am. J. Physiol. (Cell Physiol. 32): c1-c9, 1992.



Kushmerick, M.J. and R.A. Meyer. Chemical changes in rat leg muscle by nuclear magnetic resonance. Am. J. Physiol. 248: C542-C549, 1985.

Kushmerick, M.J., and R.J. Paul,. Aerobic recovery metabolism following a single isometric tetanus in frog sartorius muscle at 0 degrees C. J. Physiol. (Lond.) 254: 693-709, 1976.

Kuster, U., R. Bohnensack, and W. Kunz. Control of oxidative phosphorylation by the extramitochondrial ATP/ADP ratio. Biochim. Biophys. Acta 440: 391-402, 1976.

Kuster, U., G. Letko, W. Kunz, J. Duszynsky, K. Bogucka, and L. Wojtczak. Influence of different energy drains on the interrelationship between the rate of respiration, proton-motive force and adenine nucleotide patterns in isolated mitochondria. Biochim. Biophys. Acta 636: 32-38, 1981.

Lannergren, J., and H. Westerblad. Maximum tension and force-velocity properties of fatigued, single xenopus muscle fibres studied by caffeine and high K^+ . J. Physiol. (Lond.) 409: 473-490, 1989.

Lannergren, J., and H. Westerblad. Force decline due to fatigue and intracellular acidification in isolated fibres from mouse skeletal muscle. J. Physiol. (Lond.) 434: 307-322, 1991.

LaNoue, K.F., F.M.H. Jeffries, and G.K. Radda. Kinetic control of mitochondrial ATP synthesis. Biochem. 25: 7667-7675, 1986.

Lardy, H.A. The role of phosphate in metabolic control mechanisms. In: The Biology of Phosphorus, In Press, East Lansing, 1951: p. 131-145.

Lardy, H.A. and G.F. Maley. Metabolic Effects of Thyroid Hormones in Vitro. Recent. Progr. Hormone Resear. 10: 129-155, 1954.

Lardy, H.A. and H. Wellman. The catalytic effect of 2,4-dinitrophenol on adenosinetriphosphate hydrolysis by cell particals and soluble enzymes. J. Biol. Chem. 201: 357-370, 1953.

Lardy, H.A. and H. Wellmen. Oxidative phosphorylations: role of inorganic phosphate and acceptor systems in control of metabolic rates. Nature 215-224, 1951.

Lawrie, R.A. The relation of energy-rich phosphate in muscle to myoglobin and to cytochrome-oxidase activity. Biochem. 55: 20-309, 1953.

Lawson, J.W.R., and R.L. Veech,. Effects of pH and free Mg^{2+} on the K_{eq} of the creatine kinase reaction and other phosphate hydrolyses and phosphate transfer reactions. J. Biol. Chem. 254(14): 6528-6537, 1979.

Lehninger, A.L. Oxidative phosphorylation. Harvey Lectures 49: 176-215, 1954.

Lehninger, A.L. and S. Wagner Smith. Efficiency of phosphorylation coupled to electron transport between dihydrodiphosphopyridine nucleotide and oxygen. J. Biol. Chem. 178: 415-429, 1949.

Leigh, J.S., B. Chance, and S. Nioka. Control of oxidative metabolism and hydrogen delivery in human skeletal muscle. A steady-state analysis. NMR Biol Med 201-216, 1986.

Letko, G., U. Kuster, J. Duszynski, and W. Kunz. Investigation of the dependence of the intramitochondrial [ATP]/[ADP] ratio on the respiration rate. Biochim. Biophys. Acta 593: 196-203, 1980.

Lipmann, F. Metabolic generation and utilization of phosphate bond energy. Nature: 99-161, 1951.

Lipmann, F. Metabolic process patterns. In: Currents in Biochemical Research, edited by D.E. Green, Interscience, New York, 1946: p. 137-148.

Lynen, V.F. Die rolle der phosphate bei dehydrierungsvorgangen und ihre biologische bedeutung. Die Naturwissenschaften 30: 398-406, 1942.

Mahler, M. First-order kinetics of muscle oxygen consumption, and equivalent proportionality between QO_2 and phosphorylcreatine level. J. Gen. Physiol. 86: 135-165, 1985.

McGilvery, R.W. and T.W. Murray. Calculated equilibria of phosphocreatine and adenosine phosphates during utilization of high energy phosphate by muscle. J. Biol. Chem. 249(18): 5845-5850, 1974.

Metzger, J.M. and R.L. Moss. Greater hydrogen ion-induced depression of tension and velocity in skinned single fibers of rat fast than slow muscles. J. Physiol. (Lond.) 393: 727-742, 1987.

Meyer, R.A., M.J. Kushmerick, and T.R. Brown. Application of ^{31}P -NMR spectroscopy to the study of striated muscle metabolism. Am. J. Physiol. 242: C1-C11, 1982.

Meyer, R.A., H.L. Sweeney, and M.J. Kushmerick. A simple analysis of the phosphocreatine shuttle. Am. J. Physiol. 246: C365-C377, 1984.

Meyer, R.A., T.R. Brown, and M.J. Kushmerick. Phosphorus nuclear magnetic resonance of fast- and slow-twitch muscle. Am. J. Physiol. 248: C279-C287, 1985.

Meyer, R.A., T.R. Brown, B.L. Krilowicz, and M.J. Kushmerick. Phosphagen and intracellular pH changes during contraction of creatine depleted rat muscle. Am. J. Physiol. 250: C264-C274, 1986.

Meyer, R.A. A linear model of muscle respiration explains monoexponential phosphocreatine changes. Am. J. Physiol. 254: C548-C553, 1988.

Meyer, R.A. Linear dependence of muscle phosphocreatine kinetics on total creatine content. Am. J. Physiol. (257): C1149-C1157, 1989.

Meyer, R.A. and G.R. Adams. Stoichiometry of phosphocreatine and inorganic phosphate changes in rat skeletal muscle. NMR Biomed 3(5): 206-210, 1990.

Miller, R.G., M.D. Boska, R.S. Moussavi, P.J. Carson, and M.W. Weiner. ^{31}P nuclear magnetic resonance studies of high energy phosphates and pH in human muscle fatigue. J. Clin. Invest. 81: 1190-1196, 1988.

Mitchell, P. Coupling of phosphorylation to electron and hydrogen transfer by a chemi-osmotic type of mechanism. Nature 191: 144-148, 1961.

Mitchell, P. Keilin's respiratory chain concept and its chemiosmotic consequences. Science 206: 1148-1159, 1979.

Moon, R.B. and J.H. Richards. Determination of intracellular pH by ^{31}P magnetic resonance. J. Biol. Chem. 248(20): 7276-7278, 1973.

Nakamaru, Y. and A. Schwartz. The influence of hydrogen ion concentration on calcium binding and release by skeletal muscle sarcoplasmic reticulum. J. Gen. Physiol. 59: 22-32, 1972.

Nioka, S., Z. Argov, G.P. Dobson, R.E. Forster, H.V. Subramanian, R.L. Veech, and B. Chance. Substrate regulation of mitochondrial oxidative phosphorylation in hypercapnic rabbit muscle. J. Appl. Physiol. 72(2): 521-528, 1992.

Ochoa, S. . Nature(Lond.) 146: 267, 1940a.

Ochoa, S. "Coupling" of phosphorylation with oxidation of pyruvic acid in brain. Nature 751-773, 1940b.

Orchard, C.H., D.L. Hamilton, P. Astles, E. McCall, and B.R. Jewell. The effects of acidosis on the relationship between Ca^{2+} and force in isolated ferret cardiac muscle. J. Physiol. 436: 559-578, 1991.

Orchard, C.H., The role of the sarcoplasmic reticulum in the response of ferret and rat heart muscle to acidosis. J. Physiol. (Lond.) 384: 431-449, 1987.

Owen, C.S. and D.F. Wilson. Control of respiration by the mitochondrial phosphorylation state. Arch. Biochem. Biophys. 161: 581-591, 1974.

Partain, C.L., R.R. Price, J.A. Patton, W.H. Stephens, A.C. Price, V.M. Runge, M.R. Mitchell, R.G. Stewart, and A.E. James. Nuclear magnetic resonance imaging. RadGraph. 4: 5-25, 1984.

Phillips, C.A., and J.S. Petrofsky,. Muscle: structural and functional mechanics. In: Mechanics of Skeletal and Cardiac Muscle, edited by C.A. Phillips and J.S. Petrofsky, Charles C. Thomas, Springfield, Ill., 1983: p. 3-18.

Rall, J.A. Energetic aspects of skeletal muscle contraction: implication of fiber types. In: , 1972: p. 35-74.

Sahlin, K., L. Edstrom, H. Sojoholm, and E. Hultman. Effects of lactic acid accumulation and ATP decrease on muscle tension and relaxation. Am. J. Physiol. 240(Cell Physiol.9): C121-C126, 1981.

Saks, V.A., V. Kuznetsov, V.V. Kupriyanov, M.V. Miceli, and W.E. Jacobus. Creatine kinase of rat heart mitochondria. J. Biol. Chem. 260(12): 7757-7764, 1985.

Sapega, A.A., D.P. Sokolow, T.J. Graham, and B. Chance. Phosphorus nuclear magnetic resonance: a non-invasive technique for the study of muscle bioenergetics during exercise. Med. Sci. Sports Exec. 19(4): 410-420, 1987.

Senior, A.E., ATP synthesis by oxidative phosphorylation. Physiol. Rev. 68(1): 177-231, 1988.

Seraydarian, K., W.F.H.M. Mommaerts, A. Wallner, and R.J. Guillory. An estimation of the true inorganic phosphate content of frog sartorius muscle. J. Biol. Chem. 236(7): 2071-2075, 1961.

Shoubridge, E.A. and G.K. Radda. A gated ^{31}P NMR study of tetanic contraction in rat muscle depleted of phosphocreatine. Am. J. Physiol. 252: C532-C542, 1987.

Slater, E.C., J. Rosing, and A. Mol. The phosphorylation potential generated by respiring mitochondria. Biochim. Biophys. Acta 292: 534-553, 1973.

Slater, E.C. The discovery of oxidative phosphorylation. TIBS 226-227, 1981.

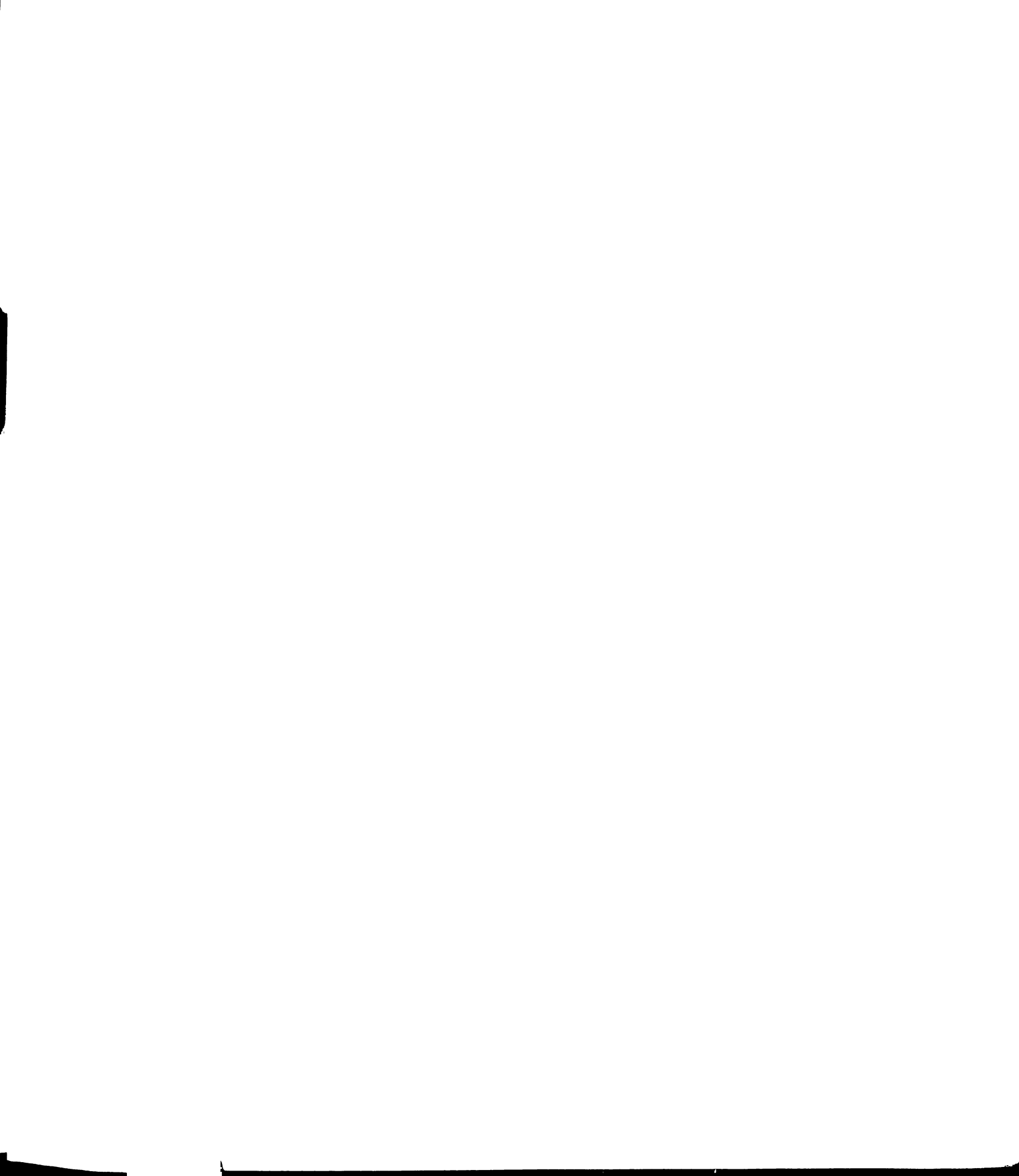
Tamura, M., O. Hazeki, S. Nioka, and B. Chance. In vivo study of tissue oxygen metabolism using optical and nuclear magnetic resonance spectroscopies. Ann. Rev. Physiol. 51: 813-834, 1989.

Taylor, D.J., P. Styles, P.M. Matthews, D.A. Arnold, D.G. Gadian, P. Bore, and G.K. Radda. Energetics of human muscle: exercise-induced ATP depletion. Mag. Res. Med. 3: 44-54, 1986.

Terjung, R.L., G.A. Dudley, and R.A. Meyer. Metabolic and circulatory limitations to muscular performance at the organ level. J. Exp. Biol. 115: 307-318, 1985.

Thompson, L.V., E.M. Balog, and R.H. Fitts. Muscle fatigue in frog semitendinosus: role of intracellular pH. Am. J. Physiol. 262(Cell Physiol.31): C1507-C1512, 1992.

Tobin, R.B., C.R. Mackerer, and M.A. Mehlman. pH effects on oxidative phosphorylation of rat liver mitochondria. Am. J. Physiol. 223: 83-88, 1972.



Van Dam, K., H.V. Westerhoff, K. Krab, R. Van Der Meer, and J.C. Arents. Relationship between chemiosmotic flows and thermodynamic forces in oxidative phosphorylation. Biochim. Biophys. Acta 591: 240-250, 1980.

Van Der Meer, R., T.P.M. Akerboom, A.K. Groen, and J.M. Tager. Relationship between oxygen uptake of perfused rat-liver cells and the cytosolic phosphorylation state calculated from indicator metabolites and a redetermined equilibrium constant. Eur. J. Biochem. 84: 421-428, 1978.

Van Der Meer, R., H.V. Westerhoff, and K. Van Dam. Linear relation between rate and thermodynamic force in enzyme-catalyzed reactions. Biochim. Biophys. Acta 591: 488-493, 1980.

Veech, R.L., J.W. Lawson, N.W. Cornell, and H.A. Krebs. Cytosolic phosphorylation potential. J. Biol. Chem. 254(14): 6538-6547, 1979.

Vignais, P.V. Molecular and physiological aspects of adenine nucleotide transport in mitochondria. Biochim. Biophys. Acta 456: 1-38, 1976.

Vincent, A. and J.McD. Blair. The coupling of the adenylate kinase and creatine kinase equilibria calculation of substrate and feedback signal levels in muscle. FEBS Letters 7(3): 239-245, 1970.

Wakata, N., Y. Kawamura, M. Kobayashi, Y. Araki, and M. Kinoshita. Histochemical and biochemical studies on the red and white muscle in rabbit. Comp. Biochem. Physiol. 97B(3): 543-545, 1990.

Westerblad, H., J.A. Lee, J. Lannergren, and D.G. Allen. Cellular mechanisms of fatigue in skeletal muscle. Am. J. Physiol. (Cell Physiol.30): C195-C209, 1991.

Westerblad, H. and J. Lannergren. The relation between force and intracellular pH in fatigued, single *Xenopus* muscle fibers. Acta Physiol. Scand. 113: 83-89, 1988.

Wilkie, D.R. Muscular fatigue: effects of hydrogen ions and inorganic phosphate. Federation Proc. 45: 2921-2923, 1986.

Wilson, D.F., M. Erecinska, C. Drown, and I.A. Silver. Effects of oxygen tension on cellular energetics. Am. J. Physiol. 233(5): C135-C140, 1977a.

Wilson, D.F., C.S. Owen, and A. Holian. Control of mitochondrial respiration: a quantitative evaluation of the roles of cytochrome c and oxygen. Arch. Biochem. Biophys. 182: 749-762, 1977b.

Wilson, D.F., C.S. Owen, and M. Erecinska. Quantitative dependence of mitochondrial oxidative phosphorylation on oxygen concentration: A mathematical model. Arch. Biochem. Biophys. 195(2): 494-504, 1979.

Wilson, D.F., M. Stubbs, R.L. Veech, M. Erecinska, and H.A. Krebs. Equilibrium relations between the oxidation-reduction reactions and the adenosine triphosphate synthesis in suspensions of isolated liver cells. Biochem. J. 140: 57-64, 1974.

Wilson, D.F., Energy transduction in biological membranes. 1993: p. 153-195.

Yoshizaki, K., H. Nishikawa, and H. Watari. Diffusivities of creatine phosphate and ATP in and aqueous solution studied by pulsed field gradient ^{31}P NMR. Japan. J. Physiol. 37: 923-928, 1987.

Yoshizaki, K., H. Watari, and G.K. Radda. Role of phosphocreatine in energy transport in skeletal muscle of bullfrog studied ^{31}P -NMR. Biochim. Biophys. Acta 1051: 144-150, 1990.



MICHIGAN STATE UNIV. LIBRARIES



31293010191777